Spatial and Temporal Variation in Primary and Secondary Productivity in the Eastern Great Australian Bight

Paul D. van Ruth

April 2009

A thesis submitted in fulfilment of the requirements for the degree of

Doctor of Philosophy,

School of Earth and Environmental Sciences,

The University of Adelaide.

Table of contents

List of tables

List of figures

Summary

The Great Australian Bight (GAB) was for many years thought to be an area of limited biological productivity due to a perceived lack of nutrient enrichment processes. These conclusions, however, were based on data from few studies in the western GAB which were assumed to reflect conditions throughout the entire GAB. More recent studies have reported the occurrence of coastal upwelling in the eastern GAB (EGAB) during summer/autumn (November-April), characterized by low sea surface temperatures and elevated concentrations of chlorophyll *a*, which suggests that certain areas of the GAB may be highly productive during certain times of the year.

The eastern Great Australian Bight (EGAB) forms part of the Southern and Indian Oceans and is an area of high ecological and economic importance. Although it supports the largest fishery in Australia (the South Australian Sardine fishery, annual catches since 2004 ~ 25,000 to 42,500 t), quantitative estimates of the primary productivity underlying this industry are open to debate. Estimates range from < 100 mg C m^{-2} day^{-1} to > 500 mg C m^{-2} day^{-1}. Part of this variation may be due to the unique upwelling circulation of shelf waters in summer/autumn (November-April), which shares some similarities with highly productive eastern boundary current upwelling systems, but differs due to the influence of a northern boundary current, the Flinders current, and a wide continental shelf. Shelf waters encompass an area of ~115,000 km^2, and the diverse coastal topography forms part of one of the longest stretches of southward facing coastline in the world. In summer-autumn, winds are upwelling favourable, and the Flinders current running along the continental slope causes the upwelling of the deep permanent thermocline from around 600 m depth

(dynamic uplift), allowing nutrient rich cold water to entrain onto the shelf. In winter-spring, the EGAB is dominated by westerly downwelling-favourable winds, and upwelling via the Flinders current is suppressed. Thus, the area is highly dynamic, with significant spatial and temporal variations in meteorology and oceanography which may drive variations in nutrient enrichment and productivity. This study represents the first intensive investigation of the primary and secondary productivity of the EGAB, and was designed to evaluate the general hypothesis that spatial and temporal variations in meteorology and oceanography in the EGAB will drive spatial and temporal variations in phytoplankton size structure, and primary and secondary productivity. It examines variations in primary and secondary productivity in the EGAB during the upwelling and downwelling seasons of 2004, and the upwelling seasons of 2005 and 2006.

Daily integral productivity calculated using the vertically generalised production model (VGPM) showed a high degree of spatial variation. Productivity was low (<800 mg C m^{-2} day^{-1}) in offshore central and western regions of the EGAB. High productivities (1600-3900 mg C m^{-2} day^{-1}) were restricted to hotspots in the east that were influenced by the upwelled water mass. There was a strong correlation between the depth of the euphotic zone and the depth of the mixed layer that suggested that ~50% of the euphotic zone lay below the mixed layer depth. As a result, high rates of primary productivity did not require upwelled water to reach the surface. A significant proportion of total productivity in the euphotic zone (57% in 2005 and 65% in 2006) occurred in the upwelled water mass below the surface mixed layer. This result has implications for daily integral productivities modelled with the VGPM, which uses surface measures of phytoplankton biomass to calculate productivity. Macro nutrient concentrations could not be used to explain the difference in the low

and high productivities (silica >1 μmol L^{-1}, nitrate/nitrite >0.4 μmol L^{-1}, phosphate >0.1 μmol L^{-1}). Mixing patterns or micro-nutrient concentrations are possible explanations for spatial variations in primary productivity in the EGAB. On a global scale, daily rates of primary productivity of the EGAB lie between the highly productive eastern boundary current upwelling systems, and less productive coastal regions of western and south eastern Australia, and the oligotrophic ocean. However, daily productivity rates in the upwelling hotspots of the EGAB rival productivities in Benguela and Humbolt currents.

Temporal variation in mixing and primary productivity was examined in upwelling influenced nearshore waters off south western Eyre Peninsula (SWEP) in the EGAB. Mixing/stratification in the region was highly temporally variable due to the unique upwelling circulation in summer/autumn, and downwelling through winter/spring. Highest productivity was associated with upwelled/stratified water (up to 2958 mg C m^{-2} d^{-1}), with low productivity during periods of downwelling and mixing (~300-550 mg C m^{-2} d^{-1}), yet no major variations in macro-nutrient concentrations were detected between upwelling and downwelling events (silica >1 μmol L^{-1}, nitrate/nitrite >0.4 μmol L^{-1}, phosphate >0.1 μmol L^{-1}). We hypothesise that upwelling enriches the region with micro-nutrients. High productivity off SWEP appears to be driven by a shallowing of mixed layer depth due to the injection of upwelled waters above Z_{cr}. Low productivity follows the suppression of enrichment during downwelling/mixing events, and is exacerbated in winter/spring by low irradiances and short daylengths.

Phytoplankton abundance and community composition was also examined in the shelf waters of the EGAB. Phytoplankton abundances were generally higher in near shore waters compared with offshore waters, and during the summer/autumn

upwelling season compared with the winter/spring downwelling season. Three distinctly different phytoplankton communities were present in the region during the upwelling and downwelling seasons of 2004, and the upwelling season of 2005, with distinctions manifest in variations in the abundance of dominant types of phytoplankton, and differences in average cell sizes. In summer/autumn, waters influenced by upwelling were characterised by high phytoplankton abundances (particularly diatoms) and larger average cell sizes, while the warmer high-nutrient-low-chlorophyll (HNLC) waters in the region had lower phytoplankton abundances and smaller average cell sizes. The winter/spring community was made up of low abundances of relatively large cells. Diatoms always dominated, but evidence of Si limitation of further diatom growth suggests there may be an upper limit to diatom productivity in the region. The maximum observed diatom concentration of ~164,000 cells L^{-1} occurred in February/March 2004, in an area influenced by the upwelled water mass. Variations in phytoplankton biodiversity in the shelf waters of southern Australia appear to be related to variations in the influence of upwelling in the region.

Meso-zooplankton abundance and community composition was examined in the coastal upwelling system of the EGAB. Spatial and temporal variations were influenced by variations in primary productivity and phytoplankton abundance and community composition, which were driven by variations in the influence of upwelling in the region. Peak meso-zooplankton abundances and biomass occurred in the highly productive upwelling influenced nearshore waters of the EGAB. However, abundances were highly variable between regions and years, reflecting the high spatial and temporal variations in primary productivity and phytoplankton abundance that characterise the shelf waters of the region. Spatial and temporal variations in community composition were driven by changes in the abundance of classes of meso-

zooplankton common to all regions in both years of this study. Meroplanktonic larvae and opportunistic colonizers dominated the community through the upwelling season, in response to increased primary productivity and phytoplankton blooms. Differences in community composition between upwelling influenced waters and the more HNLC regions appear to be reflected in the relative abundances of cladocera and appendicularia, with cladocera more abundant in productive upwelling influenced areas, and appendicularia thriving in the more HNLC regions of the EGAB. Highest potential grazing rates in the EGAB occurred in nearshore regions with highest meso-zooplankton biomass, most likely in response to the high phytoplankton biomass that occurs in the same regions. Peak meso-zooplankton grazing rates in the EGAB were ~80% less than those measured in south west Spencer Gulf in March 2007, and ~35% greater than grazing rates in the Huon Estuary in February 2005.

Productivity in the EGAB shows significant spatial and temporal variation, with changes reflecting regional and seasonal variation in meteorology and oceanography, and the water masses present in the region. The overall productivity of a summer/autumn upwelling season was highly dependent on within-season variations in wind strength and direction, which dictate the number, intensity, and duration of upwelling events. Rates of primary productivity measured in the EGAB at a given time depended on the meteorological and oceanographic conditions in the region in the lead up to, and during, the sampling event. We hypothesise that during upwelling events, high productivity in the EGAB is driven by the enrichment of waters above Z_{cr}, but below the surface mixed layer, with micro-nutrients. Low productivity within summer/autumn upwelling seasons follows the suppression of this enrichment during downwelling/mixing events, and the overall productivity of the upwelling season will depend on the number, duration and intensity of these downwelling/mixing events.

Low productivity during winter/spring is driven by the absence of upwelling, low irradiances and short daylengths.

Declaration

This work contains no material which has been accepted for the award of any other degree or diploma in any university or other tertiary institution and, to the best of my knowledge and belief, contains no material previously published or written by another person, except where due reference has been made in the text.

I give consent to this copy of my thesis, when deposited in the University Library, being made available for loan and photocopying, subject to the provisions of the Copyright Act 1968.

22nd April, 2009.

Acknowledgements

This PhD study was undertaken at the University of Adelaide, and was jointly funded by the School of Earth and Environmental Sciences and the South Australian Research and Development Institute (SARDI) Aquatic Sciences division. In addition to these supporting institutions, I am sincerely grateful to the following individuals:

- My supervisors, A/Prof George Ganf and A/Prof Tim Ward, for their continual guidance, encouragement and support
- A/Prof John Middleton and Dr John A. T. Bye for invaluable discussions on a myriad of oceanographic topics
- The master and crew of the *RV Ngerin*, Neil Chigwidden, Dave Kerr, Chris Small, and Ralf Putz, for their expertise and assistance in ensuring that sampling trips were completed safely and successfully
- Members of the SARDI Aquatic Sciences Wild Fisheries Pelagic fish group, Lachie McLeay, Paul Rogers, Alex Ivey, Wetjens Dimmlich, and Richard Saunders, for their assistance before, during, and after sampling trips
- Ralf Putz for skippering the *Tucana*, and Richard Saunders for his assistance, during the February 2006 sampling trip off south western Kangaroo Island
- Steve Brett from Microalgal Services (Victoria, Australia) for discussions regarding phytoplankton identification
- Peter Hobson for assistance with data management
- My office mates over the years have been fantastic in their support and encouragement. Special thanks to Danny Brock, Annelise Wiebkin, Michelle Roberts, Rudi Regel, Kane Aldridge and Brian Deegan
- Finally, my parents, for everything, especially the gift of self-belief

1. Introduction

Production in the ocean refers to the harnessing of solar energy to produce organic compounds that can be utilised by other trophic levels. Primary producers (the phytoplankton) form high-energy organic compounds from nutrients and light via photosynthesis. Phytoplankton are responsible for more than 95% of marine photosynthesis (Falkowski and Kolber 1995). Their health and productivity underpin the marine ecosystem, since they form the primary food source in the oceanic food web. Herbivorous secondary producers feed on the phytoplankton, and are in turn preyed upon by carnivorous higher consumers. Thus, light energy harnessed by the phytoplankton is gradually transformed into products available for consumption by higher trophic levels as it moves up the food chain.

As micro-organisms in a dynamic environment, phytoplankton are dependent on oceanographic processes like upwelling and vertical mixing to bring nutrients from depths below the euphotic zone (so-called 'new' nutrients, inorganic Si, P, and N as NO_x) to levels where they may be utilized for photosynthesis (Margalef 1978). The dynamic nature of these processes means both nutrients and phytoplankton are distributed randomly through the water column, and phytoplankton are exposed to constantly fluctuating nutrient supplies, irradiances, and turbulence. As a result, the overall productivity, size distribution and community composition of the phytoplankton in a given region in the ocean will be primarily affected by the availability of nutrients and light (Olivieri and Hutchings 1987; Daneri *et al*. 2000; Aiken *et al.* 2008), which will be dictated by spatial and temporal variations in the meteorological and oceanographic processes which govern their supply.

Early estimates of marine primary productivity suggested that the open sea, about 90% of the global ocean, had a low productivity. Estimated rates of productivity ranged from 50 g C m^{-2} $year^{-1}$ for open seas, to 100 g C m^{-2} $year^{-1}$ for costal zones. Highest rates of primary productivity were 300 g C m^{-2} $year^{-1}$ for highly productive upwelling areas, which were estimated to total only 0.1% of the ocean surface (Ryther 1969). The advent of satellite technology has provided more accurate estimates of productivity at much higher spatial resolution. Measurements of sea surface temperature (SST) and surface fluorescence can be used to model primary productivity across vast areas of the ocean. These estimates generally appeared to confirm those of Ryther (1969), with global patterns in primary productivity provided through the Sea-viewing Wide Field-of-view Sensor (SeaWiFS) and Moderate Resolution Imaging Spectroradiometer (MODIS) projects indicating low productivity in the open ocean and higher productivity in coastal and upwelling zones. There are limitations, however, to primary productivity estimates from satellite data. Satellite mounted sensors are unable to recognise any deep chlorophyll maxima, or detect productivity occurring below near-surface waters. With euphotic depths across the global ocean ranging between ~30-180 m (http://daac.gsfc.nasa.gov/oceancolor/locus/LOCUS_NASA_water_quality_info.shtml) there is likely to be a significant amount of primary productivity occurring below the surface that would not be picked up in satellite estimates. Indeed, Waite & Suthers (2007) emphasise that deep water chlorophyll maxima (DCM) occur off the Australian coast at depths of 100 to 200 m and contain 40 – 80% of the chlorophyll *a* in the water column. Hanson *et al.* (2007) related the DCM in the Leeuwin current waters off south-western Australia to nitrate concentrations that were generally higher than in the overlying surface waters. They concluded that oceanographic conditions

in Leeuwin current waters were driving variations in nitrocline depth relative to euphotic depth (Z_{eu}), leading to variations in the contribution of the primary productivity of the DCM to overall water column productivity. This highlights the need for satellite estimates of primary productivity to be validated with measured rates and estimates based on measured data.

The most productive pelagic ecosystems in the world's oceans occur off the north western and south western coasts of Africa and America, in areas dominated by eastern boundary currents and wind induced coastal upwelling (Ryther 1969; Mann and Lazier 2006). In these areas, equatorward longshore winds drive Ekman transport of water offshore at the surface, with nutrient rich water upwelled from below (Tomczak and Godfrey 1994; Mann and Lazier 2006). The strength and duration of upwelling favourable winds may be highly variable and will depend on local meteorological conditions, which may lead to large variations in rates of primary productivity. Estimates for these areas range between 1000-3500 mg C m^{-2} d^{-1} in the Benguela current upwelling system off southern Africa (Brown *et al.* 1991), and 800-5100 mg C m^{-2} day^{-1} in the Humboldt current upwelling system off the coast of Chilè (Daneri *et al.* 2000). The ecosystems supported in these regions are of high economic and ecological importance, due to the commercial fisheries and abundant sea-life they sustain.

The size distribution of the phytoplankton community has an important influence on the amount of productivity that occurs within a given region of the ocean. The efficiency of energy transfer up the food chain depends on the number of steps required to transfer carbon from phytoplankton to fish. This in turn depends on the size distribution of the phytoplankton community. Photo-autotrophic picoplankton (phytoplankton <2 µm) include both prokaryotic (cyanobacteria) and eukaryotic

(diatoms, silicoflagellates, cryptomonads, green algae, and members of the Eustigmatophyceae and Prasinophyceae families) algal species (Johnson and Sieburth 1979, 1982; Takahashi and Bienfang 1983; Takahashi and Hori 1984; Chisholm 1992; Aiken *et al.* 2008). The size, physiology and biochemistry of pico-phytoplankton provide a significant advantage over other phytoplankton size classes during periods of low or pulsed nutrient supply, or low irradiance (Stockner and Anita 1986; Stockner 1988; Raven 1998; Aiken *et al.* 2008). Pico-phytoplankton are too small to be eaten directly by meso-zooplankton, and pass into a food web known as the microbial loop. The small algal cells are eaten by ciliates and protozoans, which are then large enough to be preyed upon by meso-zooplankton. In this way, previously inaccessible carbon is made available to the zooplankton via the 'repackaging' of the pico-phytoplankton into suitably sized particles (Hewes *et al*. 1985). Pico-phytoplankton are dominant in low nutrient zones such as oligotrophic open ocean gyres, areas which have low carbon biomass, low concentrations of chlorophyll *a*, and low productivity, (Aiken *et al.* 2008). Smaller cells, and thus the less productive microbial loop, tend to dominate phytoplankton assemblages during long periods of stratification (Peterson *et al.* 1988; Teira *et al.* 2001; Aiken *et al.* 2008). These cells are more effectively able to acquire and use nutrients than larger cells, and thus have an advantage when nutrients are in short supply (Raven 1998), due to a combined effect of a thinner boundary layer (and thus reduced impact of diffusion limitation), and a very large surface area to volume ratio, which provides a larger area for solute exchange per unit volume (Raven 1998). In addition, sinking rates of natural pico-phytoplankton populations have been found to be immeasurable (Takahashi and Bienfang 1983). Pico-phytoplankton remain suspended in the euphotic zone in stratified waters where larger cells may quickly sink away from the light.

The larger size classes of phytoplankton include the nano- and micro-phytoplankton. Nano-phytoplankton (2-20 µm) grow in regions with some input of 'new' nutrients, which typically have moderate carbon biomass, chlorophyll *a* concentrations and productivity (Aiken *et al.* 2008). Micro-phytoplankton (2-2000 µm) include the diatoms and dinoflagellates, and bloom in high nutrient environments such as upwelling zones. These areas have high biomass, high concentrations of chlorophyll *a*, and high productivity (Aiken *et al.* 2008). When the primary productivity of a region is dominated by larger algal cells (typically diatoms), the carbon flux from algae to fish is more direct. Fewer steps are required before carbon is in a form that can be utilized by higher trophic levels. Production of this sort involves the more efficient classic food chain, and supports most of the large fisheries in the world (Ryther 1969; Webber and El Sayed 1987; Cushing 1989; Mann 1993; Tilstone *et al.* 1999; Teira *et al.* 2001). In these regions, where 'new' nutrients are brought into well-lit surface waters, turbulent vertical mixing reduces the impact of diffusion limitation due to the larger boundary layer of large cells, and ensures the large cells remain suspended in the euphotic zone.

Understanding the distribution and community dynamics of the zooplankton is also important when examining the fate of marine primary production and the flux of carbon through marine ecosystems. As primary consumers, zooplankton form an important link between primary producers and higher trophic levels, effectively repackaging autotrophic carbon into larger particles which are more readily available to secondary consumers and beyond (Swadling *et al.* 1997; Clark *et al.* 2001). Copepods are the most abundant of the marine meso-zooplankton (200-20,000µm body length, Parsons and Takahashi 1973; Omori and Ikeda 1984), and have been shown to dominate zooplankton communities in waters off central Chile (Grunewald

et al. 2002), during the Joint Global Ocean Flux Study (JGOFS) of the equatorial Pacific (Roman *et al.* 1995), and in studies of the northeast Atlantic (Clark *et al.* 2001), the Arabian sea (Roman *et al.* 2000), and off southwestern Africa (Verheye *et al.*1992). In recent years, however, another group of zooplankton have come under increasing scrutiny for their contribution to marine food webs and their importance in the transfer of phytoplankton carbon to higher order consumers. The micro-zooplankton are heterotrophic organisms which can pass through a <200 μm mesh screen. Micro zooplankton communities are dominated by oligotrich and tintinnid ciliates, but also include rotifers and heterotrophic dinoflagellates (Froneman and Perisinotto 1996; Froneman *et al.* 1996; Dolan *et al.* 2000). While rarely dominating zooplankton communities, micro-zooplankton still play an important role in marine food webs. They form an important food source for meso-zooplankton in the absence of suitably sized phytoplankton cells, and by consuming the smaller size classes of phytoplankton that dominate the oligotrophic ocean, these organisms make available to higher trophic levels areas of primary productivity that would otherwise be unavailable.

The impact of meso and micro-zooplankton on primary production varies widely between different oceanic regions. Despite dominating zooplankton communities, copepods are no longer thought to be the major consumers of marine primary production (Calbet and Landry 1999; Sautour *et al.* 2000). In highly productive waters such as upwelling regions, large diatoms typically dominate the algal community. These cells are large enough to be directly consumed by copepods, and the resulting classic food chain, from diatoms to meso-zooplankton to higher trophic levels, supports most of the world's large fisheries (Cushing 1989; Mann 1993; Tilstone *et al.* 1999; Teira *et al.* 2001). More recent studies, however, have reported

that a considerable part of the copepod diet consists of heterotrophic flagellates and ciliates, the micro-zooplankton (Roman and Gauzens 1997; Calbet *et al.* 2000; Calbet 2001). Feeding on phytoplankton is often insufficient to meet the metabolic costs of marine copepods, and selective feeding on micro-zooplankton often occurs (Calbet and Landry 1999; Roman *et al.* 2000; Nejstgaard *et al.* 2001). There is increasing evidence demonstrating that smaller phytoplankton are primarily consumed by micro-zooplankton, especially in unproductive waters where the grazing impact of micro-zooplankton may be four times higher than the impact of meso-zooplankton (Landry *et al.* 1993; Sautour *et al.* 2000; Calbet 2001; Nejstgaard *et al.* 2001).

The Great Australian Bight (GAB) was for many years thought to be an area of limited biological activity, much like the open sea, due to a perceived lack of nutrient enrichment processes (Motoda *et al.* 1978; Young *et al.* 2001). Primary productivity estimates ranged from 11 to 22 mg C m^{-2} hr^{-1}. Using the conversion equation of Keller (1988) these hourly productivities suggest a daily rate of between 50 and 160 mg C m^{-2} day^{-1}. It was assumed that these low productivities of the western GAB were representative of the entire GAB. However, there is significant potential for large spatial variations in primary productivity in an area as vast as the GAB. Indeed, recent studies in the eastern GAB (EGAB) have reported the occurrence of coastal upwelling in summer-autumn (November-April), characterized by low sea surface temperatures and elevated concentrations of chlorophyll *a* (Kampf *et al.* 2004; McClatchie *et al.* 2006; Ward *et al.* 2006). Middleton and Bye (2007) suggest that the upwellings that occur off Kangaroo Island and the Bonney coast are important drivers of the ecology of the region. However, they also point out that "Our understanding of upwelling here is again derived from a few studies and many questions remain as to the details and dynamics of this important system". This lack of detailed

oceanographic information is not unique to the GAB, but is emphasised by Carr *et al.* (2006) in their assessment of primary productivity estimated from ocean colour, sea surface temperature (SST), solar irradiance and mixed layer depth.

The circulation of the EGAB and south east Indian Ocean (SEIO) is unique in the global ocean. Shelf waters encompass an area of ~115,000 km^2, with a wide continental shelf and diverse coastal topography that forms part of one of the longest stretches of southward facing coastline in the world. The area is highly dynamic, with significant temporal variations in meteorology and oceanography which may drive variations in nutrient enrichment and productivity. In summer-autumn (November-April), the wind stress curl in the SEIO south of the continental shelf is positive, and leads to equatorward Sverdrup transport of water in the deep ocean. This northward Sverdrup transport is deflected to the west as it reaches the continental slope, resulting in a northern boundary current flowing from east to west along the slope, which is known as the Flinders current (Bye 1972; 1983; Middleton and Cirano 2002, Middleton and Bye 2007). The Flinders current, analogous to western boundary currents, causes the upwelling of the deep permanent thermocline from around 600 m depth (dynamic uplift), allowing nutrient rich cold water to entrain onto the shelf. The mean wind stress over the continental shelf is upwelling favourable at this time. Prevailing south-easterly winds drive Ekman transport of water offshore in the surface layer and cold water is upwelled from below (Hertzfeld and Tomczak 1997; 1999; Middleton and Platov 2003). This only occurs in areas of the EGAB with favourably angled coastlines, such as south-western Kangaroo Island, and south-western Eyre Peninsula (Middleton and Bye 2007). Strong upwelling events have also been reported to occur off the western coast of Eyre Peninsula in the absence of these upwelling favourable winds (Griffin *et al*. 1997), which suggests that upwelling in

this region of the EGAB cannot be explained by the wind field alone. Upwelling in the EGAB in the absence of favourable winds results from the eastern intensification of anticyclonic currents on the continental shelf. Current meter observations indicate a mean north-westerly flow along the coast and south-easterly flow over the shelf break (Bye 1983; Schahinger 1987; Evans and Middleton 1998), with the circulation of the GAB dominated by the presence of an anticyclonic gyre set up by the prevailing wind stress field (Hertzfeld and Tomczak 1997; 1999). Anticyclonic oceanic circulation in a basin of uniform depth provides convergent flow toward the centre of the gyre in the surface Ekman layer, and divergent flow in the bottom Ekman layer, with upwelling along the edges. This effect is intensified on the eastern edge of the gyre due to the bottom slope (Hertzfeld and Tomczak 1997; 1999). Thus, strong coastal upwelling in the EGAB may be the combined result of the upwelling favourable south-easterly winds blowing along the coast, and the eastern intensification of the wind driven anticyclonic circulation on the continental shelf, and can still occur in the absence of upwelling favourable winds. Upwelling in the EGAB is visible in analyses of sea surface temperature (SST) which reveal the presence of significantly colder water near the coast in the EGAB in summer-autumn (14-15^{o}C), with warmer waters offshore (18-20^{o}C) (Herzfeld 1997; Herzfeld and Tomczak 1997). The warm water has origins in the shallow waters of the north-western GAB and is driven eastward by the passing of anticyclonic weather systems. This water mass has a distinctly higher salinity than the waters of the Leeuwin current, which doesn't enter the GAB until mid May (Herzfeld 1997; Herzfeld and Tomczak 1997).

In winter-spring (May-October), the EGAB is dominated by westerly downwelling-favourable winds, which lead to the formation of a continuous eastward coastal current along the shelf break from Cape Leeuwin to the east coast of

Tasmania. This current results from the change in coastal sea level caused by the onshore Ekman transport of the wind field (Cirano and Middleton 2004). The presence of this coastal current suppresses the upwelling associated with the Flinders current, which flows underneath the coastal current within the permanent thermocline at around 600 m depth (Middleton and Cirano 2002). Coastal winds are downwelling favourable during winter (Cirano and Middleton 2004), and a continuous eastward current exists on the continental shelf (Bye 1983; Godfrey *et al*. 1986). Sea surface temperatures are lower inshore than offshore in winter, but the water column is well mixed, with no evidence of cold water intrusion or coastal upwelling. The water mass over the continental shelf has low nutrient levels (NO_3 <0.02 μM), high salinities (>36 ppt) and medium temperatures (~ 17°C) (Ward *et al*. 2001). The Leeuwin current enters the GAB in mid May, interacting with the warm surface water established in summer to produce a continuous band of warm water across the GAB. This water is gradually isolated from the coast and influenced by winter cooling, so that by late September-early October, SSTs are uniform across the GAB (Herzfeld, 1997; Herzfeld and Tomczak, 1997).

The summer/autumn shelf circulation south of Australia shares some characteristics with the highly productive upwelling systems outlined above, and like these systems, spatial and temporal variations in local meteorological conditions may lead to large variations in rates of primary productivity in the region. The physical oceanographic processes leading to the circulation detailed above, however, differ from those driving the upwelling circulation of the north and south western coastlines of Africa and America. The shelf circulation in the EGAB is not caused by upwelling alone, but by a combination of the actions of the Flinders current and associated dynamic uplift, adjustment to wintertime density anomalies, local winds and eastern

intensification of the anticyclonic circulation (Herzfeld and Tomczak 1999; Middleton and Platov 2003). The absence of eastern boundary currents and the distinctive circulation associated with the highly productive upwelling regions mentioned above characterize the upwelling observed in the EGAB in summer/autumn as a uniquely specialised coastal upwelling system.

While there have been many studies concerning the oceanography and circulation of the GAB (Bye 1972, 1983; Godfrey *et al.* 1986; Schahinger 1987; Griffin *et al.* 1997; Herzfeld 1997; Hertzfeld and Tomczak 1997; Evans and Middleton 1998; Hertzfeld and Tomczak 1999; Middleton and Cirano 2002; Middleton and Platov 2003; Cirano and Middleton 2004; Kampf *et al.* 2004; Middleton and Bye 2007), few have examined the biology of productivity in the region. The only information for the region consists of estimations of standing stock via surface chlorophyll *a* measurements (Motoda *et al.* 1978; Kampf *et al.* 2004; McClatchie *et al.* 2006; Ward *et al.* 2006). There have been few, if any, direct measurements of primary or secondary productivity in the region, and little is known about the abundance, composition, and spatial and temporal distribution of the phytoplankton and zooplankton communities. In summarizing information on primary and secondary productivity in Australian waters, Waite and Suthers (2007) suggest there is an overall dominance of small pico- and nano-plankton in shelf and coastal regions, and that the microbial food web dominates Australian phytoplankton dynamics and productivity. This study represents the first intensive investigation of the primary and secondary productivity of the upwelling regions of the EGAB, and was designed to evaluate the general hypothesis that spatial and temporal variations in meteorology and oceanography in the EGAB will drive spatial and temporal variations in phytoplankton size structure, and primary and secondary productivity. While

acknowledging the importance of the pico-phytoplankton to global productivity, this study focuses on the nano- and micro-phytoplankton which are more likely to be dominant in upwelling influenced ecosystems. Sampling took advantage of annual sardine surveys conducted by researchers from the Aquatic Sciences division of the South Australian Research and Development Institute. While providing excellent spatial coverage of the EGAB, the timing of these cruises meant investigations into productivity in the region were limited to snap-shots in time. As stated by Waite & Suthers (2007), however, "clearly oceanographers have yet to establish a comprehensive understanding of the processes governing productivity in Australian coastal waters". This study will provide baseline data regarding spatial and temporal variation in primary and secondary productivity in the EGAB, and guide future studies into productivity in the region at finer spatial and temporal scales.

1.1. References

Aiken, J., Hardman-Mountford, N. J., Barlow, R., Fishwick, J., Hirata, T. and Smyth, T. (2008). Functional links between bioenergetics and bio-optical traits of phytoplankton taxonomic groups: an overarching hypothesis with applications for ocean colour remote sensing. *Journal of Plankton Research* **30**(2): 165-181.

Brown, P. C., Painting, S. J. and Cochraine, K. L. (1991). Estimates of phytoplankton and bacterial biomass and production in the northern and southern Benguela ecosystems. *South African Journal of Marine Science* **11**: 537-564.

Bye, J. A. T. (1972). Oceanic circulation south of Australia. Antarctic Oceanology 2. *Antarctic Research Series* **19**: 95-100.

Bye, J. A. T. (1983). The general circulation in a dissipative ocean basin with longshore wind stresses. *Journal of Physical Oceanography* **13**: 1553-1563.

Calbet, A. (2001). Mesozooplankton grazing effect on primary production: A global comparative analysis in marine ecosystems. *Limnology and Oceanography* **46**(7): 1824-1830.

Calbet, A. and Landry, M. R. (1999). Mesozooplankton influences on the microbial food web: Direct and indirect trophic interactions in the oligotrophic open ocean. *Limnology and Oceanography* **44**(6): 1370-1380.

Calbet, A., Landry, M.R., and Scheinberg, R.D. (2000). Copepod grazing in a subtropical bay: Species-specific responses to a midsummer increase in nanoplankton standing stock. *Marine Ecology Progress Series* **193**: 75-84.

Carr, M., Friedrichs, M. A. M., Schmeltz, M., Aita, M. N., Antoine, D., Arrigo, K. R., Asanuma, I., Aumont, O., Barber, R., Behrenfeld, M., Bidigare, R., Buitenhuis, E. T., Campbell, J., Ciotti, A., Dierssen, H., Dowell, M., Dunne, J., Esaias, W., Gentili, B., Gregg, W., Groom, S., Hoepffner, N., Ishizaka, J., Kameda, T., Le Quere, C., Lohrenz, S., Marra, J., Melin, F., Moore, K., Morel, A., Reddy, T. E., Ryan, J., Scardi, M., Smyth, T., Turpie, K., Tilstone, G., Waters, K. and Yamanaka, Y. (2006). A comparison of global estimates of marine primary production from ocean color. *Deep Sea Research 2* **53**: 741-770.

Chisholm, S. W. (1992). Phytoplankton size. *in* Productivity and biogeochemical cycles in the seas. P. G. Falkowsi, and Woodhead, A.D. New York, Plenum Press**:** 213-237.

Cirano, M. and Middleton, J. F. (2004). The mean wintertime circulation along Australias southern shelves: a numerical study. *Journal of Physical Oceanography* **34**(3): 668-684.

Clark, D. R., Aazem, K. V. and Hays, G. C. (2001). Zooplankton abundance and community structure over a 4000 km transect in the north-east Atlantic. *Journal of Plankton Research* **23**(4): 365- 372.

Cushing, D. H. (1989). A difference in structure between ecosystems in strongly stratified waters and in those that are only weakly stratified. *Journal of Plankton Research* **11**: 1-13.

Daneri, G., Dellarossa, V., Quinones, R., Jacob, B., Montero, P. and Ulloa, O. (2000). Primary production and community respiration in the Humboldt Current System off Chile and associated oceanic areas. *Marine Ecology Progress Series* **197**: 41-49.

Dolan, J. R., Gallegos, C. L. and Moigis, A. (2000). Dilution effects on micro-zooplankton in dilution grazing experiments. *Marine Ecology Progress Series* **200**: 127-139.

Evans, S. R. and Middleton, J. F. (1998). A regional model of shelf circulation near Bass Strait: a new upwelling mechanism. *Journal of Physical Oceanography* **28**: 1439-1457.

Falkowski, P. G. and Kolber, Z. (1995). Variations in chlorophyll fluorescence yields in phytoplankton in the world oceans. *Australian Journal of Plant Physiology* **22**: 341-355.

Froneman, P. W. and Perisinotto, R. (1996). Structure and grazing of the microzooplankton communities of the Subtropical Convergence and a warm-core eddy in the Atlantic sector of the Southern Ocean. *Marine Ecology Progress Series* **135**: 237-245.

Froneman, P. W., Perisinotto, R. and McQuaid, C. D. (1996). Seasonal variations in micro-zooplankton grazing in the region of the Subtropical Convergence. *Marine Biology* **126**: 433-442.

Godfrey, J. S., Vaudrey, D. J. and Hahn, S. D. (1986). Observations of the shelf-edge current south of Australia, winter 1982. *Journal of Physical Oceanography* **16**: 668-679.

Griffin, D. A., Thompson, P. A., Bax, N. J., Bradford, R. W. and Hallegraeff, G. M. (1997). The 1995 mass mortality of pilchard: no role found for physical or biological oceanographic factors in Australia. *Marine and Freshwater Research* **48**: 27-42.

Grunewald, A. C., Morales, C. E., Gonzalez, H. E., Sylvester, C. and Castro, L. R. (2002). Grazing impact of copepod assemblages and gravitational flux in coastal and oceanic waters off central Chile during two contrasting seasons. *Journal of Plankton Research* **24**(1): 55-67.

Hanson, C. E., Pesant, S., Waite, A. M. and Pattiaratchi, C. B. (2007). Assessing the magnitude and significance of deep chlorophyll maxima of the coastal eastern Indian Ocean. *Deep Sea Research 2* **54**: 884-901.

Herzfeld, M. (1997). The annual cycle of sea surface temperature in the Great Australian Bight. *Progress in Oceanography* **39**: 1-27.

Herzfeld, M. and Tomczak, M. (1997). Numerical modelling of sea surface temperature and circulation in the Great Australian Bight. *Progress in Oceanography* **39**: 29-78.

Herzfeld, M. and Tomczak, M. (1999). Bottom-driven upwelling generated by eastern intensification in closed and semi-closed basins with a sloping bottom. *Marine and Freshwater Research* **50**: 613-627.

Hewes, C. D., Holm-Hansen, O. and Sakshaug, E. (1985). Alternate carbon pathways at lower trophic levels in the Antactic food web. *in* Antarctic nutrient cycles and food webs. W. R. Siegfried, Condy, P.R., and Laws, R.M. New York, Springer-Verlag.

Johnson, W. J. and Sieburth, J. M. (1979). Chroococcoid cyanobacteria in the sea: A ubiquitous and diverse phototrophic biomass. *Limnology and Oceanography* **24**: 928-935.

Johnson, W. J. and Sieburth, J. M. (1982). In-situ morphology and occurrence of eukaryotic phototrophs of bacterial sizein the picoplankton of estuarine and coastal waters. *Journal of Phycology* **18**: 318-327.

Kampf, J., Doubel, M., Griffin, D. A., Matthews, R. and Ward, T. M. (2004). Evidence of a large seasonal coastal upwelling system along the southern shelf of Australia. *Geophysical Research Letters* **31**(L09310): doi:10.1029/2003GL019221.

Keller, A. A. (1988). An empirical model of primary productivity (^{14}C) using mesocosm data along a nutrient gradient. *Journal of Plankton Research* **10**(4): 813-834.

Landry, M. R., Monger, B. C. and Selph, K. E. (1993). Time-dependency of microzooplankton grazingand phytoplankton growth in the subarctic Pacific. *Progress in Oceanography* **32**: 205-222.

Mann, K. H. (1993). Physical oceanography, food chains and fish stocks: a review. *ICES Journal of Marine Science* **50**: 105-119.

Mann, K. H. and Lazier, J. R. N. (2006). Dynamics of marine ecosystems: biological - physical interactions in the oceans. London, Blackwell Science.

Margalef, R. (1978). Life forms of phytoplankton as survival alternatives in an unstable environment. *Oceanologica Acta* **1**: 493-509.

McClatchie, S., Middleton, J. F. and Ward, T. M. (2006). Water mass analysis and alongshore variation in upwelling intensity in the eastern Great Australian Bight. *Journal of Geophysical Research* **111**(C08007): doi:10.1029/2004JC002699.

Middleton, J. F. and Bye, J. A. T. (2007). A review of the shelf slope circulation along Australia's southern shelves: Cape Leeuwin to Portland. *Progress in Oceanography* **75**: 1-41.

Middleton, J. F. and Cirano, M. (2002). A northern boundary current along Australia's southern shelves: the Flinders current. *Journal of Geophysical Research-Oceans* **107**(C9): 3129-3143.

Middleton, J. F. and Platov, G. (2003). The mean summertime circulation along Australia's southern shelves: a numerical study. *Journal of Physical Oceanography* **33**(11): 2270-2287.

Motoda, S., Kawamura, T. and Taniguchi, A. (1978). Differences in productivities between the Great Australian Bight and the Gulf of Carpentaria, Australia, in Summer. *Marine Biology* **46**: 93-99.

Nejstgaard, J. C., Naustvoll, L. J. and Sazhin, A. (2001). Correcting for underestimation of microzooplankton grazing in bottle incubation experiments with mesozooplankton. *Marine Ecology Progress Series* **221**: 59-75.

Olivieri, E. T. and Hutchings, L. (1987). Volumetric estimates of phytoplankton production in newly upwelled waters of the southern Benguela Current. *Limnology and Oceanography* **32**(5): 1099-1111.

Omori, M. and Ikeda, T. (1984). Methods in marine zooplankton ecology. New York, Wiley-Interscience.

Parsons, T. R. and Takahashi, M. (1973). Biological oceanographic processes. New York, Pergamon Press.

Peterson, W. T., Dagoberto, F. A., McManus, G. B., Dam, H., Bellantoni, D., Johnson, T. and Tiselius, P. (1988). The nearshore zone during coastal upwelling: daily variability and coupling between primary and secondary production off central Chile. *Progress in Oceanography* **20**: 1-40.

Raven, J. A. (1998). The twelfth Tansley Lecture. Small is beautiful: the picophytoplankton. *Functional Ecology* **12**: 503-513.

Roman, M., Smith, S., Wishner, K., Zhang, X. and Gowing, M. (2000). Mesozooplankton production and grazing in the Arabian sea. *Deep Sea Research 2* **47**: 1423-1450.

Roman, M. R., Dam, H. G., Gauzens, A. L., Urban-Rich, J., Foley, D. G. and Dickey, T. D. (1995). Zooplankton variability on the equator at 140 deg W during the JGOFS EqPac study. *Deep Sea Research 2* **42**(2-3): 673-693.

Roman, M. R. and Gauzens, A. L. (1997). Copepod grazing in the equatorial Pacific. *Limnology and Oceanography* **42**(4): 623-634.

Ryther, J. H. (1969). Photosynthesis and Fish Production in the Sea. *Science* **166**: 72-76.

Sautour, B., Artigas, L. F., Delmas, D., Herbland, A. and Laborde, P. (2000). Grazing impact of micro- and mesozooplankton during a spring situationin coastal waters off the Gironde estuary. *Journal of Plankton Research* **22**(3): 531-552.

Schahinger, R. B. (1987). Structure of coastal upwelling events off the south east coast of South Australia during February 1983-April 1984. *Australian Journal of Marine and Freshwater Research* **38**: 439-459.

Stockner, J. G. (1988). Phototrophic picoplankton: An overview from marine and freshwater ecosystems. *Limnology and Oceanography* **33**: 765-775.

Stockner, J. G. and Anita, N. J. (1986). Algal picoplankton from marine and freshwater ecosystems: A multidisciplinary perspective. *Canadian Journal of Fisheries and Aquatic Science* **43**: 2472-2503.

Swadling, K. M., Gibson, J. A. E., Ritz, D. A., Nichols, P. D. and Hughes, D. E. (1997). Grazing of phytoplankton by copepods in eastern Antarctic coastal waters. *Marine Biology* **128**: 39-48.

Takahashi, M. and Bienfang, P. K. (1983). Size structure of phytoplankton biomass and photosynthesis in subtropical Hawaiian waters. *Marine Biology* **76**: 203-211.

Takahashi, M. and Hori, T. (1984). Abundance of picophytoplankton in the subsurface chlorophyll maximum layer in subtropical and tropical waters. *Marine Biology* **79**: 177-186.

Teira, E., Serret, P. and Fernandez, E. (2001). Phytoplankton size-structure, particulate and dissolved organic carbon production and oxygen fluxes through microbial communities in the NW Iberian coastal transition zone. *Marine Ecology Progress Series* **219**: 65-83.

Tilstone, G. H., Figueirus, F. G., Fermin, E. G. and Arbones, B. (1999). Significance of nanophytoplankton photosynthesis and primary production in a coastal upwelling system (Ria de Vigo, NW Spain). *Marine Ecology Progress Series* **183**: 13-27.

Tomczak, M. and Godfrey, J. S. (1994). Regional oceanography: an introduction, Pergamon.

Verheye, H. M., Hutchings, L., Huggett, J. A. and Painting, S. J. (1992). Mesozooplanktonm dynamics in the Benguela ecosystem, with emphasis on the herbivorous copepods. *South African Journal of Marine Science* **12**: 561-584.

Waite, A. M. and Suthers, I. M. (2007). Open water: plankton ecology. *in* Marine Ecology. S. D. Connell and B. M. Gillanders. Melbourne, Oxford University Press.

Ward, T. M., Hoedt, F., McLeay, L. J., Dimmlich, W. F., Jackson, G., Rogers, P. J. and Jones, K. (2001). Have recent mass mortalities of the sardine *Sardinops sagax* facilitated an expansion in the distribution and abundance of the anchovy *Engraulis australis* in South Australia? *Marine Ecology Progress Series* **220**: 241-251.

Ward, T. M., McLeay, L. J., Dimmlich, W. F., Rogers, P. J., McClatchie, S., Matthews, R., Kampf, J. and van Ruth, P. D. (2006). Pelagic ecology of a northern boundary current system: effects of upwelling on the production and distribution of sardine (*Sardinops sagax*), anchovy (*Engraulis australis*) and southern bluefin tuna (*Thunnus maccoyii*) in the Great Australian Bight. *Fisheries Oceanography* **15**(3): 191-207.

Webber, L. H. and El-Sayed, S. Z. (1987). Contributions of the net, nano- and picoplankton to the phytoplankton standing crop and primary productivity in the Southern Ocean. *Journal of Plankton Research* **9**(5): 973-994.

Young, J., Nishida, T. and Stanley, C. (2001). A preliminary survey of the summer hydrography and plankton biomass of the eastern Great Australian Bight, Australia. Southern Bluefin Tuna Recruitment Monitoring and Tagging Program. *in* Report of the Eleventh Workshop. Hobart, CSIRO.

2. Hot-Spots of Primary Productivity: An Alternative Interpretation to Conventional Upwelling Models

2.1. Abstract

The eastern Great Australian Bight (EGAB) forms part of the Southern and Indian Oceans and is an area of high ecological and economic importance. Although it supports a commercial fishery, quantitative estimates of the primary productivity underlying this industry are open to debate. Estimates range from < 100 mg C m^{-2} day^{-1} to > 500 mg C m^{-2} day^{-1}. Part of this variation may be due to the unique upwelling circulation of shelf waters in summer/autumn (November-April), which shares some similarities with highly productive eastern boundary current upwelling systems, but differs due to the influence of a northern boundary current, the Flinders current, and a wide continental shelf. This study examines spatial variations in primary productivity in the EGAB during the upwelling seasons of 2005 and 2006. Daily integral productivity calculated using the vertically generalised production model (VGPM) showed a high degree of spatial variation. Productivity was low (<800 mg C m^{-2} day^{-1}) in offshore central and western regions of the EGAB. High productivities (1600-3900 mg C m^{-2} day^{-1}) were restricted to hotspots in the east that were influenced by the upwelled water mass. There was a strong correlation between the depth of the euphotic zone and the depth of the mixed layer that suggested that ~50% of the euphotic zone lay below the mixed layer depth. As a result, high rates of primary productivity did not require upwelled water to reach the surface. A significant proportion of total productivity in the euphotic zone (57% in 2005 and

65% in 2006) occurred in the upwelled water mass below the surface mixed layer. This result has implications for daily integral productivities modelled with the VGPM, which uses surface measures of phytoplankton biomass to calculate productivity. Macro nutrient concentrations could not be used to explain the difference in the low and high productivities (silica >1μmol L^{-1}, nitrate/nitrite >0.4μmol L^{-1}, phosphate >0.1μmol L^{-1}). Mixing patterns or micro-nutrient concentrations are possible explanations for spatial variations in primary productivity in the EGAB. On a global scale, daily rates of primary productivity of the EGAB lie between the highly productive eastern boundary current upwelling systems, and less productive coastal regions of western and south eastern Australia, and the oligotrophic ocean. However, daily productivity rates in the upwelling hotspots of the EGAB rival productivities in Benguela and Humbolt currents.

2.2. Introduction

The geographical boundaries of the Great Australian Bight (GAB) are ill defined but it spans an area from about 32°S to 35°S, and about 125°E to 135°E, (Motoda *et al.* 1978, Middleton and Bye 2007). Moore and Abbott (2000) suggest that the GAB forms a northern limit of the Southern Ocean and has two ecological regions, the Mid-latitude Gyre Region and Mid-latitude Coastal Region. Longhurst *et al.* (1995) classify the GAB as part of the coastal Indian Ocean in the province of Australia Southwest (AuSW). They also recognise that south of the coastal Indian Ocean province the GAB merges into the Southern Ocean, the South Subtropical Convergence (SSTC).

The GAB for many years was thought to be an area of limited biological activity, due to a perceived lack of nutrient enrichment processes (Motoda *et al.* 1978; Young

et al. 2001). Primary productivity estimates ranged from 11 to 22 mg C m^{-2} $hr^{-1}$and nitrate and phosphate concentrations were <2 µg L^{-1}. Using the conversion equation of Keller (1988) these hourly productivities suggest a daily rate of between 50 and 160 mg C m^{-2} day^{-1}. It was assumed that these low productivities of the western GAB were representative of the entire GAB. More recently, Longhurst *et al.* (1995) suggest primary productivities of 550 mg C m^{-2} day^{-1} for AuSW and 370 mg C m^{-2} day^{-1} for the SSTC or an annual productivity of 199 and 136 g C m^{-2} $year^{-1}$. These annual figures are significantly higher than the average figures estimated by Ryther (1969) of 50 for open seas, 100 for coastal zones and 300 g C m^{-2} $year^{-1}$ for upwelling areas. Recent studies in the eastern GAB (EGAB) have reported the occurrence of coastal upwelling in summer-autumn (November-March), characterized by low sea surface temperatures and elevated concentrations of chlorophyll *a* (Kampf *et al.* 2004; McClatchie *et al.* 2006; Ward *et al.* 2006). Middleton and Bye (2007) suggest that the upwellings that occur off Kangaroo Island and the Bonney coast are important drivers of the ecology of the region. The supposition is that upwelling brings nutrient rich water into the euphotic zone that promotes primary productivity. However, they also point out that "Our understanding of upwelling here is again derived from a few studies and many questions remain as to the details and dynamics of this important system". This lack of detailed oceanographic information is not unique to the GAB but is emphasised by Carr *et al.* (2006) in their assessment of primary production estimated from ocean colour, sea surface temperature (SST), solar irradiance and mixed layer depth.

The upwelling circulation of the EGAB is unique in the global ocean. Shelf waters encompass an area of ~115,000 km^2, with a wide continental shelf and diverse coastal topography that forms part of one of the longest stretches of southward facing

coastline in the world. Summer/Autumn meteorology in the EGAB is dominated by high pressure systems and south easterly winds which produce an anticyclonic gyral circulation in the GAB (Herzfeld and Tomczak 1999; Middleton and Platov 2003). Equatorward Sverdrup transport of water in the south east Indian Ocean results in a northern boundary current flowing from east to west along the slope, the Flinders current (Bye 1972; 1983; Middleton and Cirano 2002). This current is analogous to western boundary currents, and drives the upwelling of cold water from ~250m depth onto the continental shelf south of Kangaroo island (Middleton and Platov 2003; Middleton and Bye 2007). However, due to the wide shelf that characterises the region, upwelling in the EGAB is effectively a two step process. Water upwelled through the action of the Flinders current forms a sub-surface pool south and west of Kangaroo Island as it is driven to the north, then west along constant depth contours (Middleton and Bye 2007). A second upwelling event, driven by prevailing south easterly winds, is then required to bring the cold water from the Kangaroo Island pool to the surface via Ekman transport of water offshore in the surface layer, and the upwelling of water from below (Herzfeld and Tomczak 1997; 1999; Middleton and Platov 2003). This only occurs in regions with coastlines that are parallel to the south-easterly winds, which are comparable to the temporally variable longshore winds that drive upwelling in eastern boundary current systems (Middleton 2000; Middleton and Platov 2003). Such regions in the EGAB include south western Eyre Peninsula (SWEP) and south western Kangaroo Island (SWKI) (Middleton and Bye 2007).

The upwelling circulation described above does not persist constantly throughout the upwelling season. Upwelling occurs between December and March as a series of 2-4 upwelling events which are interspersed by periods of weak downwelling and

mixing. The strength and timing of these events is determined by the passage of high pressure systems through the region (Middleton and Bye 2007). In an area as large and dynamic as the EGAB, variations in meteorology and oceanography produce significant potential for spatial variations in nutrient enrichment of surface waters which may result in significant spatial variations in primary productivity.

While it is generally assumed that upwelling brings cold water rich in nitrogen and silica from great depths into surface waters, promoting primary productivity, there may also be occasions where a bottom layer of nutrient rich water exists on the continental shelf encompassed within the lower euphotic zone, that drives high primary productivity and promotes the formation of deep chlorophyll maxima (DCM). For example, Hanson *et al.* (2007) found that pigment concentrations and phytoplankton carbon in Leeuwin current waters off south-western Australia were significantly higher in the DCM, which generally occurred toward the base of the euphotic zone. The DCM was associated with increased nitrate concentrations, with generally low nutrient concentrations in the overlying surface waters. Hanson *et al.* (2007) concluded that changing oceanographic conditions in Leeuwin current waters were driving variations in nitrocline depth relative to euphotic depth (Z_{eu}), leading to variations in the contribution of primary productivity in the lower regions of the euphotic zone to overall water column productivity. The upwelled water of the Kangaroo Island pool outlined above may present another example of a bottom layer of water that provides nutrient enrichment toward the base of the euphotic zone. Waters in the layer above the Kangaroo Island pool most likely have origins in the waters of the central GAB to the west of Head of Bight, an area of the GAB with limited communication with deep water from off the shelf, and therefore unlikely to be enriched with N and Si. The influence of the Kangaroo Island pool on primary

productivity in the EGAB will depend on variations in the intensity of upwelling/downwelling events in the region, and the depth of the surface mixed layer and the Kangaroo Island pool relative to Z_{eu}.

With the complex and dynamic meteorology and oceanography of the EGAB in mind, we propose a conceptual model that relates nutrient enrichment and irradiance to primary productivity in the EGAB. The model outlines four possible scenarios that may be encountered when sampling the shelf waters of the EGAB (Fig. 2.1). The first scenario details conditions that may be expected to occur during periods of downwelling and mixing, where there is no enrichment of shelf waters and probably low productivity. The next scenarios describe the onset of upwelling that sees deep water brought onto the shelf south of Kangaroo Island moving to the north and then west to form the Kangaroo Island pool. Scenario two occurs when Z_{eu} is shallow, and does not encompass any of the Kangaroo Island pool, and is likely to result in low productivity. In Scenario 3, Z_{eu} is deep enough to include some of the water from the Kangaroo Island pool, resulting in high productivity in a bottom layer toward the base of Z_{eu}, and low productivity in the surface layer. Scenario 4 describes conditions that are likely to be found after a second upwelling event has occurred, with upwelled water from the Kangaroo island pool reaching the surface near the coast off SWKI or SWEP, and is likely to result in high productivity throughout the water column. Primary productivity levels measured in the EGAB during the upwelling season are likely to depend on which of these scenarios is occurring in the region at the time of sampling, and where in the region the sampling is done.

This study aims to investigate spatial variation in primary productivity in the shelf waters of the EGAB. It was designed to evaluate the hypotheses that spatial variations in meteorology, oceanography and coastal topography drive spatial

variations in nutrient enrichment in the EGAB, and that nutrient enrichment and primary productivity will be highest in the regions of the EGAB influenced by the upwelled water mass. The primary productivity models of Behrenfeld and Falkowski (1997a; 1997b), and Platt *et al.* (1990; 1991) were coupled with surface chlorophyll measured directly (extraction) and chlorophyll depth profiles measured via fluorescence. In addition, measurements were made of the vertical attenuation coefficient and temperature to provide estimates of the depths of the euphotic zone and the mixed layer.

2.3. Methods

Research cruises were undertaken during February/March 2005 and 2006, at stations outlined in Figure 2.2. Sampling was carried out aboard the RV Ngerin and proceeded as follows.

2.3.1. Measurements of physical parameters

Pressure, conductivity and temperature were measured using a Seabird SBE 19 plus Conductivity Temperature Depth recorder (CTD) (Sea-Bird Electronics Inc., Bellevue, WA, USA), which was lowered to within 10 m of the bottom at each station, and to 70 m at stations >80 m depth. Depth and density were derived from pressure, temperature and conductivity during data processing using Seabird SBE Data Processing win32 software. Surface contour plots and cross-shelf depth profiles of temperature and density were produced in Surfer® (Golden Software Inc., Golden, CO, USA) using a kriging interpolation algorithm. A Biospherical QSP-2300 underwater PAR sensor with log amplifier (Biospherical Instruments Inc., San Diego,

CA, USA) was used to measure underwater irradiance. The natural log of irradiance was plotted against depth, with the slope of the regression through these points providing the coefficient of downwelled irradiance, or K_d. The euphotic depth (Z_{eu}) was calculated by substituting K_d into a derivation of the Beer-Lambert equation (Kirk 1994).

$$Z_{eu} = 4.6 / K_d \quad (1)$$

Mixed layer depths (MLD) were calculated using a density based criterion according to Kara *et al.* (2000).

2.3.2. Measurements of nutrient concentrations

Water samples for nutrient analysis were collected at selected stations using a Niskin bottle (Fig. 2.2). Fifty ml of each sample was filtered through a Whatman GF/C filter and retained for analysis by the Water Studies Centre at Monash University, Victoria, Australia. Dissolved Si (APHA-AWWA-WPCF 1998c), nitrate/nitrite (NO_x) (APHA-AWWA-WPCF 1998a), and phosphate (APHA-AWWA-WPCF 1998b) were determined by flow injection analysis with a QuickChem 8000 Automated Ion Analyser.

2.3.3. Measurements of phytoplankton biomass and primary productivity

Water samples were collected from 3 m depth at each station for chlorophyll analysis. A 1 L sample from each station was filtered through a Whatman GF/C filter and the filter kept in the dark at < -5ºC until returned to the laboratory. Samples were

extracted in 90% methanol over 24 hours, with absorbances read at 750 nm (background) and 665 nm (chlorophyll *a*) using a Hitachi U-2000 spectrophotometer with 1 cm pathlength. Chlorophyll concentrations were calculated using the formulae of Talling and Driver (1963). Chlorophyll was also measured in CTD casts as fluorescence using a Chelsea Aquatracka Mk3 fluorometer (Chelsea Technologies Group, Surrey, UK) attached to the CTD. Contour plots of extracted surface chlorophyll *a* concentrations, and cross-shelf depth profiles of chlorophyll fluorescence were produced in Surfer® (Golden Software Inc., Golden, CO, USA) using a kriging interpolation algorithm.

Spatial correlations between physical parameters, nutrient concentrations and chlorophyll *a* concentrations were examined via mantel tests in PC-Ord 5 (McCune and Mefford 1999). Essentially, these tests look to correlate potential differentiation with geographical distance. Data were tested for 19 stations across the EGAB in February 2005 and 10 stations in February/March 2006. The three matrices compared in the tests included (1) Physical data (temperature and density), (2) Nutrient data (Si, NO_x, FRP, in μmol L^{-1}), and (3) Biological data (extracted chlorophyll *a* concentration). The distance measure used was Sorensen (Bray-Curtis). The standardised Mantel statistic (r) was calculated via randomization using the Monte Carlo test (5000 iterations, 0.1 significance level).

In February/March 2006, primary production was examined using a Walz phyto-PAM. Samples collected at the three nearshore stations in the eastern and central regions were dark adapted for > 30 minutes prior to measurement. Samples were corrected for background fluorescence using GF/C filtrate, then exposed to a series of irradiances to provide estimates of relative specific electron transport rates. These estimates were used to construct rapid light curves, and when fitted to the model of

Ralph and Gademann (2005), corrected for the absence of photoinhibition, provided values for the photosynthetic efficiency (α), the irradiance corresponding to light saturation of photosynthesis (I_k), and the maximum specific electron transport rate (ETR^B_{max}). Specific electron transport rates can be converted into specific rates of photosynthesis using conversion factors which consider the absorption cross section of photosystem 2 in natural phytoplankton populations, and the number of electrons required to produce one molecule of oxygen (Korner and Nicklisch 2002, Estevez-Blanco *et al.* 2006, Kromkamp *et al.* 2008). Maximum specific electron transport rates were converted to maximum specific photosynthetic rates (P^B_{max}) using a conversion factor of 0.156 (Korner and Nicklisch 2002). Maximum specific photosynthetic rates were converted from units of mg O_2 (mg chl a)$^{-1}$ h^{-1} to units of mg C (mg chl a)$^{-1}$ h^{-1} according to (Parsons *et al.* 1984), assuming a molecular photosynthetic quotient of 1 (Ganf and Horne 1975).

2.3.4. Modelling primary production

The vertically generalised production model (VGPM) of Behrenfeld and Falkowski (1997b) was used to estimate primary productivity (PP_{eu}) in the waters off south western Eyre Peninsula according to equation 2:

$$PP_{eu} = 0.66125 P^{b}_{opt} \frac{I_0}{I_0 + 4.1} C_{surf} \times Z_{eu} \times D_{irr} \qquad (2)$$

Where P^b_{opt} is the optimal specific photosynthetic rate, I_o is the daily mean surface irradiance, C_{surf} is the extracted surface chlorophyll concentration, Z_{eu} is the euphotic depth, and D_{irr} is daylength in decimal hours. I_o from all coastal weather stations in

the EGAB was provided by the Australian Bureau of Meteorology. Calculations for each station made use of the I_o from the closest weather station.

CTD-measured sea surface temperature (SST) was used to calculate P^b_{opt} according to the relation:

$$P^b_{opt} = \begin{cases} 1.13 \rightarrow if \cdot SST < -1.0 \\ 4.00 \rightarrow if \cdot SST > 28.5 \\ P^{b'}_{opt} \rightarrow otherwise \end{cases} \quad (3)$$

$$P^{b'}_{opt} = 1.2956 + 2.759\times10^{-1} SST + 6.17\times10^{-2} SST^2 - 2.05\times10^{-2} SST^3 + 2.462\times10^{-3} SST^4 - 1.348\times10^{-4} SST^5 + 3.4132\times10^{-6} SST^6 - 3.27\times10^{-8} SST^7$$

Euphotic depth (Z_{eu}) was calculated from C_{surf} according to equation 4

$$Z_{eu} = \begin{cases} 568.2(C_{tot})^{-0.746} \rightarrow if \cdot C_{tot} < 102 \\ 200.0(C_{tot})^{-0.293} \rightarrow if \cdot C_{tot} > 102 \end{cases}$$
$$where \quad (4)$$
$$C_{tot} = \begin{cases} 38.0(C_{surf})^{0.425} \rightarrow if \cdot C_{surf} < 1.0 \\ 40.2(C_{surf})^{0.507} \rightarrow if \cdot C_{surf} \geq 1.0 \end{cases}$$

D_{irr} was obtained from astronomical information on the Geoscience Australia website (www.ga.gov.au/geodesy/astro). Contour plots of PP_{eu} were produced in Surfer® (Golden Software Inc., Golden, CO, USA) using a kriging interpolation algorithm.

As a means of examining the contribution of the surface mixed layer to overall productivity in the euphotic zone, the above model was run using mixed layer depth in

place of Z_{eu},. Bottom layer productivity was calculated as the difference between productivity in the euphotic zone and productivity in the surface mixed layer.

To test the validity of VGPM estimates of primary productivity, independent estimates of daily integral primary productivity ($P_{Zeu,\ T}$) were calculated according to the model of Platt *et al.* (1991):

$$P_{Z_{eu},T} = Z_{eu} DBP_m^B (1 - \exp(-(2I_*^m / \pi K_d Z_{eu})(1 - M))) \qquad (5)$$

Where Z_{eu} is the euphotic depth, D is daylength in decimal hours, B is biomass (concentration of chlorophyll *a*), P^B_m is the maximum specific photosynthetic rate, I^m_* is the dimensionless irradiance at local noon, and M is the optical transmittance for the surface mixed layer (M = exp ($-K_dZ_{eu}$)). The mean maximum specific photosynthetic rate measured by the Phyto-PAM for the region in question was used for P^B_m. I^m_* was calculated as I^m_o/I_k, where I^m_o is the maximum daily (noon) surface irradiance, and and I_k is the irradiance corresponding to the onset of light saturation of photosynthesis. I^m_o was provided by the Australian Bureau of Meteorology from the weather station at the Adelaide Airport (34.952ºS 138.520ºE), the closest station to the study area that collects half hourly global solar data. The mean I_k measured with the Phyto-PAM for the region in question was used in calculations of I^m_*. Daily integral primary productivity in the surface mixed layer was calculated by substituting MLD for Z_{eu} in equation 7. Daily integral primary productivity in the bottom layer was estimated as the difference between productivity in the surface mixed layer and productivity in the euphotic zone.

2.4. Results

2.4.1. Spatial variation in physical parameters

SST plots reveal the presence of two different water masses in the EGAB. Cold, upwelled water (15-16°C) is visible in coastal waters off SWKI and SWEP. The upwelled water is confined in narrow regions close to the coast, squeezed between the coast and the large mass of warmer water (18-22°C) intruding from the west. This general pattern was evident in SST maps for Feb/Mar 2005 and 2006, but there were significant variations in patterns of SST between years. Upwelled water was visible off SWKI and SWEP in Feb/Mar 05, but only off SWEP in Feb/Mar 06, and temperatures off SWEP in Feb/Mar 06 were >2°C colder than those measured in Feb/Mar 05 (Fig. 2.3).

Temperature depth profiles reveal a mass of cold water moving across the shelf toward the coast in a bottom layer, which reaches the surface at certain stations (such as Q1 and 2, and L2 and 3 in Feb/Mar 05, and L1 to 4 in Feb/Mar 06). The cold water flows underneath a large surface mass of warmer water (Fig. 2.4). This pattern appears to exist across the shelf, but decreases in intensity from east to west. In both years, coldest temperatures were observed in the bottom layer of stations on transect F (off SWKI). Temperatures on the three transects examined were ~2°C colder in Feb/Mar 06 (Fig. 2.4). Density depth profiles indicate that this colder water is denser than the overlying warmer water (Fig. 2.5).

2.4.2. Spatial variations in the light regime

Mean K_d and Z_{eu} varied between regions and years (Table 2.1). K_d's were higher and consequently euphotic depths shallower in the nearshore compared with the off-

shore regions. Mixed layer depths (MLD) were also shallower in nearshore compared with the off shore regions. The euphotic depths were always > 15 m deeper than mixed layer depths. There was a strong positive correlation between Z_{eu} and mixed layer depth (r = 0.900 in 2005, 0.897 in 2006) that suggested that the surface mixed layer made up 46% of the euphotic zone in 2005 and 51% of the euphotic zone in 2006 (Fig. 2.6). Ratios of Z_{eu}:MLD ranged between 1.4 and 2.8 in Feb/Mar 05, and 1.1 and 3.5 in Feb/Mar 06.

2.4.3. Spatial variation in nutrient concentrations

Mean nutrient concentrations varied both between and within years (Table 2.2). Surface (3 m depth) phosphate concentrations ranged from 0.1 to 0.8 and from 0.2 to 0.6 μmol L^{-1} in the bottom layer below the thermocline. NO_x ranged from 0.4 to 1.3 in the surface and 0.5 to 2.6 μmol L^{-1}. The range for surface Si was 1.3 to 29.4 and 1.1 to 6.4 μmol L^{-1} in the bottom layer. In the eastern and central regions, the areas most influenced by the upwelling plume, concentrations of FRP and NO_x were generally higher in the bottom layer than the surface waters (Table 2.2).

2.4.4. Spatial variation in phytoplankton biomass and primary productivity

Surface extracted chlorophyll *a* concentrations were highest in areas influenced by the upwelled water mass. Chlorophyll concentrations in most of the EGAB ranged between < 0.1 and 0.6 μg L^{-1}. However, in Feb/Mar 2005, concentrations as high as 2.1 μg L^{-1} were measured in the surface waters off SWKI, and concentrations of 3.3 μg L^{-1} were measured in surface waters off SWEP in Feb/Mar 2006 (Fig. 2.7). High

concentrations of chlorophyll *a* were also measured nearshore around Cape Adieu (Transect V) in both Feb/Mar 2005 (1.1 μg L^{-1}) and 2006 (1.4 μg L^{-1}) (Fig. 2.7).

Fluorescence depth profiles show highest chlorophyll concentrations associated with the cold, dense upwelled water mass, both in the bottom layer and when it moves toward the surface. Chlorophyll concentrations in the overlying warmer water mass were generally < 0.2 μg L^{-1}, while concentrations in the upwelled water mass ranged between 0.2 and 1.6 μg L^{-1}, and varied greatly between years and regions (Fig. 2.8). In 2005, the highest chlorophyll concentration was 1.6 μg L^{-1} recorded at ~35 m depth at station L2, with a concentration of 1.4 μg L^{-1} measured at ~35 m depth at station Q1. Chlorophyll concentrations > 1.2 μg L^{-1} were also recorded in the waters between 15 and 35 m depth at station F2. In 2006, the highest chlorophyll concentration was 1.6 μg L^{-1} measured at ~35 m depth at station L1, with high concentrations also measured in the top 20 m of the water column at stations L2 and L3.

In February 2005 there were no significant associations between chlorophyll concentrations and nutrient concentrations in the EGAB ($p > 0.1$). There was a significant weak association between the physical data and chlorophyll *a* concentrations ($p = 0.082$, $r = -0.170$), but no significant association between the physical data and nutrient concentrations ($p > 0.4$). In February/March 2006 there was a significant, weak association between chlorophyll concentrations and nutrient concentrations ($p = 0.065$, $r = -0.234$), and a significant, strong association between physical data and chlorophyll *a* concentrations ($p = 0.002$, $r = 0.907$). There was also a significant, weak association between the physical data and nutrient concentrations ($p = 0.022$, $r = -0.227$).

Levels of VGPM modelled primary productivity in the EGAB were highly variable both within and between years, with the highest levels recorded in areas influenced by the upwelled water mass (Fig. 2.9). Levels of primary productivity in most of the EGAB were < 1000 mg C m^{-2} d^{-1}, with particularly low rates (< 400 mg C m^{-2} d^{-1}) measured in the offshore western region in 2005 and in the offshore central region in 2006. The highest level of primary productivity observed was 3916 mg C m^{-2} d^{-1} at station K1 off SWEP in 2006. In 2005, the highest productivity level was recorded for station E1 off SWKI (3483 mg C m^{-2} d^{-1}). Relatively high levels of productivity (~2000 mg C m^{-2} d^{-1}) were also associated with the waters off Cape Adieu in both 2005 and 2006.

Nearshore VGPM modelled rates of primary productivity were only greater than offshore productivity in areas influenced by the upwelled water mass (Table 2.3). Offshore productivity was generally greater than nearshore productivity, due to deeper Z_{eu}. Primary productivity in the surface mixed layer modelled using the VGPM accounted for 66% of the total productivity in the euphotic zone in 2005, but only 37% of the total productivity in the euphotic zone in 2006 (Fig. 2.10).

Rapid light curves in February/March 2006 varied between regions and depths, with modelled ETR values highest at the surface in the east, and at the DCM in the central region (Fig. 2.11). There was also variation in photosynthetic parameters between regions and depths. Highest photosynthetic efficiency (α) occurred at the DCM in the central nearshore region, while maximum specific photosynthetic rates (P^B_{max}) and irradiances corresponding to the onset of light saturation of photosynthesis (I_k) were highest at the surface in the nearshore east (Table 2.4). P^B_{max} were generally higher at the surface than at the DCM, with more pronounced differences in the east.

Nearshore rates of primary productivity modelled according to Platt *et al.* (1991) were only greater than offshore rates of productivity in areas influenced by the upwelled water mass (Table 2.5). Offshore productivity was, again, generally greater than nearshore productivity, due to deeper Z_{eu}. Primary productivity in the surface mixed layer modelled according to Platt *et al.* (1991) accounted for 74% of the total productivity in the euphotic zone in 2005, but only 45% of the total productivity in the euphotic zone in 2006 (Fig. 2.12).

Regression analyses indicate a close relationship between the Platt and the VGPM model results for productivities > 200 mg C m^{-2} day^{-1} ($r^2 = 0.77$, $p < 0.001$), but no significant relationship between productivities < 200 mg C m^{-2} day^{-1} ($r^2 = 0.02$, $p = 0.643$).

2.5. Discussion

Surface chlorophyll concentrations < 0.2 μg L^{-1} are within the range for the Mid-latitude Gyre ecological region of the Southern Ocean and concentrations of > 1 μg L^{-1} coincide with the SeaWiFS estimates of chlorophyll concentrations for the Mid-latitude Coastal Region of the EGAB during the austral summer (Moore and Abbott 2000). Furthermore, concentrations of > 2 μg L^{-1} coincide with the upwelling areas of SWEP and SWKI as observed by Moore and Abbott (2000). The chlorophyll concentrations in the offshore waters in the western segment of the GAB (Station Q) are similar to those reported by Motoda *et al.* (1978) (0.1 to 0.4 μg L^{-1}). However, the deepwater chlorophyll concentrations found in the coastal regions of transects Q, L and F are an order of magnitude higher than previously reported for the GAB.

The spatial variation in primary productivity in the shelf waters of the EGAB is illustrated by:

- Offshore areas of the eastern, central and western waters have low daily integral productivities (< 800 mg C m^{-2} d^{-1}, Fig. 2.9) that compare well with values reported for the oligotrophic waters of the Leeuwin current off south west Western Australia (110-530 mg C m^{-2} d^{-1}, Hanson et al. 2005), the AuSW and SSTC provinces of Longhurst *et al.* (1995) and the north and south Atlantic sub-tropical gyres (18-362 mg C m^{-2} d^{-1}, Maranon *et al.* 2003). They are significantly higher than the average values reported by Ryther (1969) and those of Motoda *et al.* (1978).
- Mid-shelf and coastal waters have intermediate productivities (800-1600 mg C m^{-2} d^{-1}, Fig. 2.9) that are comparable to those reported for localised upwellings off south west Western Australia (840-1310 mg C m^{-2} d^{-1}, Hanson *et al.* 2005), and for the waters of Bass Strait and the east coast of Tasmania (336-2880 mg C m^{-2} d^{-1}, highest rates associated with the spring bloom, Harris *et al.* 1987).
- Higher productivities are also achievable, but are restricted to distinct hotspots in the region. Productivity levels in waters off SWEP, SWKI, and Cape Adieu (1600-3900 mg C m^{-2} d^{-1}, Fig. 2.9) were within the range of productivities measured in the highly productive upwelling systems of the Benguela current off southern Africa (1000-3500 mg C m^{-2} d^{-1}, Brown *et al.* 1991), and the Humboldt current off the coast of Chilè (800-5100 mg C m^{-2} day^{-1}, Daneri *et al.* 2000).

Thus, certain regions of the EGAB have a potential productivity that rivals the most productive areas of the global ocean, and overall productivity is relatively high in a regional and global sense.

The absence of any strong associations between parameters in the EGAB in February 2005 may indicate a more or less homogenous water mass that one might expect to find during periods of downwelling/mixing. The strong association between physical parameters and chlorophyll *a* concentrations found in February/March 2006 is indicative of a region encompassing clearly defined water masses with distinct physical/biological characteristics, such as might be found during upwelling events. These water masses may be the warm, dense, less productive GAB warm pool, and the colder, denser, more productive upwelled Kangaroo Island Pool. The weak association between physical parameters and chlorophyll concentrations in February/March 2005 may be indicative of recent past periods of upwelling/stratification with accompanied variations in water column primary productivity. These results are indicative of the potential impact of temporal variations in physical factors on primary productivity in the EGAB.

High productivity in the EGAB is promoted by the presence of an upwelled water mass. Highest levels of primary productivity and highest surface chlorophyll concentrations in the EGAB are associated with this upwelled water mass. However, high levels of primary productivity are not restricted to surface waters. The deeper region of the euphotic zone in the EGAB at times encompassed a significant portion of the upwelled water mass (as postulated in scenario 3 in the conceptual model in Fig. 2.1), with highest chlorophyll fluorescences measured in this water below the surface mixed layer. Both the VGPM and the model of Platt *et al.* (1991) use surface chlorophyll concentrations to calculate daily integral productivity, which neglects any productivity that may be occurring below the surface mixed layer, and may thus underestimate total primary productivity. This study has shown that the contribution of the surface mixed and bottom layers of the euphotic zone to total primary

productivity in the EGAB can vary considerably between years. At times, the surface mixed layer may account for < 40% of total productivity despite the fact that it makes up > 50% of the euphotic zone. It is, therefore, highly likely that daily integral productivity levels in some areas of the EGAB, most likely in the mid shelf waters of the eastern and central regions that include the upwelled Kangaroo Island pool, are higher than indicated by modelled results presented in Figure 2.9. Overall primary productivity in the EGAB was heavily influenced by the presence of the upwelled water mass, but did not require that water mass to reach the surface. High productivity levels appear to be achievable after the first upwelling event which drives the formation of the Kangaroo Island Pool. These results have implications for previous conclusions about productivity in the region based on satellite derived data, and emphasise the importance of ground-truthing satellite and modelled data.

Ratios of Z_{eu}:MLD in this study fall toward the lower end of the range reported for data collected during the Warm Core Rings Experiment (0.1-12.2), and toward the higher end of the range reported for data from the Optical Dynamics experiment III (0.8-2.7) (Brown *et al.* 1995). This ratio has been used to make inferences about the influence of mixing on water column primary productivity (Patterson 1991). Patterson's empirical model explores the coupling between photosynthesis and mixing, in particular, the influence of timescales of the response of phytoplankton to changes in irradiance relative to timescales of mixing. Results suggest that when Z_{eu} > MLD, short term responses of phytoplankton photosynthesis to changes in irradiance are more important to overall water column productivity than the effects of mixing. When Z_{eu} < MLD, the influence of these effects diminishes, and water column productivity becomes increasingly dependent on the degree of mixing. In this study, Z_{eu} was always greater than MLD which indicates that short term responses of

phytoplankton to variations in irradiance have more influence on primary productivity in the EGAB during the upwelling season than the effects of mixing. However, downwelling/mixing events that may occur in the EGAB during the upwelling season may significantly alter the Z_{eu}:MLD ratio and drive temporal variations in the influence of mixing on water column productivity.

Two water masses were identified using the physical data in this study, the productive upwelled water mass drawn from off the shelf south of Kangaroo Island, and the less productive GAB warm pool with its origins in the shallow coastal waters to the west of Head of Bight (Herzfeld 1997; Herzfeld and Tomczak 1997). Despite large contrasts in productivity between the GAB warm pool and the upwelled water mass, there were no patterns in nutrient concentrations that could be used to differentiate between them. N:P ratios indicate potential nitrogen limitation in all regions of the EGAB sampled in this study, in the surface mixed layer and below the thermocline (N:P < 10). N limitation is expected in the coastal marine environment, with data suggesting that N:P ratios are often very low in coastal areas due to increased input of phosphorus in low N:P freshwaters manifest as terrestrial runoff (Downing 1997). Si:N ratios also reveal potential nitrogen limitation in most samples collected in this study, but suggest silica limitation in upwelled waters below the thermocline in the offshore eastern region in 2005 (Si:N = 0.7), and in the nearshore eastern region in 2006 (Si:N = 0.6). Stoichiometric ratios only become useful as indicators of potential nutrient limitation of primary productivity if nutrient concentrations are below levels consider limiting to phytoplankton growth. It is difficult to put a figure to limiting nutrient concentrations since phytoplankton show great variation in their nutrient uptake efficiencies. Nutrient uptake by phytoplankton generally follows Michaelis-Menten kinetics. Half saturation constants (K_s, the

nutrient concentration supporting half the maximum uptake rate) can be calculated using the Michaelis-Menten equation, and reflect the relative ability of phytoplankton to use low levels of nutrients (Dugdale 1967; Eppley *et al.* 1969; Lehman *et al.* 1975; Nelson and Dortch 1996). Nutrient concentrations < K_s could be considered limiting to phytoplankton growth. Lehman et al. (1975) summarised K_s values for marine phytoplankton from a number of studies, and reported K_s for NO_3 uptake that ranged between 0.1 and 3.8 µmol L^{-1}, and K_s for Si uptake between 0.8 and 3.5 µmol L^{-1}. Nelson and Dortch (1996) report K_s for Si uptake between 0.5 and 5.3 µmol L^{-1}. Si limitation is further complicated by the fact that diatoms can maintain close to maximum division rates even when Si uptake is < maximum, by decreasing frustule silica content (Leynaert et al. 2001; Nelson et al. 2001). However, studies have indicated that Si uptake does cease below certain low substrate concentrations, with most reported threshold concentrations < 0.5 µmol L^{-1} (Paasche 1973; Conway and Harrison 1977). For the purposes of this study, NO_x concentrations < 0.1 µmol L^{-1} were considered limiting to phytoplankton productivity since these concentrations are less than K_s values reported for an array of marine phytoplankton species similar to those expected to be found in the EGAB (Lehman et al. 1975). Si concentrations below the < 0.5 µmol L^{-1} threshold concentration were considered limiting to diatom productivity.

The absence of any strong associations with nutrient concentrations suggests there is little differentiation between waters masses in macro-nutrient concentrations. Concentrations of NO_x and Si in the EGAB were at all times above those that may be considered limiting to phytoplankton growth, and there was no indication of nutrient limitation of primary productivity in the EGAB. Despite this, productivity levels in the GAB warm pool can be up to an order of magnitude lower than productivities in

areas influenced by the upwelled water mass. So the question remains, what is the component of the upwelled water mass that promotes productivity that is not present in the GAB warm pool? Iron has been shown to limit growth in large parts of the ocean particularly high nutrient low chlorophyll (HNLC) regions such as the sub-arctic and equatorial Pacific, and the southern ocean around Antarctica (Martin and Fitzwater 1988; Martin *et al.* 1989; Martin 1990). Iron deficiency may explain the low levels of primary productivity associated with the HNLC waters of the GAB warm pool. The absence of direct measurements of dissolved iron concentrations in the different water masses makes it impossible to confidently draw conclusions. There are many other trace metals/vitamins/chelating agents whose presence or absence in the GAB warm pool relative to the upwelled water mass may promote/suppress primary productivity. Finer scale studies of spatial variations in macro and micro nutrient cycling in the water masses of the EGAB will provide a better understanding of the factors that promote high productivity in the upwelled water. Future studies should include analysis of iron concentrations/deposition rates, sedimentation rates, the influence of benthic-pelagic and ocean-atmospheric coupling on nutrient cycling, and potential nutrient limitation in phytoplankton.

The general spatial trends in productivity were similar in both models of productivity. The VGPM was chosen for this study since it provides a useful method for estimating primary productivity on large spatial scales. However, the VGPM was largely developed from measurements of productivity in the North Atlantic, hence the model of Platt *et al.* (1991) was run for selected stations in the EGAB to ground-truth the results of the VGPM. Variations between the two models may be attributed to the likelihood that some of the constants used in the VGPM, and the assumed relationship between temperature and assimilation number, are inappropriate for use in the shelf

waters of the EGAB. That the relationship breaks down at productivities below 200 mg C m^{-2} day^{-1} may relate to incident irradiances. Low irradiances, possibly exacerbated by cloud cover, may give rise to low and variable estimates of primary productivity, whereas higher, more consistent irradiances may result in more uniform estimates for both models. We believe the model of Platt *et al.* (1991) to be more accurate than the VGPM since it uses direct measures of P-I parameters from the EGAB in calculations. These parameters were only available for selected stations in the region, consequently the VGPM was required to provide estimates of productivity for the entire EGAB.

It should be noted that measurements taken during the sampling periods of this investigation represent snapshots in time, and may not represent conditions and productivity levels that are prevalent in the EGAB through the entire upwelling season. Comparisons made in this study are not representative of the entire years of 2005 and 2006 but reflect differences between short periods within each year. Primary productivity levels at a given time in the EGAB are likely to depend on which of the scenarios outlined in the conceptual model (Fig. 2.1) occurs in the region at the time of sampling, and where in the region the sampling is done. Temporal variations in meteorology may drive significant variations in the timing and intensity of mixing/stratification events, which could have an impact on the water masses present in the euphotic zone, and affect nutrient availability and primary productivity. The potential for large temporal variations in productivity levels both within and between upwelling seasons in the EGAB can be seen in Figure 2.9, with high levels of primary productivity found around SWKI (probably reflecting scenario 4 in the conceptual model) but not around SWEP in February/March 2005 (probably reflecting scenario 3 in the model, with high productivity in the bottom layer at the

base of the euphotic zone that is not showing up in the modelled results in Figure 2.9 which used surface chlorophyll concentrations to calculate primary productivity). The reverse pattern is observed in February/March 2006. Variations in the timing and intensity of mixing/stratification events (Popova *et al.* 2006) within upwelling seasons may affect the overall seasonal productivity of the EGAB region. Mixing appears to play a significant role in temporal variations in primary productivity in the EGAB. An investigation of the impact of temporal variations in mixing and stratification on total EGAB primary production will provide a greater understanding of the impact of longer term climatic variation on the EGAB ecosystem.

2.6. References

APHA-AWWA-WPCF (1998a). Method 4500-NO3-I. Standard methods for the examination of water and wastewater. L. S. Clesceri, A. E. Greenberg and A. D. Eaton. Washington, American Public Health Association**:** pp. 4-121.

APHA-AWWA-WPCF (1998b). Method 4500-PG. Standard methods for the examination of water and wastewater. L. S. Clesceri, A. E. Greenberg and A. D. Eaton. Washington, American Public Health Association**:** pp. 4-149.

APHA-AWWA-WPCF (1998c). Method 4500-SiO2-F. Standard methods for the examination of water and wastewater. L. S. Clesceri, A. E. Greenberg and A. D. Eaton. Washington, American Public Health Association**:** pp. 4-169.

Behrenfeld, M. J. and Falkowski, P. G. (1997a). A consumers guide to phytoplankton productivity models. *Limnology and Oceanography* **42**(7): 1479-1491.

Behrenfeld, M. J. and Falkowski, P. G. (1997b). Photosynthetic rates derived from satellite-based chlorophyll concentration. *Limnology and Oceanography* **42**(1): 1-20.

Brown, C. W., Esaias, W. E. and Thompson, A. M. (1995). Predicting phytoplankton composition from space - using the ratio of euphotic depth to mixed-layer depth: An evaluation. *Remote Sensing of Environment* **53**: 172-176.

Brown, P. C., Painting, S. J. and Cochraine, K. L. (1991). Estimates of phytoplankton and bacterial biomass and production in the northern and southern Benguela ecosystems. *South African Journal of Marine Science* **11**: 537-564.

Bye, J. A. T. (1972). Oceanic circulation south of Australia. Antarctic Oceanology 2. *Antarctic Research Series* **19**: 95-100.

Bye, J. A. T. (1983). The general circulation in a dissipative ocean basin with longshore wind stresses. *Journal of Physical Oceanography* **13**: 1553-1563.

Carr, M., Friedrichs, M. A. M., Schmeltz, M., Aita, M. N., Antoine, D., Arrigo, K. R., Asanuma, I., Aumont, O., Barber, R., Behrenfeld, M., Bidigare, R., Buitenhuis, E. T., Campbell, J., Ciotti, A., Dierssen, H., Dowell, M., Dunne, J., Esaias, W., Gentili, B., Gregg, W., Groom, S., Hoepffner, N., Ishizaka, J., Kameda, T., Le Quere, C., Lohrenz, S., Marra, J., Melin, F., Moore, K., Morel, A., Reddy, T. E., Ryan, J., Scardi, M., Smyth, T., Turpie, K., Tilstone, G., Waters, K. and Yamanaka, Y. (2006). A comparison of global estimates of marine primary production from ocean color. *Deep Sea Research 2* **53**: 741-770.

Conway, H. L. and Harrison, P. J. (1977). Marine diatoms grown in chemostats under silicate or ammonium limitation. IV. Transient response of *Chaetoceros deblis, Skeletonema costatum,* and *Thalassiosira gravida* to a single addition of the limiting nutrient. *Marine Biology* **43**: 33-43.

Daneri, G., Dellarossa, V., Quinones, R., Jacob, B., Montero, P. and Ulloa, O. (2000). Primary production and community respiration in the Humboldt Current System off Chile and associated oceanic areas. *Marine Ecology Progress Series* **197**: 41-49.

Downing, J. A. (1997). Marine nitrogen:phosphorus stoichiometry and the global N:P cycle. *Biogeochemistry* **37**: 237-252.

Dugdale, R. C. (1967). Nutrient limitation and the sea: Dynamics, identification and significance. *Limnology and Oceanography* **12**: 685-695.

Eppley, R. W., Rogers, J. N. and McCarthy, J. J. (1969). Half saturation constants for uptake of nitrate and ammonium by marine phytoplankton. *Limnology and Oceanography* **14**: 912-920.

Estevez-Blanco, P., Cermeno, P., Espineira, M., and Fernandez, E. (2006). Phytoplankton photosynthetic efficiency and primary production rates estimated from fast repetition rate fluorometry at coastal embayments affected by upwelling (Rias Biaxas, NW of Spain). *Journal of Plankton Research* **28**: 1153-1165.

Ganf, G. G. and Horne, A. J. (1975). Diurnal stratification, photosynthesis and nitrogen-fixation in a shallow, equatorial lake (Lake George, Uganda). *Freshwater Biology* **5**: 13-39.

Hanson, C. E., Pattiaratchi, C. B. and Waite, A. M. (2005). Sporadic upwelling on a downwelling coast: Phytoplankton responses to spatially variable nutrient dynamics off the Gascoyne region of Western Australia. *Continental Shelf Research* **25**: 1561-1582.

Hanson, C. E., Pesant, S., Waite, A. M. and Pattiaratchi, C. B. (2007). Assessing the magnitude and significance of deep chlorophyll maxima of the coastal eastern Indian Ocean. *Deep Sea Research 2* **54**: 884-901.

Harris, G., Nilsson, C., Clementson, L. and Thomas, D. (1987). The water masses of the east coast of Tasmania: seasonal and interannual variability and the influence on phytoplankton biomass and productivity. *Australian Journal of Marine and Freshwater Research* **38**: 569-590.

Herzfeld, M. (1997). The annual cycle of sea surface temperature in the Great Australian Bight. *Progress in Oceanography* **39**: 1-27.

Herzfeld, M. and Tomczak, M. (1997). Numerical modelling of sea surface temperature and circulation in the Great Australian Bight. *Progress in Oceanography* **39**: 29-78.

Herzfeld, M. and Tomczak, M. (1999). Bottom-driven upwelling generated by eastern intensification in closed and semi-closed basins with a sloping bottom. *Marine and Freshwater Research* **50**: 613-627.

Kampf, J., Doubel, M., Griffin, D. A., Matthews, R. and Ward, T. M. (2004). Evidence of a large seasonal coastal upwelling system along the southern shelf of Australia. *Geophysical Research Letters* **31**(L09310): doi:10.1029/2003GL019221.

Kara, A. B., Rochford, P. A. and Hurlburt, H. E. (2000). An optimal definition for ocean mixed layer depth. *Journal of Geophysical Research* **105**(C7): 16,803-16,821.

Keller, A. A. (1988). An empirical model of primary productivity (^{14}C) using mesocosm data along a nutrient gradient. *Journal of Plankton Research* **10**(4): 813-834.

Kirk, J. T. O. (1994). Light and photosynthesis in aquatic ecosystems. Cambridge, Cambridge University Press.

Korner, S. and Nicklisch, A. (2002). Allelopathic growth inhibition of selected phytoplankton species by submerged macrophytes. *Journal of Phycology* **38**: 862-871.

Kromkamp, J.C., Dijkman, N.A., Peene, J., Simis, S.G.H., and Gons, H.J. (2008). Estimating phytoplankton primary production in Lake Ijsselmeer (The Netherlands) using variable fluorescence (PAM-FRRF) and C-uptake techniques. *European Journal of Phycology* **43**: 327-344.

Lehman, J. T., Botkin, D. B. and Likens, G. E. (1975). The assumptions and rationales of a computer model of phytoplankton population dynamics. *Limnology and Oceanography* **20**(3): 343-364.

Leynaert, A., Treguer, P., Lancelot, C. and Rodier, M. (2001). Silicon limitation of biogenic silica production in the Equatorial Pacific. *Deep Sea Research Part I* **48**: 639-660.

Longhurst, A., Sathyendranath, S., Platt, T. and Caverhill, C. (1995). An estimate of global primary production in the ocean from satellite radiometer data. *Journal of Plankton Research* **17**(6): 1245-1271.

Maranon, E., Behrenfeld, M. J., Gonzalez, N., Mourino, B. and Zubkov, M. V. (2003). High variability of primary production in oligotrophic waters of the Atlantic ocean: uncoupling from phytoplankton biomass and size structure. *Marine Ecology Progress Series* **257**: 1-11.

Martin, J. H. (1990). Glacial-interglacial carbon dioxide change: The iron hypothesis. *Paleoceanography* **5**: 1-13.

Martin, J. H. and Fitzwater, S. E. (1988). Iron deficiency limits phytoplankton growthin the north-east Pacific subarctic. *Nature* **331**: 341-343.

Martin, J. H., Gordon, R. M., Fitzwater, S. and Broenkow, W. W. (1989). VERTEX: phytoplankton/iron studies in the Gulf of Alaska. *Deep Sea Research* **36**: 649-680.

McClatchie, S., Middleton, J. F. and Ward, T. M. (2006). Water mass analysis and alongshore variation in upwelling intensity in the eastern Great Australian Bight. *Journal of Geophysical Research* **111**(C08007): doi:10.1029/2004JC002699.

McCune, B. and Mefford, M. J. (1999). PC-ORD. Multivariate Analysis of Ecological Data, Version 5., MjM Software Design, Gleneden Beach, Oregon, USA.

Middleton, J. F. (2000). Wind forced upwelling: the role of the surface mixed layer. *Journal of Physical Oceanography* **30**: 745-763.

Middleton, J. F. and Bye, J. A. T. (2007). A review of the shelf slope circulation along Australia's southern shelves: Cape Leeuwin to Portland. *Progress in Oceanography* **75**: 1-41.

Middleton, J. F. and Cirano, M. (2002). A northern boundary current along Australia's southern shelves: the Flinders current. *Journal of Geophysical Research-Oceans* **107**(C9): 3129-3143.

Middleton, J. F. and Platov, G. (2003). The mean summertime circulation along Australia's southern shelves: a numerical study. *Journal of Physical Oceanography* **33**(11): 2270-2287.

Moore, J. K. and Abbott, M. R. (2000). Phytoplankton chlorophyll distributions and primary production in the Southern Ocean. *Journal of Geophysical Research* **105**: 28,709-28,722.

Motoda, S., Kawamura, T. and Taniguchi, A. (1978). Differences in productivities between the Great Australian Bight and the Gulf of Carpentaria, Australia, in Summer. *Marine Biology* **46**: 93-99.

Nelson, D. M., Brzezinski, M. A., Sigmon, D. E. and Franck, V. M. (2001). A seasonal progression of Si limitation in the Pacific sector of the Southern Ocean. *Deep Sea Research Part II* **48**: 3973-3395.

Nelson, D. M. and Dortch, Q. (1996). Silicic acid depletion and silicon limitation in the plume of the Mississippi River: evidence from kinetic studies in spring and summer. *Marine Ecology Progress Series* **136**: 163-178.

Paasche, E. (1973). Silicon and the ecology of marine diatoms II. Silicate-uptake kinetics of five diatom species. *Marine Biology* **19**: 262-269.

Parsons, T. R., Maita, Y. and Lalli, C. M. (1984). A Manual of Chemical and Biological Methods for Seawater Analysis. Oxford, Pergamon Press Ltd.

Patterson, J. C. (1991). Modelling the effects of motion on primary production in the mixed layer of lakes. *Aquatic Sciences* **53**: 218-238.

Platt, T., Bird, D. F. and Sathyendranath, S. (1991). Critical depth and marine primary production. *Proceedings of the Royal Society of London B* **246**: 205-217.

Platt, T., Sathyendranath, S. and Ravindran, P. (1990). Primary production by phytoplakton: analytic solutions for daily rates per unit area of water surface. *Proceedings of the Royal Society of London B* **241**: 101-111.

Popova, E. E., Coward, A. C., Nurser, G. A., de Cuevas, B., Fasham, M. J. R. and Anderson, T. R. (2006). Mechanisms controlling primary and new production in a global ecosystem model - Part 1: Validation of the biological simulation. *Ocean Science* **2**: 249-266.

Ralph, P. J. and Gademann, R. (2005). Rapid light curves: A powerful tool to assess photosynthetic activity. *Aquatic Botany* **82**: 222-237.

Ryther, J. H. (1969). Photosynthesis and Fish Production in the Sea. *Science* **166**: 72-76.

Talling, J. F. and Driver, D. (1963). Some problems in the estimation of chlorophyll *a* in phytoplankton. Conference on Primary Productivity Measurement, Marine and Freshwater., U.S. Atomic Energy Commission.

Ward, T. M., McLeay, L. J., Dimmlich, W. F., Rogers, P. J., McClatchie, S., Matthews, R., Kampf, J. and Van Ruth, P. D. (2006). Pelagic ecology of a northern boundary current system: effects of upwelling on the production and distribution of sardine (*Sardinops sagax*), anchovy (*Engraulis australis*) and southern bluefin tuna (*Thunnus maccoyii*) in the Great Australian Bight. *Fisheries Oceanography* **15**(3): 191-207.

Young, J., Nishida, T. and Stanley, C. (2001). A preliminary survey of the summer hydrography and plankton biomass of the eastern Great Australian Bight, Australia. Southern Bluefin Tuna Recruitment Monitoring and Tagging Program. Report of the Eleventh Workshop. Hobart, CSIRO.

2.7. Tables

Table 2.1. Spatial variation in euphotic depth and mixed layer depth in the EGAB. Kd = coefficient of downwelled irradiance (m^{-1}), R^2 = regression coefficient for the relationship between irradiance and depth, Zeu = euphotic depth (m), MLD = mixed layer depth (m). Values are mean ± standard error, n = 3. Regions outlined in Figure 2.2.

		2005				2006			
		K_d	R^2	Z_{eu}	MLD	K_d	R^2	Z_{eu}	MLD
Nearshore	East	0.08 (± 0.004)	0.99	57.5 (± 2.7)	37.0 (±0.4)	0.08 (± 0.01)	0.99	57.5 (± 6.1)	33.8 (±2.4)
	Central	0.11 (± 0.002)	0.99	41.6 (± 0.8)	25.7 (±1.5)	0.14 (± 0.02)	0.99	35.4 (± 7.3)	16.3 (±6.8)
	West	0.09 (± 0.1)	0.99	50.1 (± 5.4)	23.2 (±1.8)	-	-	-	29.6 (±2.7)
	Far West	0.12 (± 0.1)	0.99	40.5 (± 5.2)	-	0.11 (± 0.03)	0.99	45.6 (± 9.2)	-
Offshore	East	0.05 (± 0.004)	0.99	100.9 (± 8.8)	53.8 (±0.4)	0.05 (± 0.01)	0.99	88.9 (± 11.6)	47.8 (±2.8)
	Central	0.04 (± 0.002)	0.99	114.5 (± 5.1)	62.3 (±2.5)	0.05 (± 0.001)	0.99	100.9 (± 3.3)	54.4 (±2.9)
	West	0.04 (± 0.005)	0.99	105.9 (± 13.0)	59.8 (±0.9)	0.06 (± 0.01)	0.99	79.7 (± 8.6)	54.4 (±6.5)

Table 2.2. Spatial variation in nutrient concentrations in the EGAB. P = phosphate, NO_x = nitrite/nitrate, Si = silica. Concentrations μmol L^{-1} ± standard error, n = 3. Regions outlined in Figure 2.2.

		2005						2006					
		Surface layer			Bottom layer			Surface layer			Bottom layer		
		FRP	NO_x	Si	FRP	NO_x	Si	FRP	NO_x	Si	FRP	NO_x	Si
Nearshore	East	0.2 (± 0.1)	1.3 (± 0.9)	4.6 (± 3.8)	0.5 (± 0.3)	1.8 (± 1.2)	1.1 (± 0.2)	0.2 (± 0.05)	0.6 (± 0.1)	1.7 (± 0.8)	0.4 (± 0.02)	2.6 (± 0.4)	1.5 (± 0.2)
	Central	0.2 (± 0.1)	0.4 (± 0.1)	3.5 (± 1.0)	0.3 (± 0.1)	0.5 (± 0.2)	4.2 (± 3.4)	0.2 (± 0.04)	0.6 (± 0.1)	11.1 (± 5.4)	0.3 (± 0.1)	1.4 (± 0.6)	1.7 (± 0.4)
	West	0.6 (± 0.1)	1.2 (± 0.4)	5.1 (± 2.6)	0.4 (± 0.04)	1.0 (± 0.3)	2.7 (± 0.2)						
	Far West	0.3 (± 0.05)	1.2 (± 0.1)	29.4 (± 6.3)	0.6 (± 0.1)	0.7 (± 0.1)	4.0 (± 0.3)						
Offshore	East	0.1 (± 0.1)	0.9 (± 0.5)	2.2 (± 1.6)	0.2 (± 0.05)	1.8 (± 1.0)	1.1 (± 0.4)	0.1 (± 0.06)	0.5 (± 0.4)	7.0 (± 0.3)	0.2 (± 0.1)	1.5 (± 1.4)	1.4 (± 0.0)
	Central	0.4 (± 0.1)	0.6 (± 0.1)	1.3 (± 0.6)	0.3 (± 0.1)	1.4 (± 1.0)	1.7 (± 0.6)	0.1 (± 0.02)	0.4 (± 0.1)	7.9 (± 1.4)	0.2 (± 0.1)	1.7 (± 1.0)	1.5 (± 1.0)
	West	0.8 ± (0.7)	1.0 (± 0.8)	9.1 (± 6.3)	0.3 (± 0.03)	0.6 (± 0.05)	6.4 (± 3.3)						

Table 2.3. Spatial variation in VGPM modelled primary productivity in different sections of the water column in the EGAB. SML = productivity in the surface mixed layer. Productivity is reported in units of mg C m^{-2} day^{-1} ± standard error, n = 3. Regions outlined in Figure 2.2.

		2005		2006	
		Euphotic zone	SML	Euphotic zone	SML
Nearshore	East	719.2 (±243.5)	467.1 (±253.0)	300.9 (±25.4)	198.6 (±17.9)
	Central	127.6 (±79.0)	78.9 (±50.2)	529.1 (±319.9)	214.5 (±111.6)
	West	365.5 (±33.5)	148.3 (±10.4)		
Offshore	East	228.2 (±48.0)	125.0 (±23.6)	162.1 (±59.1)	74.3 (±30.7)
	Central	460.4 (±144.1)	245.8 (±72.6)	141.2 (±16.2)	75.9 (±10.7)
	West	434.9 (±35.8)	249.2 (±15.3)	169.5 (±123.5)	96.0 (±60.7)

Table 2.4. Photosynthetic parameters measured in nearshore regions using Phyto-PAM, February/March 2006. α = photosynthetic efficiency (mg C (mg chl *a*)$^{-1}$ hr^{-1} (µmol m^{-2} s^{-1})$^{-1}$), I_k = the irradiance corresponding to the onset of light saturation of photosynthesis (µmol m^{-2} s^{-1}), P^B_{max} = maximum specific photosynthetic rate (mg C (mg chl *a*)$^{-1}$ hr^{-1}). Values are means ± standard error, n = 3. Regions outlined in Figure 2.2.

Region/Depth		α	I_k	P^B_{max}
east	Surface	0.014 (±0.001)	412.1 (±82.4)	5.7 (±0.5)
	DCM	0.012 (±0.001)	229.6 (±49.4)	2.7 (±0.4)
central	Surface	0.014 (±0.001)	308.7 (±17.8)	4.3 (±0.3)
	DCM	0.016 (±0.001)	237.1 (±47.9)	3.5 (±0.6)

Table 2.5. Spatial variation in primary productivity modelled according to Platt *et al.* (1991) in different sections of the water column in the EGAB. SML = productivity in the surface mixed layer. Productivity is reported in units of mg C m^{-2} day^{-1} ± standard error, n = 3. Regions outlined in Figure 2.2.

		2005		2006	
		Euphotic zone	SML	Euphotic zone	SML
Nearshore	East	2769.2 (±1228.1)	1351.6 (±549.6)	247.8 (±107.1)	213.3 (±87.1)
	Central	471.9 (±28.4)	428.3 (±41.5)	1356.3 (±815.6)	693.0 (±327.1)
	West	401.3 (±151.9)	165.3 (±81.6)	-	-
Offshore	East	1403.8 (±352.3)	958.6.3 (±205.7)	519.9 (±209.5)	372.9 (±129.1)
	Central	1100.0 (±300.4)	788.0 (±183.0)	747.2 (±51.2)	559.7 (±49.1)
	West	1017.3 (±211.7)	739.9 (±104.0)	1067.0 (±127.0)	874.8 (±91.8)

2.8. Figures

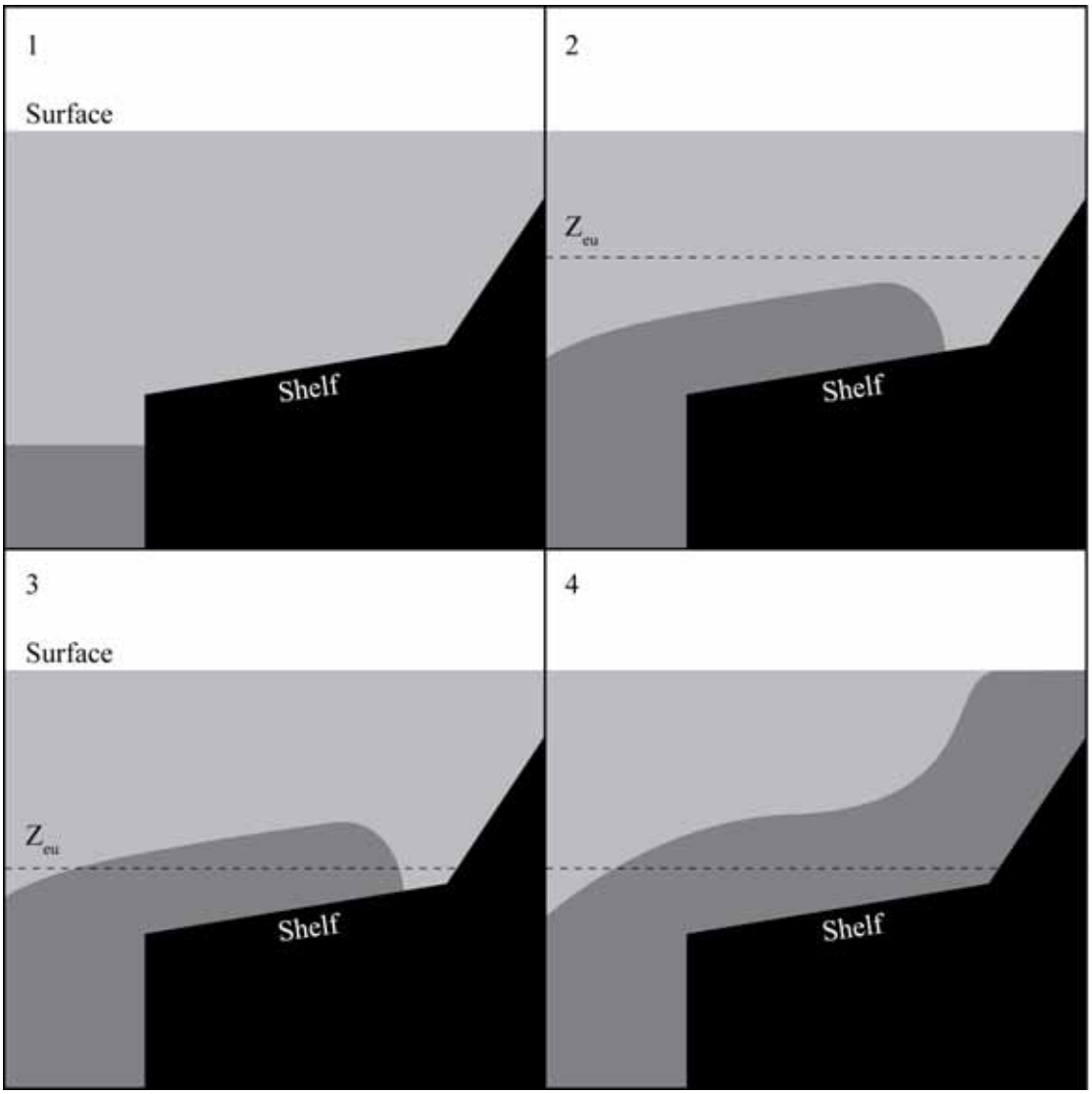

Figure 2.1. Conceptual model of water mass formation and nutrient enrichment in the upwelling region of the EGAB. The black section represents the land mass encompassing the continental slope, the continental shelf and the shore. The dark grey section represents the upwelled water mass. The light grey section represents overlying warmer water. Dashed line indicates euphotic depth (Z_{eu}). Scenarios are described in the text.

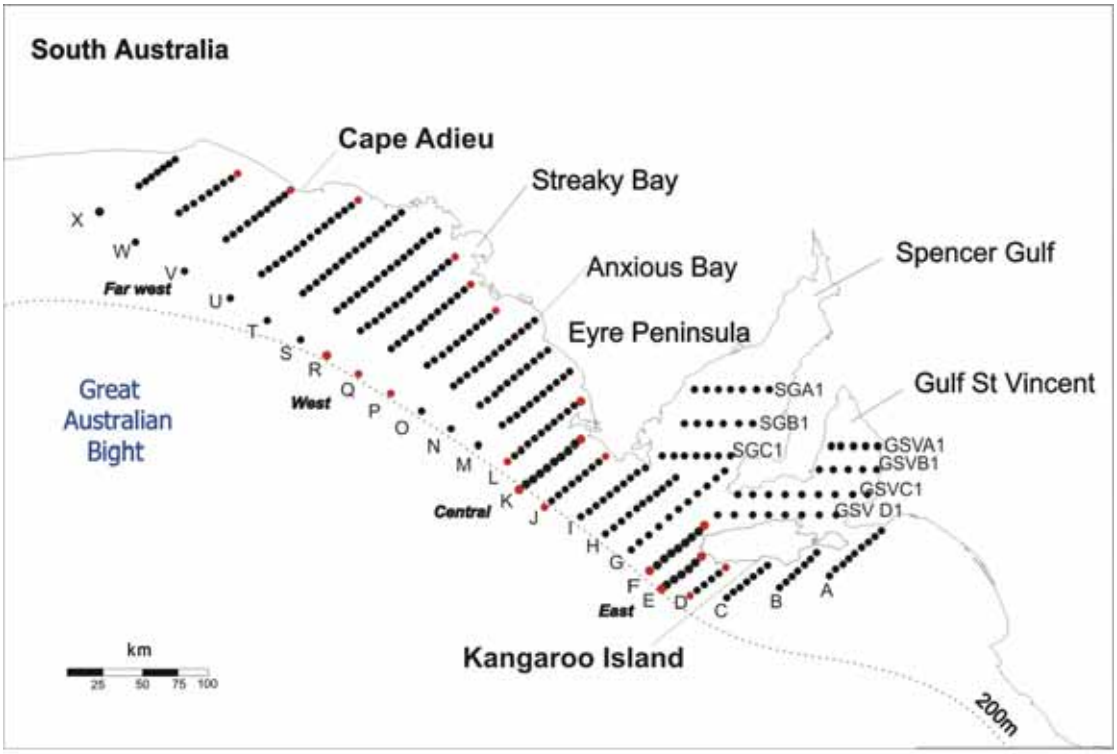

Figure 2.2. Sampling station locations. Black circles represent CTD and extracted chlorophyll sampling stations. Red circles represent stations that were also sampled for nutrients. Different regions in the EGAB denoted east, central, west, and far west. Dashed line represents the 200 m isobath.

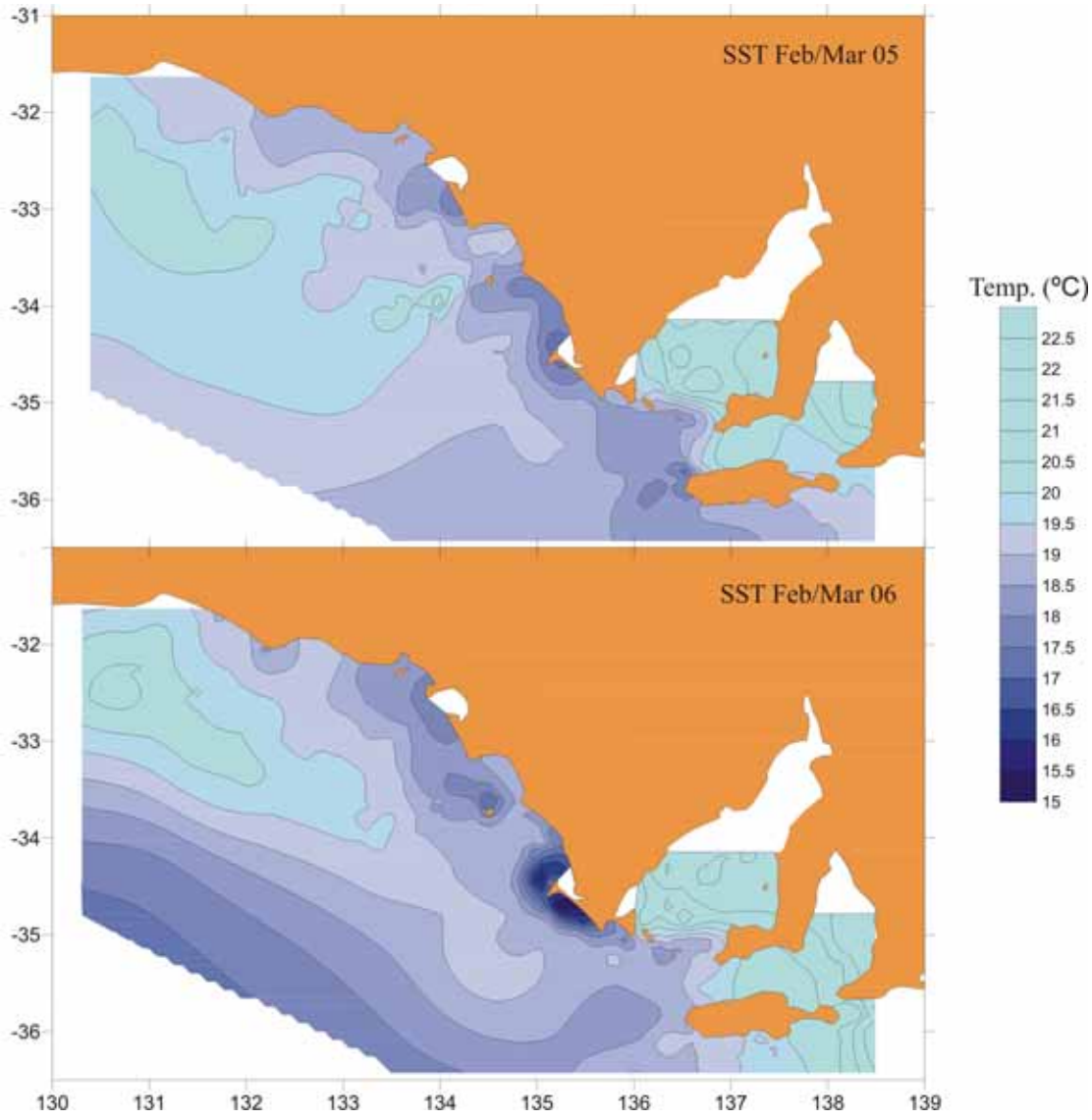

Figure 2.3. Spatial variation in CTD measured SST in the EGAB in February/March 2005 (top) and 2006 (bottom).

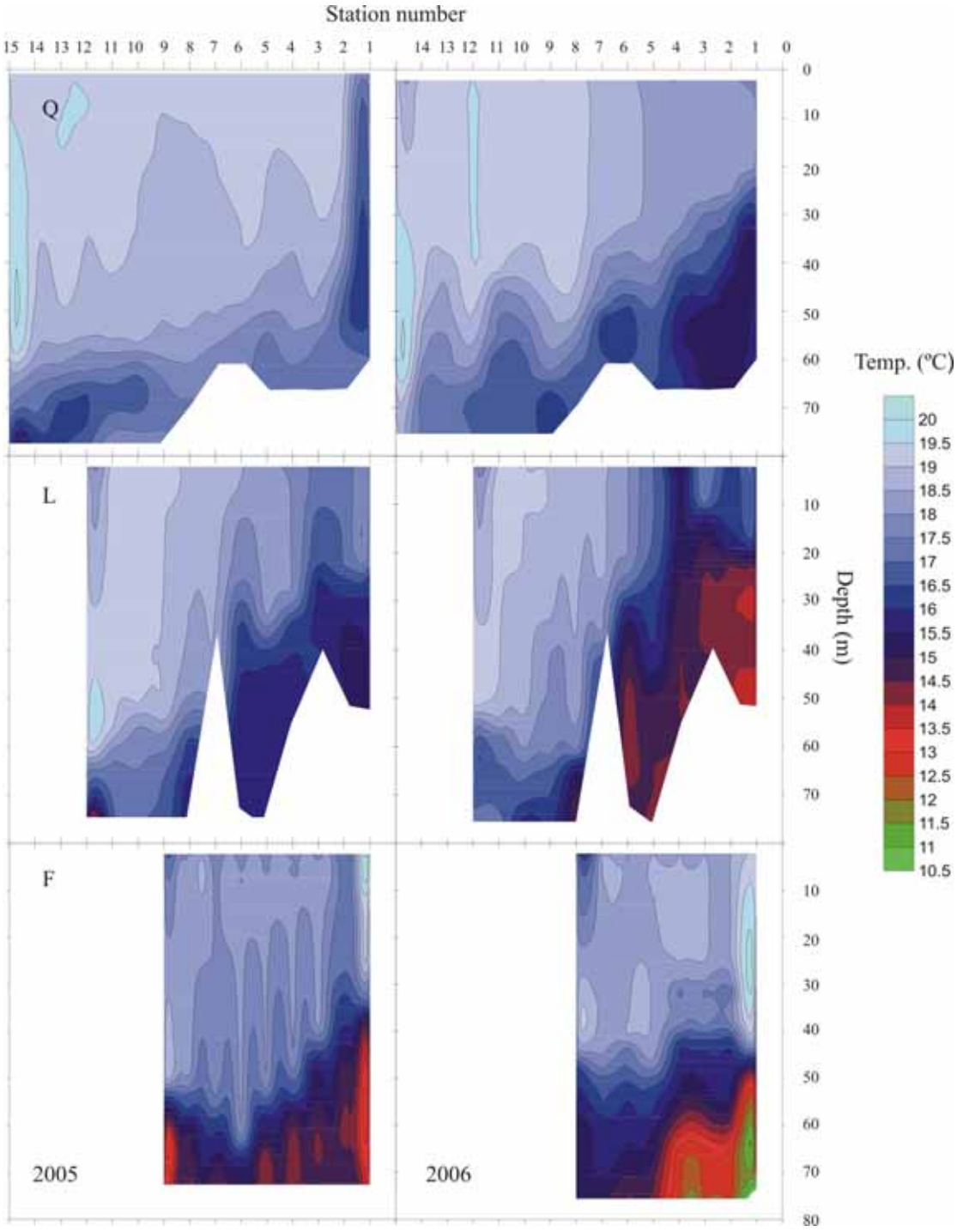

Figure 2.4. CTD temperature depth profiles for cross-shelf transects in the EGAB in February/March 2005 (left) and 2006 (right). Transects in the figure are transect F (east, bottom), transect L (central, middle), and transect Q, (west, top).

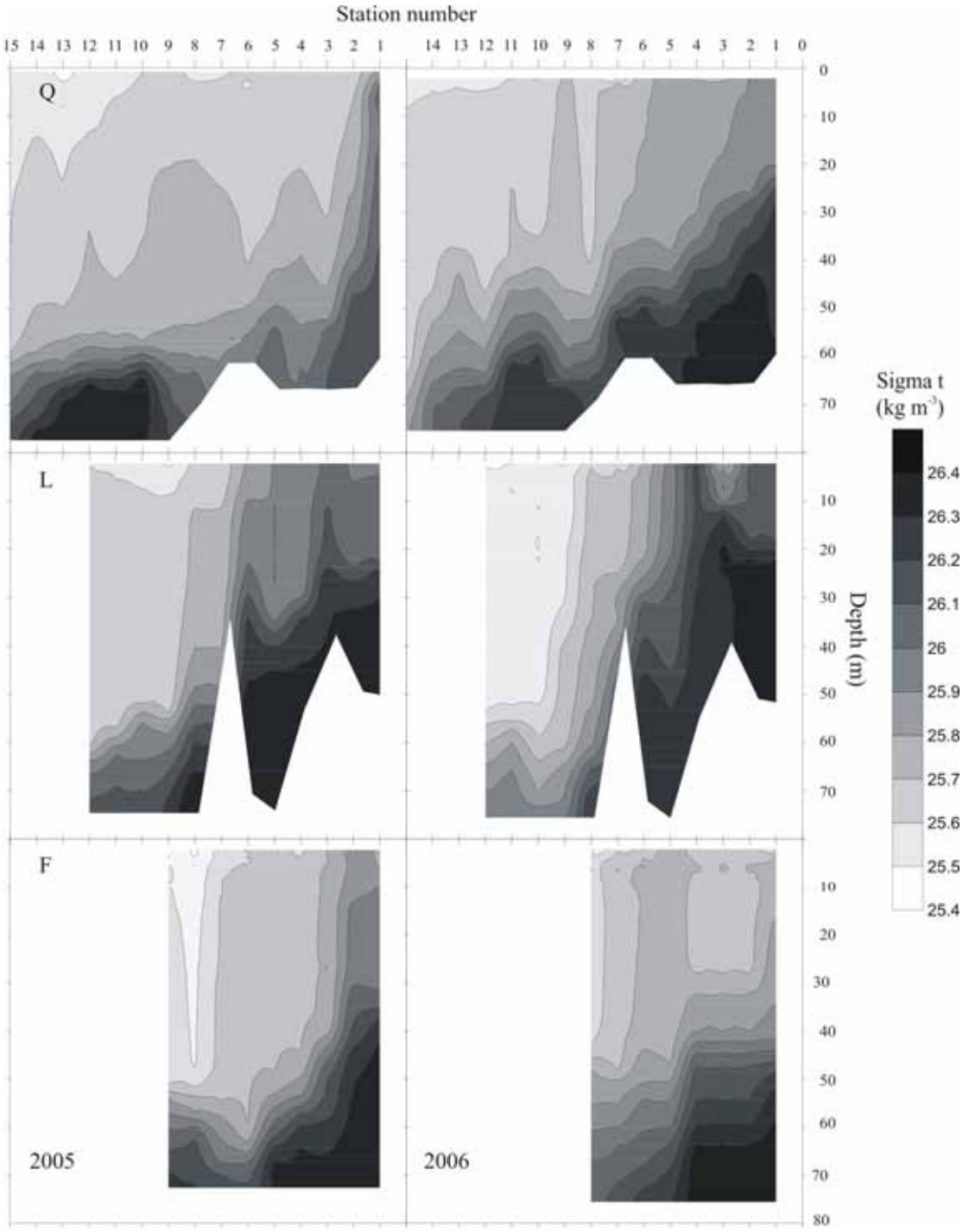

Figure 2.5. CTD density depth profiles for cross-shelf transects in the EGAB in February/March 2005 (left) and 2006 (right). Transects in the figure are transect F (east, bottom), transect L (central, middle), and transect Q, (west, top).

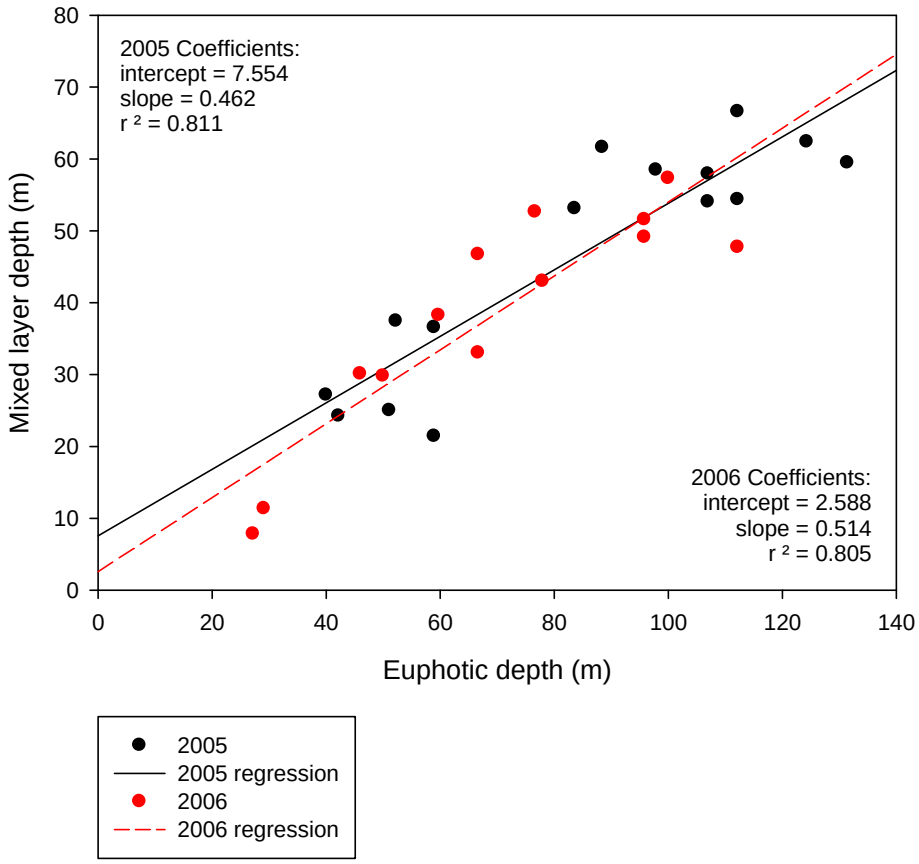

Figure 2.6. Relationship between mixed layer depth and euphotic depth at selected stations in the EGAB. Data presented were derived from the stations indicated by red circles in Figure 2.1. The slope of the regressions indicates the proportion of the euphotic zone that is made up by the surface mixed layer.

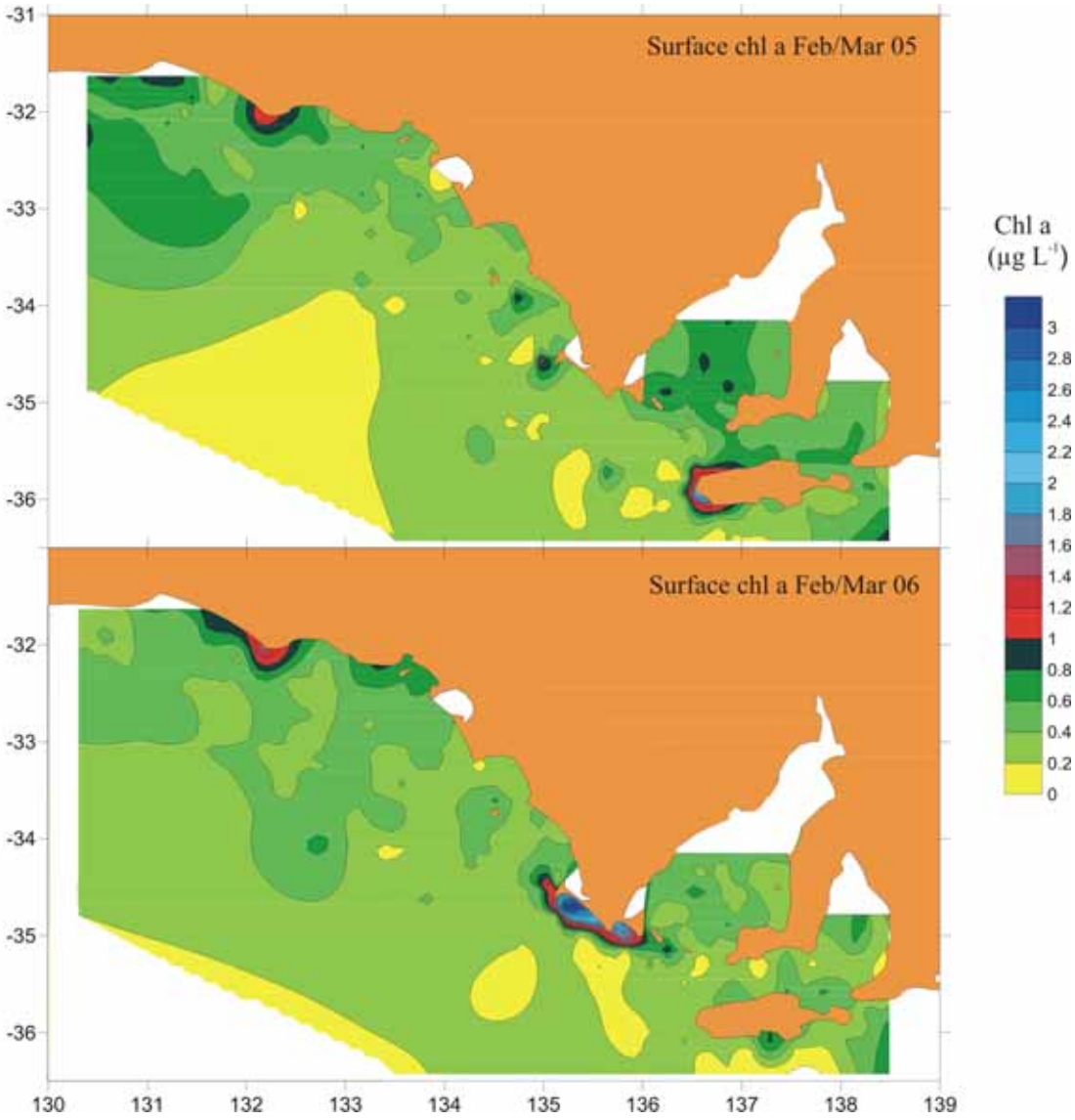

Figure 2.7. Spatial variation in surface extracted chlorophyll *a* concentrations in the EGAB in February/March 2005 (top) and 2006 (bottom).

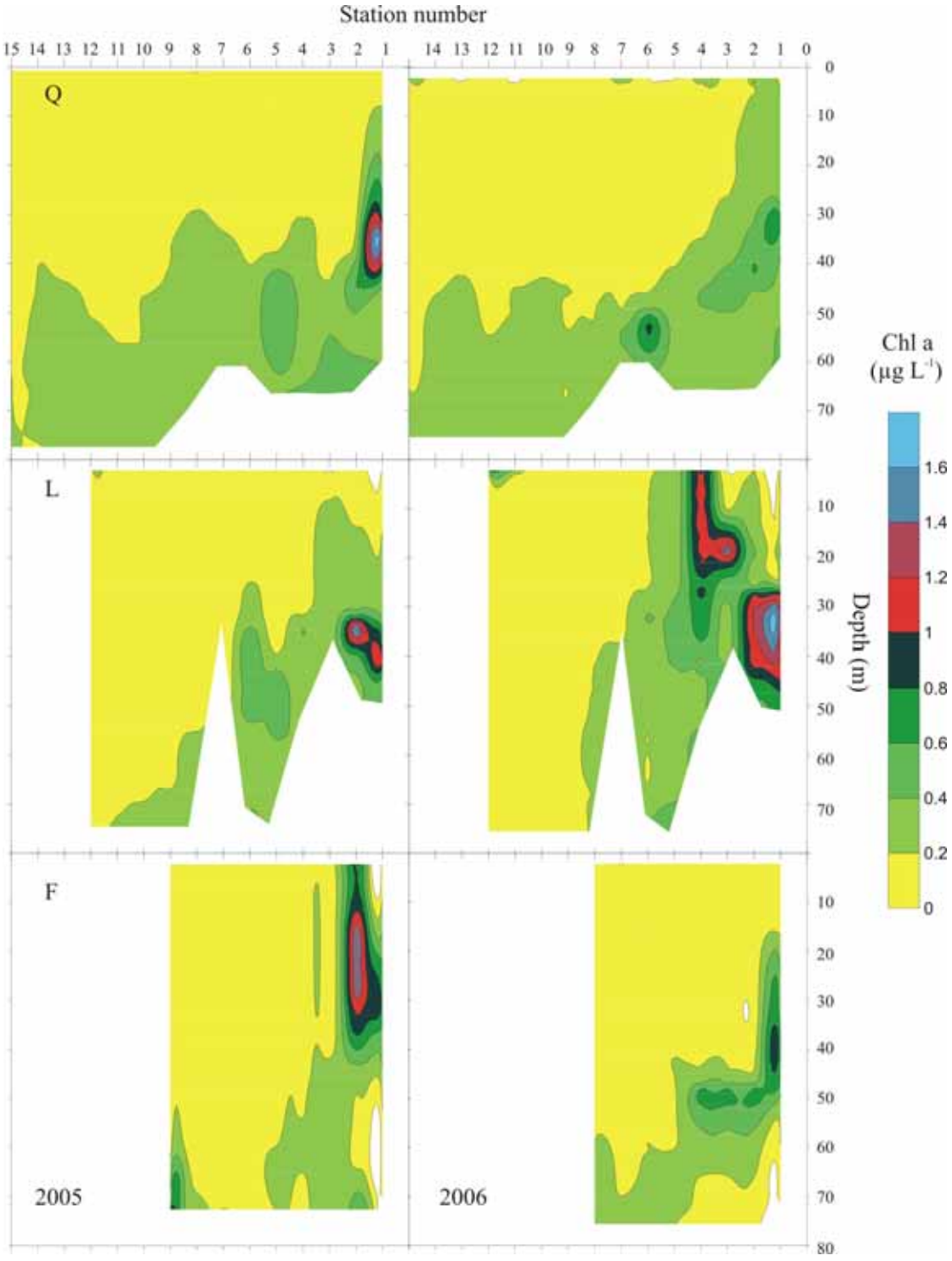

Figure 2.8. CTD fluorescence depth profiles for cross-shelf transects in the EGAB in February/March 2005 (left) and 2006 (right). Transects in the figure are transect F (east, bottom), transect L (central, middle), and transect Q, (west, top).

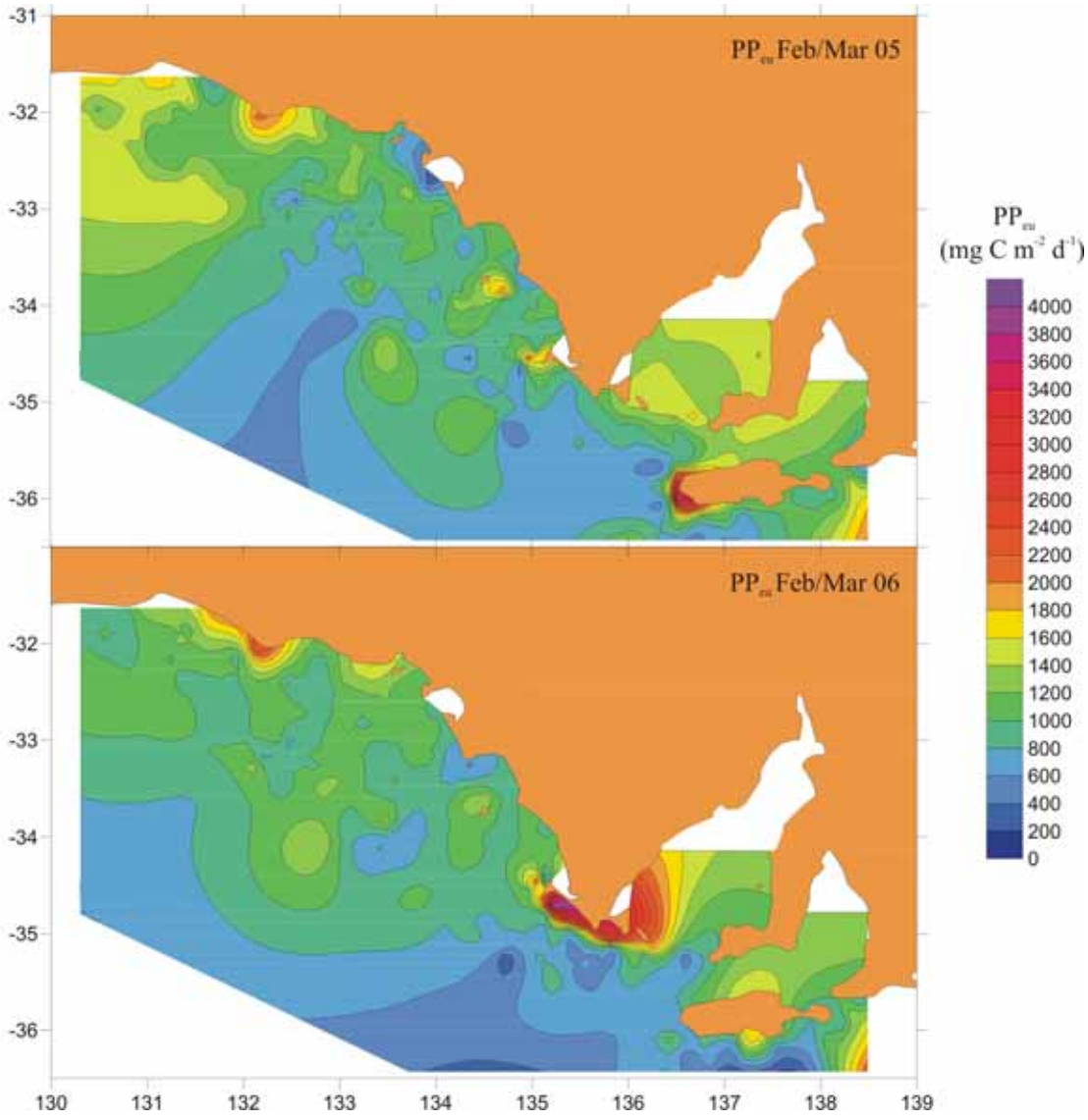

Figure 2.9. Spatial variation in VGPM modelled primary productivity in the EGAB in February/March 2005 (top) and 2006 (bottom).

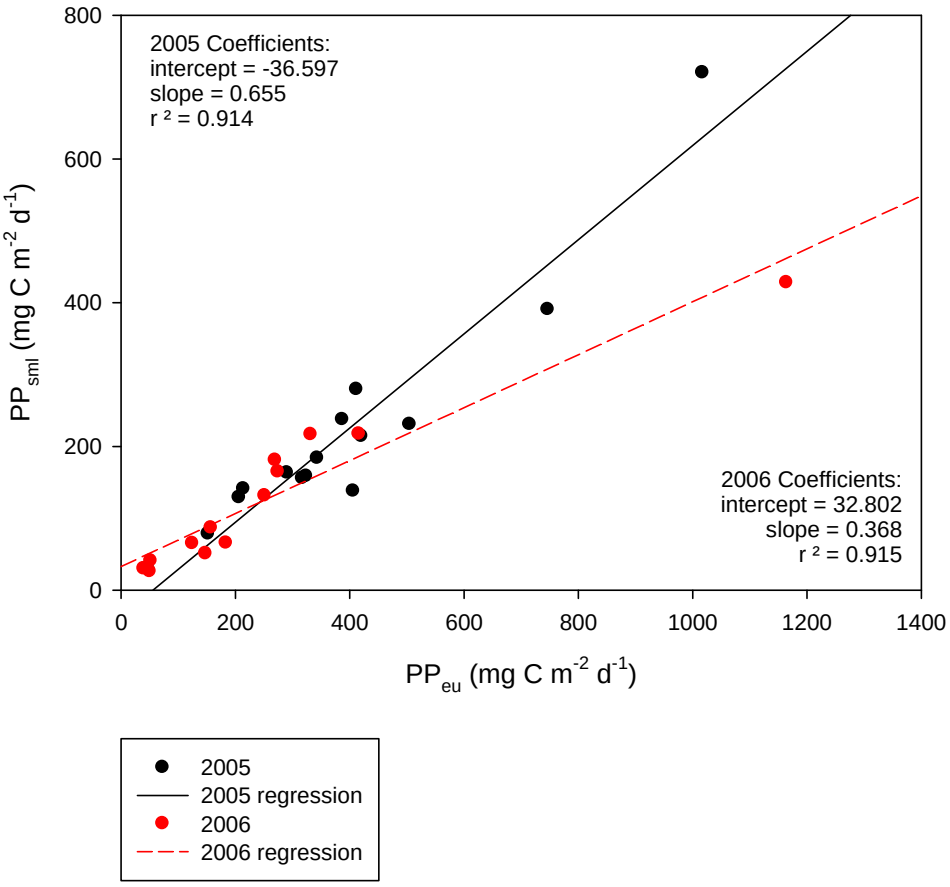

Figure 2.10. Relationship between VGPM modelled primary productivity in the surface mixed layer and total primary productivity in the euphotic zone, calculated using CTD fluorescence. Data presented were derived from the stations indicated by red circles in Figure 2.1. The slope of the regressions indicates the proportion of total productivity that is made up by productivity in the surface mixed layer.

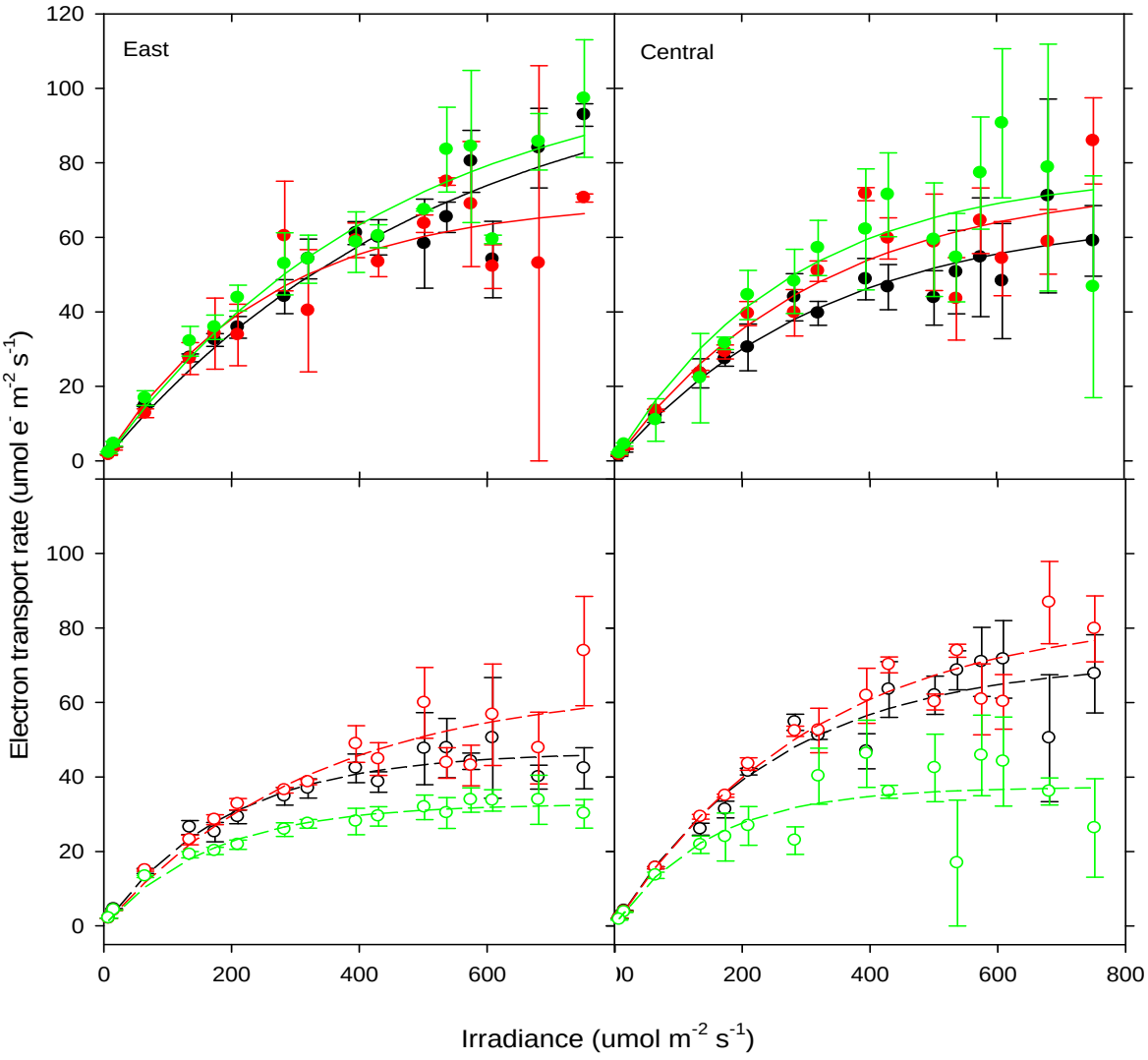

Figure 2.11. Electron transport rates (ETR) measured in the EGAB in February/March 2006 using Phyto-PAM. Circles represent mean ETR ± standard error (n = 3), curves modelled according to Ralph and Gademann (2005). Closed circles = surface samples, open circles = samples from the DCM. Regions outlined in Figure 2.2.

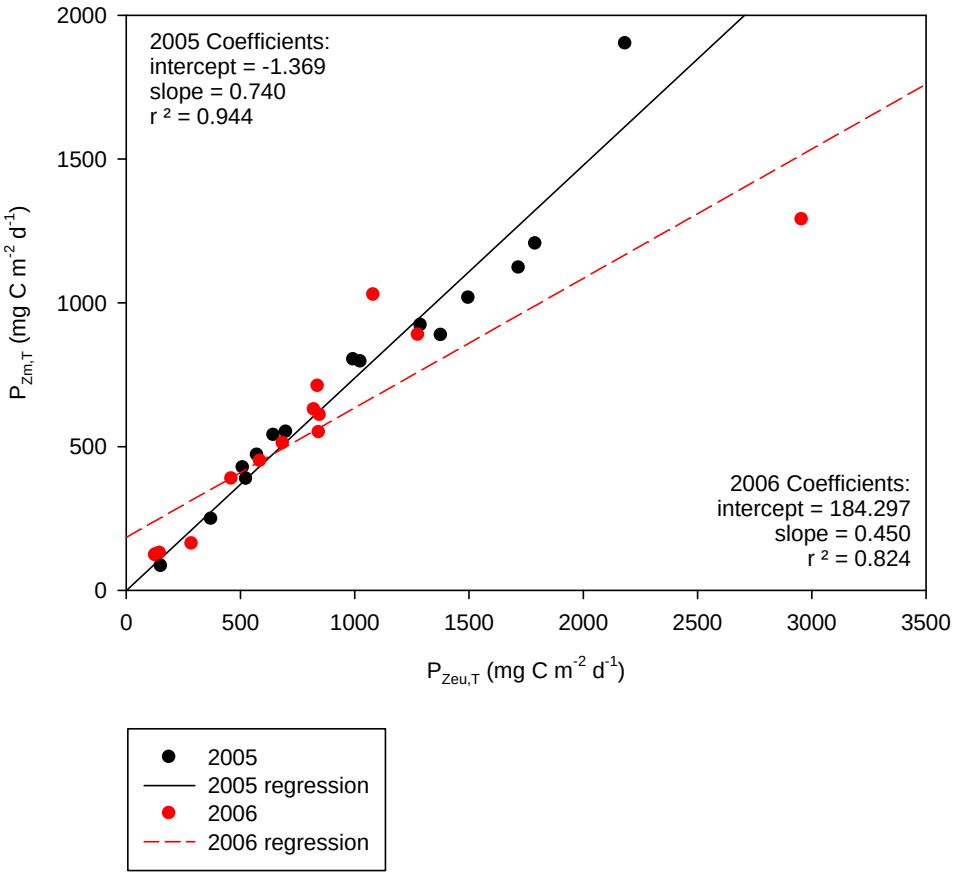

Figure 2.12. Relationship between primary productivity, in the surface mixed layer and total primary productivity in the euphotic zone, modelled according to Platt *et al.* (1991) using CTD fluorescence. Data presented were derived from the stations indicated by red circles in Figure 2.1. The slope of the regressions indicates the proportion of total productivity that is made up by productivity in the surface mixed layer.

3. The Influence of Mixing on Primary Productivity: A Unique Application of Classical Critical Depth Theory

3.1. Abstract

Mixing and primary productivity was examined in upwelling influenced nearshore waters off south western Eyre Peninsula (SWEP) in the eastern Great Australian Bight (EGAB), the economically and ecologically important shelf region off southern Australia that forms part of the Southern and Indian oceans. Mixing/stratification in the region was highly temporally variable with a unique upwelling circulation in summer/autumn (November-April), and downwelling through winter/spring (May-September). Highest productivity was associated with upwelled/stratified water (up to 2958 mg C m^{-2} d^{-1}), with low productivity during periods of downwelling and mixing (~300-550 mg C m^{-2} d^{-1}), yet no major variations in macro-nutrient concentrations were detected between upwelling and downwelling events (silica >1μmol L^{-1}, nitrate/nitrite >0.4μmol L^{-1}, phosphate >0.1μmol L^{-1}). We hypothesise that upwelling enriches the region with micro-nutrients. High productivity off SWEP appears to be driven by a shallowing of mixed layer depth due to the injection of upwelled waters above Z_{cr}. Low productivity follows the suppression of enrichment during downwelling/mixing events, and is exacerbated in winter/spring by low irradiances and short daylengths.

3.2. Introduction

Mixing processes such as upwelling and vertical mixing are generally thought to promote primary productivity by bringing nutrients from great depths into well lit surface waters. Indeed, areas influenced by upwelling are some of the most productive in the global ocean. Mixing processes, however, also influence the overall light conditions encountered by phytoplankton, and may affect net primary productivity in the water column by influencing the balance between community photosynthesis and respiration.

Sverdrup (1953) examined the balance between phytoplankton photosynthesis and respiration. In a well mixed water column with an even distribution of phytoplankton, he suggested that photosynthesis decreases logarithmically with depth, in accordance with the logarithmic decrease in light intensity, while respiration remains independent of depth due to the even distribution of the phytoplankton in the mixed layer. Sverdrup defined the depth at which photosynthesis equals respiration as the compensation depth (Z_c). The irradiance at which this occurred was termed the compensation irradiance (I_c). He suggested that an increase in the phytoplankton population can only occur at depths where total photosynthetic gains in carbon exceed total losses due to respiration, and observed that "This implies that there must exist a critical depth (Z_{cr}) such that blooming can occur only if the depth of the mixed layer is less than the critical value". The value of Z_{cr} depends on the time-averaged amount of effective incoming radiation (I_e, the total incoming irradiance (I_o), corrected for a fraction lost by reflection from the sea surface and wavelengths absorbed in the upper few metres of the water column (~82%)), the attenuation of light with depth (as indicated by the attenuation coefficient, K), and I_c, according to:

$$Z_{cr} = (\overline{I_e} / kI_c)(1 - e^{-kZ_{cr}}) \qquad (1)$$

There are large uncertainties associated with critical depth values calculated using equation 1, and several studies have set out to increase the accuracy of Z_{cr}. Nelson and Smith (1991) indicated that "(Eqn. 1), as normally applied, contains two large compensating errors…that were not part of the original derivation". The first error was in the estimation of the optical correction term for the amount of incoming radiation. They point out that the correction factor used by Sverdrup to calculate I_e was based on total solar energy rather than PAR, and propose to use time averaged PAR (ΣI_o) in calculations of Z_{cr}. Losses of PAR due to reflection at the ocean surface generally range between 4-7% under all atmospheric and wind conditions, and are toward the lower end of this range at low latitudes (Jerlov 1976; Campbell and Aarup 1989). Coupled with this loss, wavelengths of light >650nm are absorbed strongly in the upper few metres of the water column, leading to ~15% loss of PAR (Jerlov 1976; Kirk 1994). These factors together suggest a 20% reduction in ΣI_o (i.e. a correction factor of 0.8) is required to account for surface reflectance and near-surface absorbance of PAR (Nelson and Smith 1991), which is considerably less than the 82% suggested in original calculations of Z_{cr}.

The second compensating error that was identified by Nelson and Smith (1991) concerns the method used to calculate I_c. Published I_c values typically come from experiments on phytoplankton cultures and are calculated as the minimum irradiance required for a culture to survive. These values range between 1.2 and 9.3 μmol m^{-2} s^{-1} (Raymont 1980; Langdon 1988). Nelson and Smith (1991) proposed that a value termed

the net photo-compensation irradiance (I_n, defined as "the value of photosynthetically active radiation (PAR) that results in a net phytoplankton growth rate of zero in the presence of most naturally occurring losses") be used in place of I_c, citing Perry and Marra's unpublished calculations of I_n which ranged between 30 and 40 μmol m^{-2} s^{-1}. However, natural community loss factors such as grazing and sinking, and variations in community structure are not accounted for in culture based estimates or Perry and Marra's calculations (Sverdrup 1953; Smetacek and Passow 1990; Nelson and Smith 1991). Community-level I_c estimates which consider these loss factors have a broad range, between 4.0 and 40.0 μmol m^{-2} s^{-1} (Riley 1957; Najjar and Keeling 1997). Siegel *et al.* (2002) set out to provide more accurate community-level estimates of I_c, using satellite and hydrographic datasets. They report median community I_c values for the north Atlantic spring bloom across different latitudes (from 35°N to 75°N) of between 11.1 and 20.2 μmol m^{-2} s^{-1}.

Community level phytoplankton loss factors were also included in an alternative critical depth model developed by Platt *et al.* (1991). These authors "combine an analytical solution for the daily rate of primary production (Platt *et al.* 1990) with currently plausible estimates of phytoplankton loss to provide an analytical model for critical depth". They found that critical depth values calculated using a combined loss value that includes losses due to respiration, grazing, sedimentation and excretion were considerably shallower than estimates based on respiration alone.

Sverdrup (1953) suggested that for blooming of phytoplankton to occur, production of organic matter by photosynthesis must exceed destruction by respiration. When the mixed layer depth (MLD) is deeper than Z_{cr}, phytoplankton are mixed into areas of the

water column where total respiration is greater than total photosynthesis, and there is zero net productivity. High net productivity and phytoplankton blooms occur in vertically stratified regions with MLD above Z_{cr} (Sverdrup 1953; Smetacek and Passow 1990; Nelson and Smith 1991; Kirk 1994; Mann and Lazier 1996). However, studies suggest that phytoplankton blooms can develop in the absence of vertical water column stratification, i.e. before the decrease in MLD to depths above Z_{cr} (Townsend *et al.* 1992; Eilertsen 1993). Huisman *et al.* (1999) developed a model to explain these deviations from classical critical depth theory. Sverdrup's critical depth theory assumes that the phytoplankton community in a well mixed water column is relatively evenly distributed (Sverdrup 1953). The model of Huisman *et al.* (1999) allowed the dynamics of phytoplankton growth and turbulent mixing to govern the distribution of phytoplankton in the water column, and indicated that a bloom can develop if MLD is shallower than Z_{cr}, or if turbulent mixing rates are less than a critical turbulence. Thus, there appear to be two mechanisms that may drive high net productivity and phytoplankton blooms. If mixing is intense, a decrease in the MLD to areas of the water column above Z_{cr} will promote high net productivity and phytoplankton blooms. If mixing is weak, or there is a relaxation of turbulent mixing, phytoplankton growth rates may be high enough to overcome vertical mixing rates, allowing net gains in productivity to be achieved before turbulent mixing takes phytoplankton below Z_{cr} (Huisman *et al.* 1999; Huisman and Sommeijer 2002).

The shelf waters off south western Eyre Peninsula (SWEP) in the eastern Great Australian Bight (EGAB) support a rich pelagic ecosystem that includes populations of important predators such as Australian sea lions (*Neophoca cinerea*), New Zealand fur

seals (*Arctocephalus forsteri*) and southern blue fin tuna (*Thunnus maccoyii*) (Page *et al.* 2006; Ward *et al.* 2006; Fowler *et al.* 2007; Goldsworthy and Page 2007), and large populations of small pelagic fish such as Australian sardine (*Sardinops sagax*), anchovy (*Engraulis australis*) and mackerel (*Scomber spp.* and *Trachurus spp.*) (Ward *et al.* 2006; Ward *et al.* 2008). Understanding temporal variations in primary productivity in the waters off SWEP is important for the management of these ecologically and economically important species. The area is highly dynamic, with significant seasonal variations in meteorology and oceanography that may drive variations in mixing and stratification. Winds are downwelling favourable through winter, shelf waters are well mixed from surface to bottom, and a continuous eastward current flows along the continental shelf (the coastal current), suppressing upwelling associated with the Flinders current (Middleton and Cirano 2002; Middleton and Bye 2007). The Flinders current drives upwelling of cold water from ~250 m depth onto the shelf in summer/autumn, and coastal upwelling events off SWEP are driven by dominant southeasterly winds (Middleton and Bye 2007). Stratification may develop in the water column with cold water upwelling beneath a shallow surface mixed layer, promoting high rates of primary productivity (chapter 2). Upwelling events may be interspersed with periods of downwelling and mixing (Chapter 2, Middleton and Bye 2007) which may break down this stratification and facilitate mixing between upwelled water and the surface water mass. With this information in mind, we propose a conceptual model of mixing and productivity in the EGAB (Fig. 3.1). The model incorporates three scenarios. Scenario 1 outlines conditions that may be expected to occur during downwelling and strong mixing in winter. Phytoplankton are likely to spend significant amounts of time mixed below

Z_{cr}, and with upwelling suppressed by the coastal current, net primary production will be low. Scenario 2 describes conditions during an upwelling event, when stratification develops, with a shallow surface mixed layer and a volume of upwelled water forced above Z_{cr} driving significant contributions to total water column productivity (chapter 2). Scenario 3 depicts conditions during downwelling/mixing events that occur periodically through the upwelling season. If these events are strong, increased mixing may take phytoplankton below Z_{cr} for long periods of time and productivity will be suppressed. If they are weak, with turbulences less than the critical turbulence, relatively high rates of productivity may still be achieved. The entrainment of upwelled water into the surface layer during this scenario may enrich surface waters and promote overall seasonal primary productivity. In addition, mixing may provide a mechanism for phytoplankton from the surface mixed layer to entrain into the upwelled water mass, providing the seed for future bursts of productivity. Temporal variations in primary productivity off SWEP will depend on which of the above mixing/enrichment scenarios is operating in the region at the time of sampling.

Variations in primary productivity off SWEP may have implications for the productivity of other economically and ecologically important species in the region. There have been many studies concerning temporal variation in the oceanography and circulation of the EGAB, but few have examined variations in primary productivity. This study aims to investigate temporal variations in primary productivity in the upwelling region off SWEP using a series of measurements taken between 2004 and 2006. The study was designed to examine the hypotheses that net primary productivity in the coastal waters off SWEP will be highest during the upwelling season, and that primary

productivity will be highest during upwelling events, when mixed layer depths are shallow and water is upwelled to depths above Z_{cr}.

3.3. Methods

Research cruises occurred during February and September 2004, February 2005 and February/March 2006 aboard the RV Ngerin. Samples were collected in coastal waters off southwest Eyre Peninsula (SWEP), within the upwelling region of the Eastern Great Australian Bight (Fig. 3.2). Sampling occurred at an eastern, a central, and a western station (E, C, and W in Fig. 3.2) in daylight hours.

3.3.1. Measurements of upwelling intensity

Three hourly wind data (U) for the study period was provided by the Australian Bureau of Meteorology in the form of wind speed and direction measured by the Neptune Island automatic weather station. The wind stress (τ) was calculated as:

$$\boldsymbol{\tau} = \rho_a C_D \boldsymbol{U} \left|\boldsymbol{U}\right| \qquad (2)$$

where ρ_a is the density of air (0.1 kg m^{-3}) and C_D is a drag coefficient given by (Gill 1982). The alongshore component of wind stress (τ_o) was subsequently calculated at an angle of 315ºT. Positive values of τ_o correspond to upwelling (Middleton and Bye 2007). The three day average of wind stress was used in evaluations of upwelling intensity since

this duration provides sufficient time for enough water movement to occur for an upwelling event to take place.

3.3.2. Measurements of hydrological parameters

Pressure, conductivity and temperature were measured using a Seabird SBE 19 plus Conductivity Temperature Depth recorder (CTD) (Sea-Bird Electronics Inc., Bellevue, WA, USA), which was lowered to within 10 m of the bottom at each station. Depth, salinity and density were derived from pressure, temperature and conductivity during data processing using *Seabird* SBE Data Processing win32 software. In September 2004, February 2005 and February/March 2006, a Biospherical QSP-2300 underwater PAR sensor with log amplifier (Biospherical Instruments Inc., San Diego, CA, USA) was used to measure underwater irradiance. The coefficient of downwelled irradiance (K_d) was derived from the slope of the semilog plot of irradiance versus depth. The euphotic depth (Z_{eu}) was calculated by substituting K_d into the Beer-Lambert equation (Kirk 1994):

$$Z_{eu} = 1/K_d \times Ln(100/1) \qquad (3)$$

Mixed layer depths were determined using a density based criterion according to Kara *et al.* (2000).

Water samples for nutrient analysis were collected at each station using a Niskin bottle. Samples were collected at three depths; 3 m, the deep chlorophyll maximum (DCM) as determined by CTD fluorescence, and 10 m below DCM. 50 ml of each sample was filtered through a Whatman GF/C filter and retained for analysis by the

Water Studies Centre at Monash University, Victoria, Australia. Dissolved Si (APHA-AWWA-WPCF 1998c), nitrate/nitrite (NO_x) (APHA-AWWA-WPCF 1998a), and phosphate (APHA-AWWA-WPCF 1998b) were determined by flow injection analysis with a QuickChem 8000 Automated Ion Analyser.

3.3.3. Measurements of biomass and primary productivity

Water samples were collected from 3 m depth at each station for chlorophyll analysis. A 1L sample from each station was filtered through a Whatman GF/C filter and the filter kept in the dark at <-5ºC until returned to the laboratory. Samples were extracted in 90% methanol over 24 hours, with absorbances read at 750 nm (background) and 665 nm (chlorophyll *a*) using a Hitachi U-2000 spectrophotometer with 1cm pathlength. Chlorophyll concentrations were calculated using the formulae of Talling and Driver (Talling and Driver 1963). Chlorophyll was also measured in CTD casts as fluorescence using a Chelsea Aquatracka Mk3 fluorometer (Chelsea Technologies Group, Surrey, UK) attached to the CTD.

In February/March 2006, primary productivity was examined using a Walz phyto-PAM. Samples were dark adapted for > 30 minutes prior to measurement. Samples were corrected for background fluorescence using GF/C filtrate, then exposed to a series of irradiances to provide estimates of relative specific electron transport rates. These estimates were used to construct rapid light curves, and when fitted to the model of Ralph and Gademann corrected for the absence of photoinhibition (Ralph and Gademann 2005), provided values for the photosynthetic efficiency (α), the irradiance corresponding to light saturation of photosynthesis (I_k), and the maximum specific electron transport rate

(ETR^{B}_{max}). Specific electron transport rates can be converted into specific rates of photosynthesis using conversion factors which consider the absorption cross section of photosystem 2 in natural phytoplankton populations, and the number of electrons required to produce one molecule of oxygen (Korner and Nicklisch 2002, Estevez-Blanco *et al.* 2006, Kromkamp *et al.* 2008). Maximum specific electron transport rates were converted to maximum specific photosynthetic rates (P^{B}_{max}) using a conversion factor of 0.156 (Korner and Nicklisch 2002). Maximum specific photosynthetic rates were converted from units of mg O_2 (mg chl a)$^{-1}$ h^{-1} to units of mg C (mg chl a)$^{-1}$ h^{-1} according to Parsons *et al.* (1984), assuming a molecular photosynthetic quotient of 1 (Ganf and Horne 1975).

3.3.4. Modelling primary production

The vertically generalised production model (VGPM) of Behrenfeld and Falkowski (1997) was used to estimate primary productivity (PP_{eu}) in the waters off south western Eyre Peninsula following:

$$PP_{eu} = 0.66125 P^{b}_{opt} \frac{I_0}{I_0 + 4.1} C_{sat} \times Z_{eu} \times D_{irr} \qquad (4)$$

Where P^{b}_{opt} is the optimal specific photosynthetic rate, I_o is the monthly mean surface irradiance, C_{sat} is the satellite surface chlorophyll concentration, Z_{eu} is the euphotic depth, and D_{irr} is daylength in decimal hours. The monthly mean C_{sat} (February for summer, September for winter) for 35ºS 136ºE was obtained from the NASA Giovanni website

(http://reason.gsfc.nasa.gov/OPS/Giovanni/mpcomp.ocean.shtml), and monthly mean I_o was provided by the Australian Bureau of Meteorology for 36ºS 138ºE. The NASA Poet website (http://poet.jpl.nasa.gov/) provided monthly mean SST for 34.73ºS 135.15ºE that was used to calculate P^b_{opt} as:

$$P^b_{opt} = \begin{cases} 1.13 \rightarrow if\ SST < -1.0 \\ 4.00 \rightarrow if\ SST > 28.5 \\ P^{b'}_{opt} \rightarrow if\ -1.0 \le SST \le 28.5 \end{cases}$$

$$\begin{aligned} &where \\ &P^{b'}_{opt} = 1.2956 + 2.759\times10^{-1} SST + 6.17\times10^{-2} SST^2 - 2.05\times10^{-2} SST^3 \\ &+2.462\times10^{-3} SST^4 - 1.348\times10^{-4} SST^5 + 3.4132\times10^{-6} SST^6 - 3.27\times10^{-8} SST^7 \end{aligned} \quad (5)$$

The euphotic depth (Z_{eu}) was calculated from C_{sat} estimates following:

$$Z_{eu} = \begin{cases} 568.2(C_{tot})^{-0.746} \rightarrow if\ C_{tot} < 102 \\ 200.0(C_{tot})^{-0.293} \rightarrow if\ C_{tot} > 102 \end{cases}$$

$$\begin{aligned} &where \\ &C_{tot} = \begin{cases} 38.0(C_{sat})^{0.425} \rightarrow if\ C_{sat} < 1.0 \\ 40.2(C_{sat})^{0.507} \rightarrow if\ C_{sat} \ge 1.0 \end{cases} \end{aligned} \quad (6)$$

The monthly mean D_{irr} was obtained from astronomical information on the Geoscience Australia website (www.ga.gov.au/geodesy/astro).

To ground-truth estimates obtained from the VGPM, the above model was run with measured data, including extracted chlorophyll concentrations, and mean Z_{eu} calculated using irradiances measured by the CTD. Mean maximum photosynthetic rate (P_{max})

measured using phyto-PAM in February/March 2006 was used in place of P^b_{opt}. The daily mean I_o for 36ºS 138ºE and daylength for the day of sampling was used in place of the monthly mean I_o and D_{irr}.

To test the validity of VGPM estimates of primary productivity, independent estimates of daily integral primary productivity ($P_{Zm,\,T}$) were calculated according to the model of Platt *et al.* (1991):

$$P_{Z_m,T} = Z_m DBP_m^B(1-\exp(-(2I_*^m/\pi KZ_m)(1-M))) \qquad (7)$$

Where Z_m is the mixed layer depth, D is daylength in decimal hours, B is biomass (concentration of chlorophyll *a*), P^B_m is the maximum specific photosynthetic rate, I^m_* is the dimensionless irradiance at local noon, K is the vertical attenuation coefficient for irradiance, and M is the optical transmittance for the surface mixed layer (M = exp (-KZ_m)). The mean maximum specific photosynthetic rate measured by the Phyto-PAM was used for P^B_m. I^m_* was calculated as I^m_o/I_k, where I^m_o is the maximum daily (noon) surface irradiance, and I_k is the irradiance corresponding to the onset of light saturation of photosynthesis. I^m_o was provided by the Australian Bureau of Meteorology from the weather station at the Adelaide Airport (34.952ºS 138.520ºE), the closest station to the study area that collects half hourly global solar data. The mean I_k measured with the Phyto-PAM in this study was used in calculations of I^m_*.

3.3.5. Calculating the critical depth

Critical depth (Z_{cr}) was calculated according to a modification of Nelson and Smith's reformulation of Sverdrup's critical depth equation (Nelson and Smith 1991):

$$Z_{cr} = 0.8 \times 11.57 \times \sum I_o / I_c \times K_d \qquad (8)$$

Where 0.8 is a correction factor for reflectance and near surface absorbance of PAR, ΣI_o is the daily mean surface irradiance for the day of sampling provided by the Australian Bureau of Meteorology for 36ºS 138ºE, 11.57 is a factor used to convert ΣI_o from units of mol m^{-2} d^{-1} to μmol m^{-2} s^{-1}, and I_c is the compensation irradiance. In calculations in this study, the median I_c value obtained by Siegel *et al.*(2002) for 35-40°N (19.6 μmol m^{-2} s^{-1}) was used, since the study region off SWEP encompasses similar latitudes in the southern hemisphere. Satellite data indicates similar sea surface temperatures in the two regions.

The calculation of the critical depth according to Platt *et al.* (1991) makes use of primary productivity in the surface mixed layer, which can be calculated using equation 7 with Z_m in place of Z_{eu}. The biomass specific phytoplankton loss rate (L^b) was calculated as the sum of losses due to respiration (R^b), grazing (G^b), excretion (E^b) and sedimentation (S^b). R^b was estimated as alpha * I_c, G^b used grazing rates measured in the region (chapter 5), E^b was estimated as 5% of the gross photosynthetic rate and $S^b = X / (24Z_m)$, where X is the carbon to chlorophyll ratio, in this case taken as 40. L^b was then used to calculate daily integrated carbon loss in the surface mixed layer according to:

$$L_{Z_m,T} = 24 Z_m B L^b \qquad (9)$$

The critical depth is the depth at which phytoplankton gains equal phytoplankton losses, that is, the depth at which $P_{Zm,T} = L_{Zm,T}$. This can be found by changing the value of Z_m in equations 7 and 9 until the left sides of both equations balance (Platt *et al.* 1991).

3.4. Results

3.4.1. Temporal variation in upwelling intensity

Upwelling intensity varied considerably in the EGAB during the study period. Mean wind stress in the region was upwelling favourable in the peak of summer, and downwelling favourable in winter (Fig. 3.3). A closer examination of wind stress, however, reveals a high degree of variability in the number and timing of upwelling events during the upwelling seasons each year (Fig. 3.4). The first positive wind stress for the upwelling season of 2003/2004 was recorded in mid October 03. Between mid October 03 and mid January 04, the wind stress was characterised by several positive peaks interspersed with periods of downwelling favourable negative wind stress. Wind stress for the remainder of the upwelling season was upwelling favourable. The end of the 03-04 upwelling season is identifiable as a sharp peak in downwelling favourable negative wind stress in mid May 04 (Fig. 3.4). The onset of the 04/05 upwelling season can be seen as a peak in positive wind stress in late October 04. This season was characterised by a series of short, sharp peaks of positive wind stress broken up by peaks of negative wind stress which occurred throughout the season, until its end in mid May 05 (Fig. 3.4). The onset of upwelling in the 2005/2006 season did not occur until early

January 06, and unlike the previous two seasons was less variable with many fewer negative wind stresses. The season was characterised by a series of wide peaks, with extended periods of upwelling favourable positive wind stress occurring until the season ended with a strong trough of negative wind stress in late April 2006 (Fig. 3.4).

3.4.2. Temporal variation in hydrological parameters

CTD data from February 2004 was deemed unsuitable for this analysis due to insufficient calibration, and is not reported here. Mean CTD measured SST from the three stations sampled in the region was 14.5 ± 0.03 ºC (mean ± standard error) in September 2004, 17.8 ± 0.4 ºC in February 2005, and 16.1 ± 0.5 ºC in March 2006 (Fig. 3.5). To put these results into context, figure 3.5. also displays the mean satellite SST for the sampling period, which showed a clear seasonal pattern, with peaks in January/February, and troughs in August/September.

In September 2004, the water column was well mixed at all stations sampled, and temperatures were low (~14.5 ºC), (Fig. 3.6). There is evidence of recent mixing and stratification at the eastern station during February 2005, with the water column characterised by relatively large changes in temperature and salinity over short vertical distances. The water column toward the west of the study area is characterised by the formation of a surface layer of warm (~17 ºC), less dense (~26.0 kg m^{-3}) water overlaying a colder (~15.5 ºC) denser (26.4 kg m^{-3}) bottom layer. The water column across the region was more stable in February/March 2006, with a warm (15.5-16.5 ºC), less dense (26.2 kg m^{-3}) surface layer overlaying a bottom layer of colder (13.5-14 ºC), denser (~26.5 kg m^{-3}) water at all stations.

The underwater light regime in the waters off south western Eyre Peninsula showed considerable variation between seasons (Table 3.1). K_d's were generally lower in winter than in summer, and corresponding Z_{eu} were deeper in winter than in summer. EGAB shelf waters were well mixed in September 2004. Mixed layer depths were ~24-27m in February 2005 and ~8-30m in February/March 2006.

Nutrient concentrations were highly variable between years and seasons with no clear patterns evident from depth profiles. Concentrations of FRP were generally < 0.5 µmol L^{-1}, but reached as high as 1 µmol L^{-1} at 40 m depth at the eastern station in February 04. Concentrations of NO_x were generally < 2 µmol L^{-1}, with a concentration of 6 µmol L^{-1} measured at 40 m depth at the eastern station in February 04. Silica concentrations were generally < 5 µmol L^{-1}, with the highest concentration (27 µmol L^{-1}) measured at 3 m depth at the western station in March 06 (Fig. 3.7). Stoichiometric ratios (Si:N and N:P, Fig.8) reveal potential silica limitation in February 04, September 04, and February 05. Potential nitrogen limitation was evident in all months sampled, but there was no indication of phosphorus limitation (Fig. 3.8).

3.4.3. Temporal variation in biomass and primary productivity

Mean extracted chlorophyll concentrations in waters off south western Eyre Peninsula did not vary markedly between February 2004 and February 2005, ranging from 0.6 ± 0.1 µg L^{-1} (mean ± standard error) in February 2004, to 0.4 ± 0.1 µg L^{-1} in September 2004, and 0.3 ± 0.1 µg L^{-1} in February 2005. The highest mean surface chlorophyll concentration measured during the study period was 1.9 ± 1.4 µg L^{-1}, in March 2006 (Fig. 3.9). Figure 3.9 also displays satellite measured monthly mean surface fluorescence.

Extracted surface chlorophyll concentrations generally agreed closely with monthly satellite means, except during February 06 when the mean extracted chlorophyll concentration was double the satellite monthly mean.

Extracted surface chlorophyll concentrations were around 0.5 μg L^{-1} for all stations sampled during February and September 2004 and February 2005, and for the western station in March 2006. However, extracted surface concentrations measured at the eastern and central stations in February/March 2006 were 3-6 times greater than concentrations measured at any other time during this study (Fig. 3.10). CTD fluorescences were always lower than extracted chlorophyll concentrations. Fluorescence was homogenous throughout the water column in September 2004, with little variation with depth (Fig. 3.10). In February 2005 and February/March 2006, fluorescences increased gradually with depth, and a deep chlorophyll maximum was observed in the waters below the surface mixed layer (Fig. 3.10). The exception was the eastern station in February/March 2006, where fluorescence decreased slightly with depth, and the maximum was observed in the surface mixed layer.

Rapid light curves in February/March 2006 were similar for all stations (Fig. 3.11), though modelled specific ETR values slightly increased when moving from east to west in the study area. There was some variation in photosynthetic parameters between stations in the region. Moving from east to west, photosynthetic efficiencies (α) and maximum specific photosynthetic rates (P^B_{max}) increased, while the irradiance corresponding to the onset of light saturation of photosynthesis (I_k) decreased (Table 3.2). The mean P^B_{max} measured for surface waters in the region was 4.3 ± 0.3 mg C (mg chl)$^{-1}$ h^{-1}, and the mean I_k was 308.7 ± 30.9 μmol m^{-2} s^{-1}.

Productivity levels estimated using the VGPM and satellite data varied greatly between years and seasons, but were an order of magnitude higher in summer than in winter, with the highest productivity recorded in February 2004 (Table 3.3). Similar variation occurred in productivity levels estimated using the VGPM and measured data. The highest productivity estimated using measured data was recorded in February/March 2006. No estimate was available for February 2004 due to the absence of irradiance data, and therefore, a calculated Z_{eu}. The magnitude of estimated daily integral production depended on the type of data used in calculations. Productivities estimated using satellite data were 1-2 orders of magnitude higher than estimates obtained using measured data in September 2004 and February 2005. Daily integral production estimated using satellite data for February/March 2006 fell within the range calculated using measured data for the same season (Table 3.3).

Daily integral productivities calculated with the model of Platt *et al*. (1991) were in relatively good agreement with VGPM calculations, and showed similar temporal patterns (Table 3.4). Productivity ranged between 375 and 434 mg C m^{-2} d^{-1} in September 2004, 430 and 526 mg C m^{-2} d^{-1} in February/March 2005, and 288 and 2958 mg C m^{-2} d^{-1} in February/March 2006.

3.4.4. Temporal variation in the critical depth

Critical depths calculated according to Nelson and Smith (1991) were ~120 m deeper than MLD in February 2005 and ~70-130 m deeper than MLD in February/March 2006. Critical depths in September 2004 were ~20-80 m shallower than those measured in February 2005 and February/March 2006 (Table 3.1).

Daily integral phytoplankton losses were greatest at the central station in February/March 2006, corresponding with the highest grazing losses (Table 3.5). Grazing losses were also relatively high at the eastern and central stations in February 2005. Losses due to respiration were < 0.35 mg C (mg chl)$^{-1}$ hr^{-1} in all sampling periods. Critical depths calculated according to Platt *et al.* (1991) were an order of magnitude lower than those calculated according to Nelson and Smith (1991) (Table 3.6). The deepest critical depth of 21.3 m occurred at the eastern station in February/March 2006. Critical depths were only deeper than mixed layer depths at the eastern and western stations in February/March 2006. No credible critical depth could be calculated for the central station at this time since losses were > gains at all depths.

3.5. Discussion

The coastal waters off SWEP have a potential primary productivity that could rival even the most productive areas of the ocean. For example, levels of primary productivity measured in February/March 2006 fall within ranges reported for the productive eastern boundary current upwelling systems off southern Africa (1000-3500 mg C m^{-2} d^{-1}, Brown *et al.* 1991), South America (800-5100 mg C m^{-2} d^{-1}, Daneri *et al.* 2000), and south western USA (500-2600 mg C m^{-2} d^{-1}, Pilskaln *et al.* 1996). The mean surface chlorophyll concentration observed in February/March 2006 was an order of magnitude greater than concentrations measured during previous summers of the study period, and was double the satellite monthly mean. Chlorophyll concentrations measured off south western Eyre Peninsula during February/March 2006 were an order of magnitude greater than those reported for oligotrophic waters off western and south eastern Australia (0.1-

0.7 µg L^{-1}, Gibbs *et al.* 1986; Hallegraeff and Jeffrey 1993; Hanson *et al.* 2005). These concentrations were comparable to those measured in short-term localised upwellings off New South Wales (2-8 µg L^{-1} Hallegraeff and Jeffrey 1993), and fall within the lower range of concentrations reported during upwelling events in the Benguela (0.8-24 µg L^{-1}, Brown 1984), Humbolt (1-30 µg L^{-1}, Peterson *et al.* 1988) and California current systems (0.5-57 µg L^{-1}, Dickson and Wheeler 1995). However, daily integral productivities measured during September 2004 and February 2005 fell towards the higher end of the range reported for the oligotrophic waters of the Leeuwin current (110-530 mg C m^{-2} d^{-1}, Hanson *et al.* 2005). Chlorophyll concentrations measured during September 2004 were relatively low by global standards, and were comparable to those measured throughout the year in the oligotrophic waters off western and south eastern Australia (Gibbs *et al.* 1986; Hallegraeff and Jeffrey 1993; Hanson *et al.* 2005). These temporal variations in primary productivity in coastal waters off SWEP may be explained by variations in the mixing scenario that is occurring during the time of sampling, which will be dictated by the timing and intensity of upwelling/downwelling events in the region, driven by variations in the wind field. Our results suggest, however, that these variations in productivity may not be dictated by variations in mixing in the classical sense.

Critical depth calculations using the model of Nelson and Smith (1991) have indicated that Z_{cr} is deeper than depicted in the conceptual model (indeed, deeper than the water depth), and is not influencing variations in primary productivity in the waters off SWEP. This is probably due to the fact that this method neglects phytoplankton loss factors that may be affecting the balance between community photosynthesis and respiration (such as grazing, sedimentation, excretion and respiration). When these

factors were considered in the calculation of the critical depth, as in the model of Platt *et al.* (1991), a more accurate determination of Z_{cr} was achieved, which was more useful in the explanation of variations in primary productivity in the region.

The waters off SWEP in the EGAB appear to represent a unique situation that doesn't always comply with conventional theory regarding mixing and productivity, which is generally used to explain the phytoplankton spring bloom. Results from February 2005 seem to resemble the conventional model. MLD were ~7 m deeper than the critical depth and productivity was low. This was the weakest upwelling season of the study, and sampling occurred during a period of downwelling and mixing. In February/March 2006 however, MLD were shallow at the western and eastern stations. At the western station, MLD was 1.7 m above Z_{cr}. Despite this result, integrated losses > integrated production, most likely due to a high grazing impact. At the eastern station, MLD was 13.5 m above Z_{cr}, and productivity was high. Results in chapter 2 indicated that primary productivity in the surface mixed layer in February/March 2006 was accounting for < 40% of primary productivity in the euphotic zone. It follows that > 60% of primary productivity was occurring in the waters below the surface mixed layer but above Z_{cr}. Higher productivity during 2006, the strongest upwelling season, was due to the entrainment of a larger volume of upwelled water from the bottom layer on the shelf southeast of Eyre Peninsula (the Kangaroo Island pool) into nearshore areas of the water column above Z_{cr}. The high rates of primary productivity, medium biomass and low grazing impact observed at the eastern station may indicate the onset of a phytoplankton bloom driven by access to large volumes of upwelled water. In contrast, at the central station in 06, no credible Z_{cr} could be calculated since losses were always > productivity. Indeed, integrated losses were

~650% of primary productivity, most likely due to high grazing impact. Despite this fact, biomass was largest at the central station in February/March 2006. The presence of such a large biomass, despite relatively low rates of primary productivity, and such high grazing losses may signal the peak/decline of a phytoplankton bloom.

The summer/autumn decreases in MLD identified in the waters off SWEP in this study were also documented by Condie and Dunn (2006) in an analysis of seasonal characteristics of the surface mixed layer in the Australasian region, and are supported by analysis of mixed layer depth data for the region from http://las.pfeg.noaa.gov/las/main.pl. The blooming of phytoplankton in the waters off SWEP appears to be regulated by changes in MLD, but not because it leads to an increase in surface layer primary productivity. Variations in MLD drive phytoplankton blooms by dictating the volume of upwelled water that can entrain from the bottom layer into nearshore areas of the water column above Z_{cr}. These results suggest that there is some component of the upwelled water mass that is not present in the overlying surface water that promotes primary productivity. In the absence of any evidence of macro-nutrient limitation, differences in micro-nutrient concentrations between the upwelled water mass and the overlying surface water of the GAB warm pool have been suggested to be responsible for variations in primary productivity between the two water masses (Chapter 2). Macro-nutrient concentrations in this study were highly variable with no clear pattern between periods of upwelling/downwelling, and there was no evidence of limitation in waters off SWEP at any time during this study. Higher productivity during the upwelling season may be driven by enrichment of waters off SWEP with micro-nutrients, which is absent during winter/spring due to the suppression of upwelling by the coastal current,

and the dominant downwelling favourable winds. Temporal variations in mixing scenarios between and within seasons may affect primary productivity in the waters off SWEP by changing the influence of the upwelled water mass on waters in the region.

Daily integral productivity calculated with satellite data indicates that productivity off SWEP during the upwelling season was an order of magnitude higher than productivity during periods of downwelling and mixing. Validation with measured data in both the VGPM and the model of Platt *et al.* (1991) suggests that low productivity may also occur during downwelling events within the upwelling season, as indicated in results from February 2005, when levels of primary productivity were considerably lower than the highest productivity during the strong upwelling of February/March 2006, and were slightly lower than the range reported for September 2004. Productivity levels modelled using measured data collected in September 2004 were within the range calculated for February/March 2006. However, in the absence of other productivity data, the mean P^{B}_{max} measured with the Phyto-PAM during February/March 2006 was used for all VGPM calculations using measured data. Given the lower irradiances and absence of enrichment via upwelling, one would expect maximum photosynthetic rates to be lower in September 2004 than in February/March 2006. With this in mind, daily integral productivities in September 2004 were probably lower than the modelled productivities reported in Table 3.3 using measured data. The advantage in using the VGPM with monthly mean satellite data to model primary productivity is that it allowed us to model productivity in February 2004, when data was limited. Testing the validity of model results with daily means and directly measured data provided us with a more accurate understanding of variations in primary productivity of SWEP. Independent estimates of

daily integral productivity calculated according to Platt *et al*. (1991) were in good agreement with the general patterns of VGPM productivity estimates, with the highest productivities observed during the strong upwelling season of 2006. An analysis of the influence of the various parameters in the model on primary productivity may be made by fixing the value of all parameters bar one, and calculating primary productivity incrementally over the full range of that parameter, as observed in this study. This analysis indicated that the main driving forces in the model are daylength, incoming irradiance, biomass, and the attenuation coefficient K. In essence, this suggests that the rate of primary productivity at a given time will depend on the volume of biomass able to be productive, the intensity of incoming irradiance and its attenuation, and the length of time the irradiance is available for photosynthesis accumulated productivity.

Variations in primary productivity in the coastal waters off SWEP may be explained by the scenarios in the conceptual model (Fig. 3.1). Sampling in February 2004 took place during an upwelling event, signified by a peak in three day averaged wind stress (Fig. 3.4), that occurred within a relatively strong upwelling season (Fig. 3.3). Conditions during sampling in February 2004 are possibly best represented by scenario 2 in the conceptual model, with high productivity driven by stratification and the intrusion of upwelled waters above Z_{cr}. Low productivity in September 2004 was driven by high mixing rates arising after long periods of downwelling favourable winds (Figs. 3.3 and 3.4) and the absence of micro-nutrient enrichment via upwelling, probably reflecting conditions in mixing scenario 1. Primary productivity in September 2004 also appears to be inhibited by lower irradiances and shorter daylengths which are characteristic of winter and early spring in the region (Table 3.3). In February 2005 sampling occurred

during a downwelling event at the end of a short peak in upwelling favourable winds (Fig. 3.4), but within a season of weak mean upwelling favourable wind stress (Fig. 3.3). During this time, we expect conditions in the region to be similar to those outlined in scenario 3, with increased mixing from downwelling favourable winds suppressing wind driven upwelling, but gradually enriching surface waters of the SWEP via entrainment of upwelled water into the surface mixed layer. These periods of mixing may also provide the seed for a burst of primary productivity during the next upwelling/stratification event, by allowing phytoplankton from the surface mixed layer to entrain into areas of the water column influenced by the upwelled water mass. If this is indeed occurring, we expect the phytoplankton community in the waters off SWEP to be homogenous with depth. Productivity levels were highest in February/March 2006, after a sustained period of upwelling favourable winds. Sampling occurred during a strong upwelling event (Fig. 3.4), in a season of greater than average upwelling favourable wind stress (Fig. 3.3), when conditions reflected scenario 2 in the conceptual model (Fig. 3.1). During this time, high daily integral productivity was driven by shallow MLD's which allowed the entrainment of upwelled waters to areas above Z_{cr}, and gradual overall enrichment of shelf waters during a two month period of strong upwelling events that occurred in the lead up to the sampling period (Fig. 3.4).

The waters off SWEP represent a unique situation that does not always comply with conventional theory regarding mixing and productivity. Temporal variations in primary productivity are linked to variations in mixing and stratification, but relate to changes in the influence of upwelling in the region, driven by variations in the wind field. Major variations in macro-nutrient concentrations between upwelling and downwelling events

were not detected in the waters of SWEP, yet productivity during upwelling events was up to an order of magnitude higher than during periods of downwelling and mixing. We hypothesise that during upwelling events, high productivity off SWEP is driven by the enrichment of waters above Z_{cr}, but below the surface mixed layer, with micro-nutrients. Low productivity within summer/autumn upwelling seasons follows the suppression of this enrichment during downwelling/mixing events, and the overall productivity of the upwelling season will depend on the number, duration and intensity of these downwelling/mixing events. Low productivity during winter/spring is driven by the absence of upwelling, low irradiances and short daylengths.

3.6. References

APHA-AWWA-WPCF (1998a). Method 4500-NO3-I. Standard methods for the examination of water and wastewater. L. S. Clesceri, A. E. Greenberg and A. D. Eaton. Washington, American Public Health Association**:** pp. 4-121.

APHA-AWWA-WPCF (1998b). Method 4500-PG. Standard methods for the examination of water and wastewater. L. S. Clesceri, A. E. Greenberg and A. D. Eaton. Washington, American Public Health Association**:** pp. 4-149.

APHA-AWWA-WPCF (1998c). Method 4500-SiO2-F. Standard methods for the examination of water and wastewater. L. S. Clesceri, A. E. Greenberg and A. D. Eaton. Washington, American Public Health Association**:** pp. 4-169.

Behrenfeld, M. J. and Falkowski, P. G. (1997). Photosynthetic rates derived from satellite-based chlorophyll concentration. *Limnology and Oceanography* **42**(1): 1-20.

Brown, P. C. (1984). Primary production at two contrasting nearshore sites in the southern Benguela upwelling region, 1977-1979. *South African Journal of Marine Science* **2**: 205-215.

Brown, P. C., Painting, S. J. and Cochraine, K. L. (1991). Estimates of phytoplankton and bacterial biomass and production in the northern and southern Benguela ecosystems. *South African Journal of Marine Science* **11**: 537-564.

Campbell, J. W. and Aarup, T. (1989). Photosynthetically available radiation at high latitudes. *Limnology and Oceanography* **34**(8): 1490-1499.

Condie, S. A. and Dunn, J. R. (2006). Seasonal characteristics of the surface mixed layer in the Australasian region: implications for primary production regimes and biogeography. *Marine and Freshwater Research* **57**: 569-590.

Daneri, G., Dellarossa, V., Quinones, R., Jacob, B., Montero, P. and Ulloa, O. (2000). Primary production and community respiration in the Humboldt Current System off Chile and associated oceanic areas. *Marine Ecology Progress Series* **197**: 41-49.

Dickson, M. and Wheeler, P. A. (1995). Nitrate uptake rates in a coastal upwelling regime: A comparison of PN-specific, absolute, and Chl a-specific rates. *Limnology and Oceanography* **40**(3): 533-543.

Eilertsen, H. C. (1993). Spring blooms and stratification. *Nature* **363**: 24.

Estevez-Blanco, P., Cermeno, P., Espineira, M., and Fernandez, E. (2006). Phytoplankton photosynthetic efficiency and primary production rates estimated from fast repetition rate fluorometry at coastal embayments affected by upwelling (Rias Biaxas, NW of Spain). *Journal of Plankton Research* **28**: 1153-1165.

Fowler, S. L., Costa, D. P. and Gales, N. (2007). Ontogeny of movements and foraging ranges in the Australian sea lion. *Marine Mammal Science* **23**: 598-614.

Ganf, G. G. and Horne, A. J. (1975). Diurnal stratification, photosynthesis and nitrogen-fixation in a shallow, equatorial lake (Lake George, Uganda). *Freshwater Biology* **5**: 13-39.

Gibbs, C. F., Tomczak, M. and Longmore, A. R. (1986). The nutrient regime of Bass Strait. *Marine and Freshwater Research* **37**: 451-466.

Gill, A. E. (1982). Atmosphere-Ocean dynamics, Academic press.

Goldsworthy, S. D. and Page, B. C. (2007). A risk assessment approach to evaluating the significance of seal bycatch in two Australian fisheries. *Biological Conservation* **139**: 269-285.

Hallegraeff, G. M. and Jeffrey, S. W. (1993). Annually recurrent diatom blooms in spring along the New South Wales coast of Australia. *Marine and Freshwater Research* **44**: 325-334.

Hanson, C. E., Pattiaratchi, C. B. and Waite, A. M. (2005). Sporadic upwelling on a downwelling coast: Phytoplankton responses to spatially variable nutrient dynamics off the Gascoyne region of Western Australia. *Continental Shelf Research* **25**: 1561-1582.

Huisman, J. and Sommeijer, B. (2002). Population dynamics of sinking phytoplankton in light limited environments: simulation techniques and critical parameters. *Journal of Sea Research* **48**: 83-96.

Huisman, J., van Oostveen, P. and Weissing, F. J. (1999). Critical depth and critical turbulence: Two different mechanisms for the development of phytoplankton blooms. *Limnology and Oceanography* **44**(7): 1781-1787.

Jerlov, N. G. (1976). Marine optics. Amsterdam, Elsevier.

Kara, A. B., Rochford, P. A. and Hurlburt, H. E. (2000). An optimal definition for ocean mixed layer depth. *Journal of Geophysical Research* **105**(C7): 16,803-16,821.

Kirk, J. T. O. (1994). Light and photosynthesis in aquatic ecosystems. Cambridge, Cambridge University Press.

Korner, S. and Nicklisch, A. (2002). Allelopathic growth inhibition of selected phytoplankton species by submerged macrophytes. *Journal of Phycology* **38**: 862-871.

Kromkamp, J.C., Dijkman, N.A., Peene, J., Simis, S.G.H., and Gons, H.J. (2008). Estimating phytoplankton primary production in Lake Ijsselmeer (The Netherlands) using variable fluorescence (PAM-FRRF) and C-uptake techniques. *European Journal of Phycology* **43**: 327-344.

Langdon, C. (1988). On the causes of interspecific differences in the growth-irradiance relationship for phytoplankton. II. A general review. *Journal of Plankton Research* **10**(6): 1291-1312.

Mann, K. H. and Lazier, J. R. N. (1996). Dynamics of marine ecosystems. London, Blackwell Science.

Middleton, J. F. and Bye, J. A. T. (2007). A review of the shelf slope circulation along Australia's southern shelves: Cape Leeuwin to Portland. *Progress in Oceanography* **75**: 1-41.

Middleton, J. F. and Cirano, M. (2002). A northern boundary current along Australia's southern shelves: the Flinders current. *Journal of Geophysical Research-Oceans* **107**(C9): 3129-3143.

Najjar, R. G. and Keeling, R. F. (1997). Analysis of the mean annual cycle of the dissolved oxygen anomaly in the world ocean. *Journal of Marine Research* **55**: 117-151.

Nelson, D. M. and Smith, W. O. (1991). Sverdrup revisited: Critical depths, maximum chlorophyll levels, and the control of Southern Ocean productivity by the irradiance-mixing regime. *Limnology and Oceanography* **36**(8): 1650-1661.

Page, B. C., McKenzie, J., Sumner, M. D., Coyne, M. and Goldsworthy, S. D. (2006). Spatial separation of foraging habits among New Zealand fur seals. *Marine Ecology Progress Series* **323**: 263-279.

Parsons, T. R., Maita, Y. and Lalli, C. M. (1984). A Manual of Chemical and Biological Methods for Seawater Analysis. Oxford, Pergamon Press Ltd.

Peterson, W. T., Dagoberto, F. A., McManus, G. B., Dam, H., Bellantoni, D., Johnson, T. and Tiselius, P. (1988). The nearshore zone during coastal upwelling: daily variability and coupling between primary and secondary production off central Chile. *Progress in Oceanography* **20**: 1-40.

Pilskaln, C. H., Paduan, J. B., Chavez, F. P., Anderson, R. Y. and Berelson, W. M. (1996). Carbon export and regeneration in the coastal upwelling system of Monterey Bay, central California. *Journal of Marine Research* **54**: 1149-1178.

Platt, T., Bird, D. F. and Sathyendranath, S. (1991). Critical depth and marine primary production. *Proceedings of the Royal Society of London B* **246**: 205-217.

Platt, T., Sathyendranath, S. and Ravindran, P. (1990). Primary production by phytoplakton: analytic solutions for daily rates per unit area of water surface. *Proceedings of the Royal Society of London B* **241**: 101-111.

Ralph, P. J. and Gademann, R. (2005). Rapid light curves: A powerful tool to assess photosynthetic activity. *Aquatic Botany* **82**: 222-237.

Raymont, J. E. G. (1980). Plankton and productivity in the oceans, Pergamon.

Riley, G. A. (1957). Phytoplankton of the North Central Sargasso sea, 1950-1952. *Limnology and Oceanography* **2**(3): 252-270.

Siegel, D. A., Doney, S. C. and Yoder, J. A. (2002). The North Atlantic spring phytoplankton bloom and Sverdrup's critical depth hypothesis. *Science* **296**: 730-733.

Smetacek, V. and Passow, U. (1990). Spring bloom initiation and Sverdrup's critical-depth model. *Limnology and Oceanography* **35**(1): 228-234.

Sverdrup, H. U. (1953). On conditions for the vernal blooming of phytoplankton. *J. Cons. Cons. Int. Explor. Mer.* **18**: 287-295.

Talling, J. F. and Driver, D. (1963). Some problems in the estimation of chlorophyll *a* in phytoplankton. Conference on Primary Productivity Measurement, Marine and Freshwater., U.S. Atomic Energy Commission.

Townsend, D. W., Keller, M. D., Sieracki, M. E. and Ackleson, S. G. (1992). Spring phytoplankton blooms in the absence of vertical water column stratification. *Nature* **360**: 59-62.

Ward, T. M., McLeay, L. J., Dimmlich, W. F., Rogers, P. J., McClatchie, S., Matthews, R., Kampf, J. and van Ruth, P. D. (2006). Pelagic ecology of a northern boundary current system: effects of upwelling on the production and distribution of sardine (*Sardinops sagax*), anchovy (*Engraulis australis*) and southern bluefin tuna (*Thunnus maccoyii*) in the Great Australian Bight. *Fisheries Oceanography* **15**(3): 191-207.

Ward, T. M., Rogers, P. J., Keane, J. P., Lowry, M., McLeay, L. J., Neira, F. J., Ovenden, J. R., Saunders, R. S., Schmarr, D., Whittington, I. D. and Williams, D. (2008).

Development and evaluation of egg-based stock assessments for blue mackerel *Scomber australasicus* in southern Australia. Final report to Fisheries Research and Development Council, SARDI Aquatic Sciences.

3.7. Tables

Table 3.1. Temporal variation in bio-oceanographic parameters off south western Eyre Peninsula. K_d = coefficient of downwelled irradiance (m^{-1}), R^2 = regression coefficient for the relationship between irradiance and depth, Z_{eu} = euphotic depth (m), MLD = mixed layer depth (m), Z_{cr} = critical depth, calculate according to Nelson and smith (1991). Stations outlined in Figure 3.2.

Sampling period	Station	K_d	R^2	Z_{eu}	MLD	Z_{cr}
Sep-04	East	0.08	0.94	54.8	-	84.4
	Central	0.05	0.99	102.2	-	135.1
	West	0.11	0.99	42.6	-	61.4
Feb-05	East	0.11	0.99	42.2	24.2	154.6
	Central	0.12	0.98	40.0	27.2	141.7
	West	0.11	0.99	42.6	-	154.6
Feb/March 06	East	0.17	0.98	27.2	7.8	161.7
	Central	0.09	0.99	50.0	29.8	148.0
	West	0.16	0.99	29.1	11.4	83.2

Table 3.2. Photosynthetic parameters measured using Phyto-PAM, February/March 2006. α = photosynthetic efficiency (mg C (mg chl *a*)$^{-1}$ hr^{-1} (µmol m^{-2} s^{-1})$^{-1}$), I_k = the irradiance corresponding to the onset of light saturation of photosynthesis (µmol m^{-2} s^{-1}), P^B_{max} = maximum specific photosynthetic rate (mg C (mg chl *a*)$^{-1}$ hr^{-1}). Stations outlined in Figure 3.2.

Station	α	I_k	P^B_{max}
East	0.012	334.6	3.9
Central	0.014	316.9	4.4
West	0.017	274.5	4.6
Mean	0.014	308.7	4.3
St. dev.	0.002	30.9	0.3

Table 3.3. Temporal variations in VGPM parameters. C_{sat}/C_{ext} = surface chlorophyll concentration (µg L^{-1}), P^{b}_{opt} = optimal specific photosynthetic rate (mg C mg chl^{-1} hr^{-1}), P_{max} = maximum photosynthetic rate (mg C mg chl^{-1} hr^{-1}), I_o = surface irradiance (mol m^{-2} d^{-1}), Z_{eu} = euphotic depth (m), D_{irr} = daylength (decimal hours), PP_{eu} = daily integral productivity in euphotic zone (mg C m^{-2} d^{-1}). Calculations with satellite data used monthly mean I_o and D_{irr}, calculations with measured data used daily means.

	VGPM with satellite data						VGPM with measured data					
Sampling period	**C_{sat}**	**P^{b}_{opt}**	**Z_{eu}**	**I_o**	**D_{irr}**	**PP_{eu}**	**C_{ext}**	**P_{max}**	**Z_{eu}**	**I_o**	**D_{irr}**	**PP_{eu}**
September 04	0.4	5.8	50.4	26.2	11.9	793.0	0.3-0.6	4.3	45.8-102.2	14.3	11.7	448.5-769.2
February 05	0.5	6.5	46.9	41.0	13.3	1215.5	0.3	4.3	40.0-42.6	36.0	13.4	367.5-494.6
Feb/Mar 06	0.7	6.4	42.2	44.9	13.4	1545.0	0.6-3.3	4.3	27.2-50.0	58.2	12.9	541.5-5466.5

Table 3.4. Temporal variation in daily integral productivity calculated according to Platt *et al.* (1991). B = biomass (µg L^{-1}), I_o^m = maximum surface irradiance at local noon (µmol m^{-2} s^{-1}), I_k = the irradiance correspondiong to light saturation of photosynthesis (µmol m^{-2} s^{-1}), I_*^m = dimensionless irradiance at local noon, M = the optical transmittance for the euphotic zone (dimensionless), and $P_{Zeu,T}$ = daily integral productivity in the euphotic zone (mg C m^{-2} d^{-1}). Stations outlined in Figure 3.2.

Sampling period	Station	B	I_o^m	I_k	I_*^m	M	$P_{Zeu,T}$
Sep 04	East	0.6	631.8	308.7	2.0	0.010	374.7
	Central	0.3	631.8	308.7	2.0	0.004	304.6
	West	0.4	1495.5	308.7	4.8	0.010	433.6
Feb/Mar 05	East	0.3	2187.9	308.7	7.1	0.010	526.3
	Central	0.3	2187.9	308.7	7.1	0.010	430.7
	West	0.3	2187.9	308.7	7.1	0.010	458.6
Feb/Mar 06	East	1.7	2035.9	308.7	6.6	0.010	2958.0
	Central	3.3	2035.9	308.7	6.6	0.010	823.3
	West	0.6	2035.9	308.7	6.6	0.010	287.6

Table 3.5. Temporal variation in loss factors used in Platt *et al.*'s (1991) calculation of daily integrated losses in the surface mixed layer. R^b = biomass specific losses due to respiration (mg C (mg chl)$^{-1}$ h^{-1}), E^b = biomass specific losses due to excretion (mg C (mg chl)$^{-1}$ h^{-1}), G^b = biomass specific losses due to grazing (mg C (mg chl)$^{-1}$ h^{-1}), S^b = biomass specific losses due to sedimentation (mg C (mg chl)$^{-1}$ h^{-1}), L^b = biomass specific generalised loss rate (mg C (mg chl)$^{-1}$ h^{-1}), $L_{Zm,T}$ = daily integrated losses in the surface mixed layer (mg C m^{-2} d^{-1}). Stations outlined in Figure 3.2.

Sampling period	Station	R^b	E^b	G^b	S^b	L^b	$L_{Zm,T}$
Sep 04	East	0.2	-	0.6	-	-	-
	Central	0.3	-	1.2	-	-	-
	West	0.3	-	0.3	-	-	-
Feb/Mar 05	East	0.2	0.10	1.8	0.02	2.2	435.0
	Central	0.3	0.09	1.7	0.02	2.1	410.1
	West	0.3	-	0.3	-	-	-
Feb/Mar 06	East	0.2	0.10	0.3	0.70	1.3	423.3
	Central	0.3	0.09	2.1	0.03	2.4	5759.2
	West	0.3	0.10	1.4	0.04	1.9	307.1

Table 3.6. Temporal variation in critical depth (Z_{cr}, m) in the coastal waters off SWEP, calculated using the model of Platt *et al.* (1991). $P_{Zm,\ T}$ = daily integral productivity for the mixed layer (mg C m^{-2} d^{-1}), $L_{Zm,\ T}$ = daily integral losses for the mixed layer (mg C m^{-2} d^{-1}). Stations outlined in Figure 3.2.

Sampling period	Station	$P_{Zm,T}$	$L_{Zm,T}$	Z_{cr}
	East	306.6	306.6	17.1
Feb/Mar 05	Central	368.1	368.1	18.3
	West	-		-
	East	2236.0	2236.0	21.3
Feb/Mar 06	Central	0.3	0.3	0.01
	West	177.5	177.4	13.1

3.8. Figures

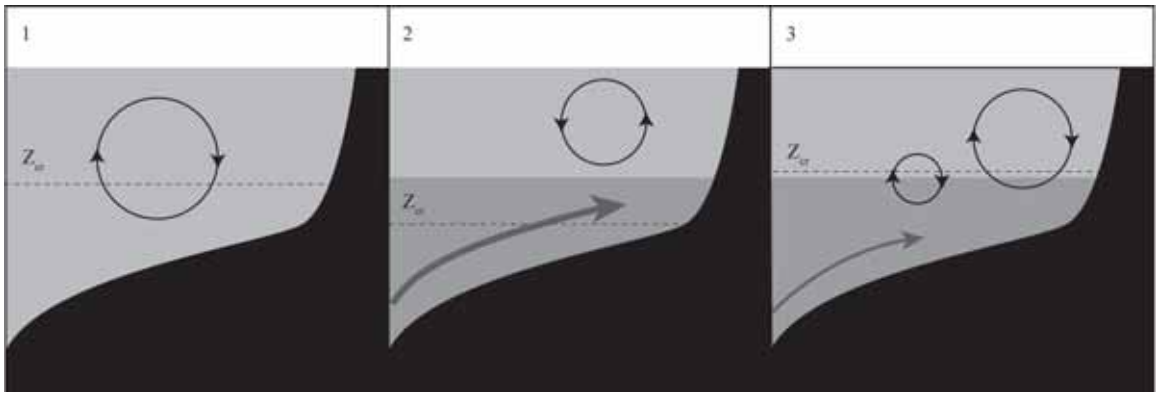

Figure 3.1. Conceptual model of mixing and productivity in the shelf waters off SWEP. Z_{cr} is the critical depth, and dark grey colour indicates upwelled water. Scenarios are described in the text.

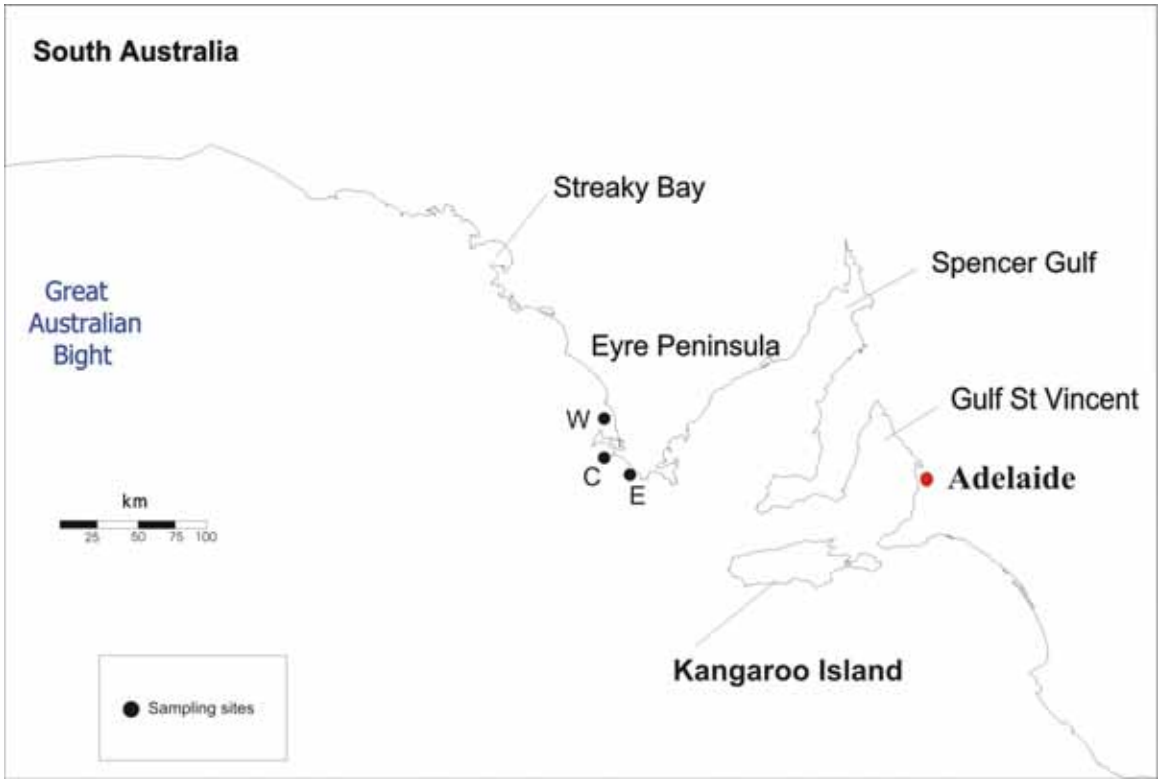

Figure 3.2. Sampling stations used for measurements of bio-oceanographic parameters and levels of primary production in the eastern Great Australian Bight.

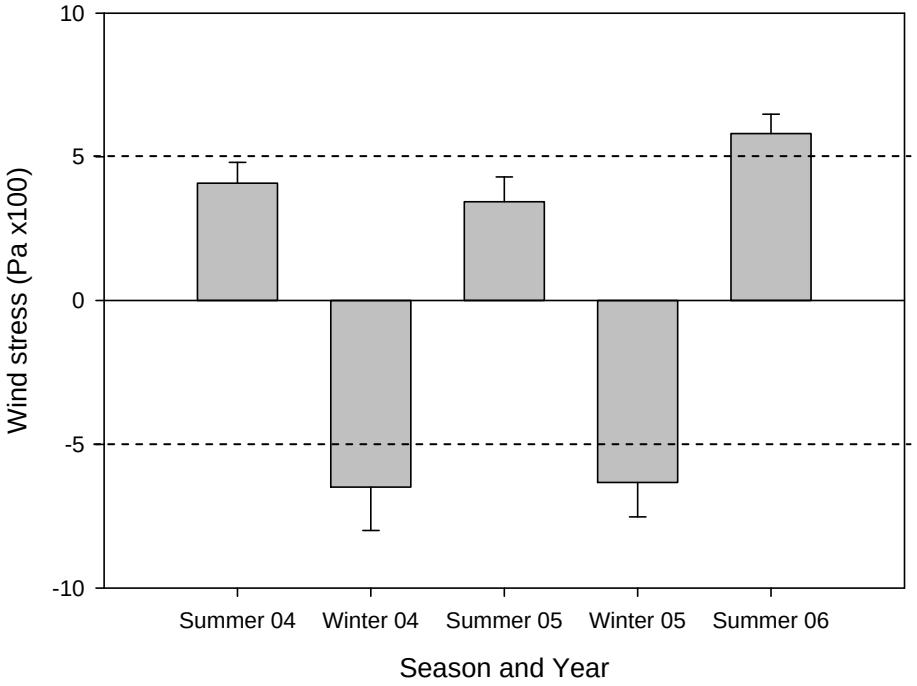

Figure 3.3. Neptune Island mean wind stress (± standard error) calculated over three month periods (Summer, Jan-Mar; Winter, Jul-Sept). Dashed lines represent the long-term summer and winter means. Positive values indicate upwelling favourable conditions.

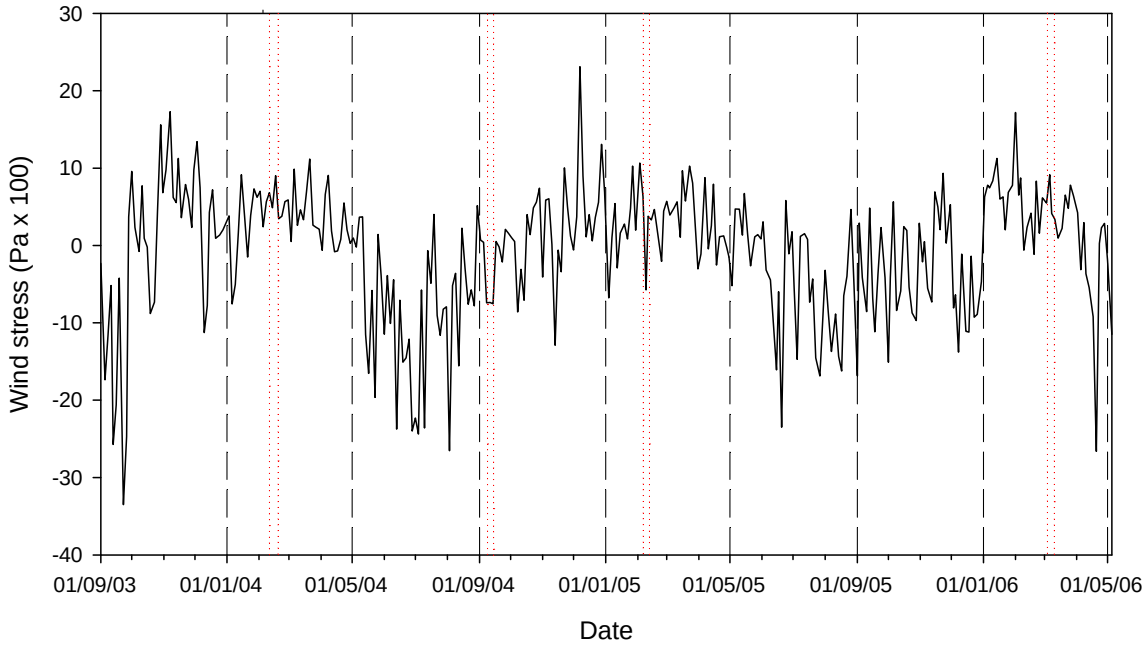

Figure 3.4. Three day averaged wind stress from Neptune Island, for the period September 2003 to May 2006. Red lines indicate sampling periods. Positive values indicate upwelling favourable conditions.

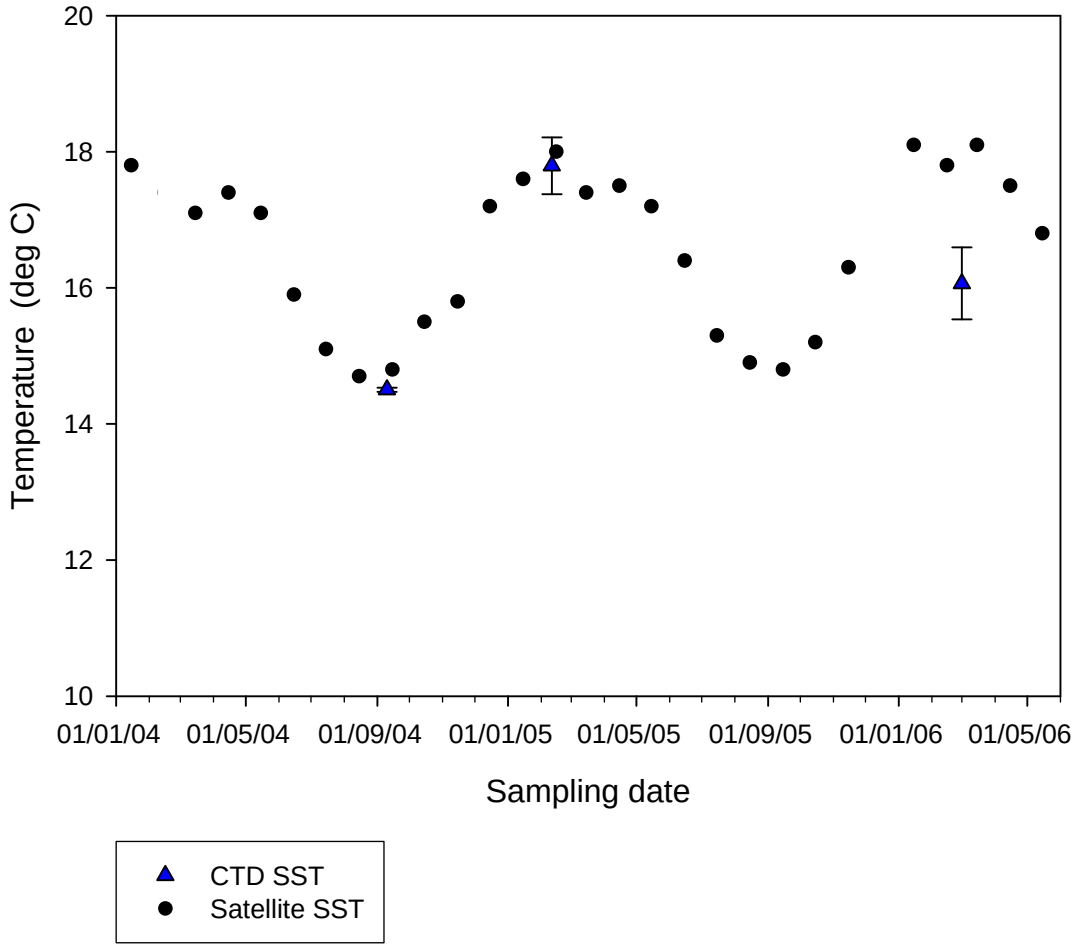

Figure 3.5. Seasonal variation in sea surface temperature in waters off south western Eyre Peninsula. Mean calculated using SST measured at three stations off south western Eyre Peninsula with a CTD. Black circles represent monthly mean satellite SST taken from the NASA Poet website (http://poet.jpl.nasa.gov/). Error bars indicate standard deviation.

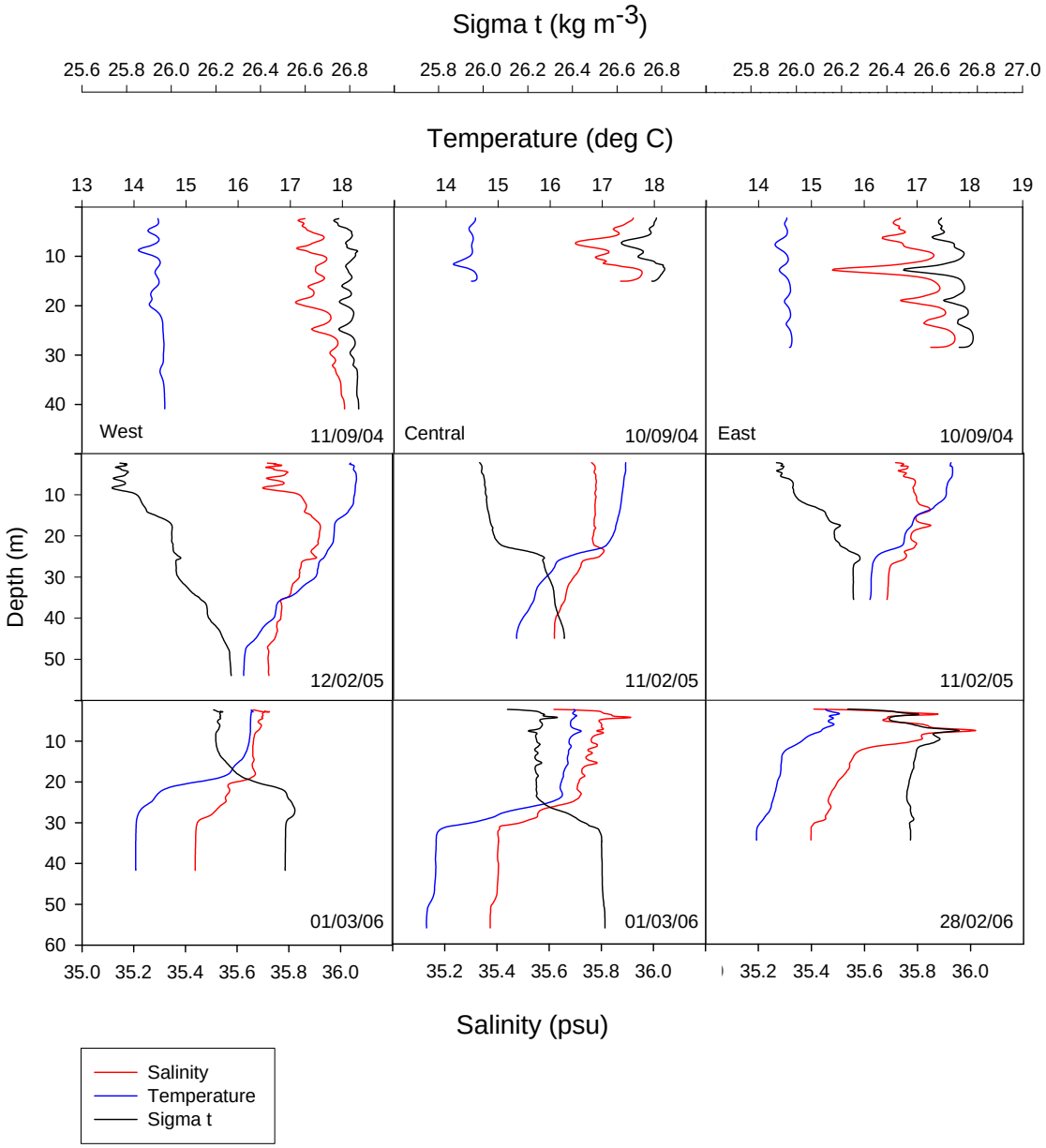

Figure 3.6. Seasonal variation in depth profiles of bio-oceanographic parameters in waters off south western Eyre Peninsula.

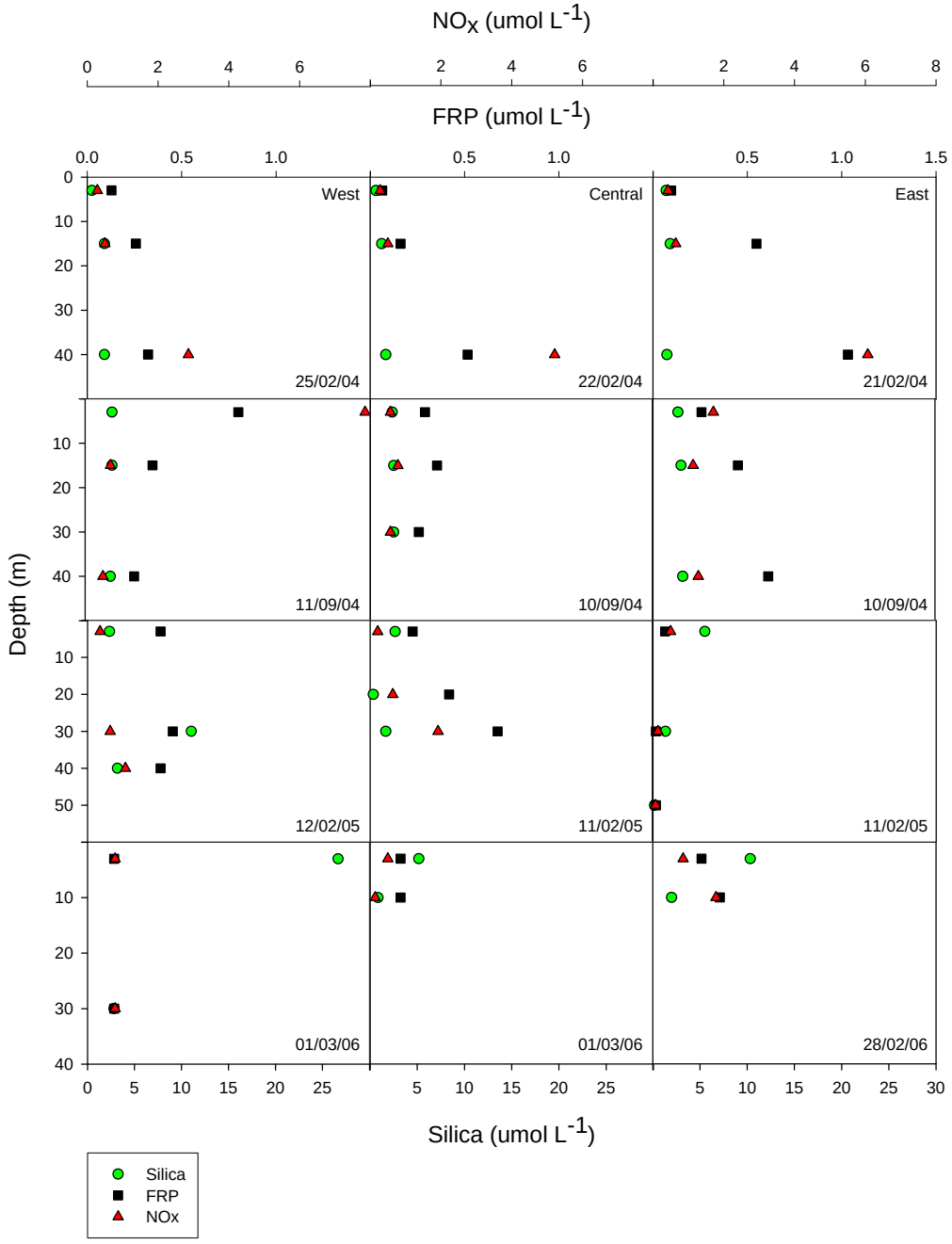

Figure 3.7. Seasonal variation in nutrient depth profiles in waters off south west Eyre Peninsula.

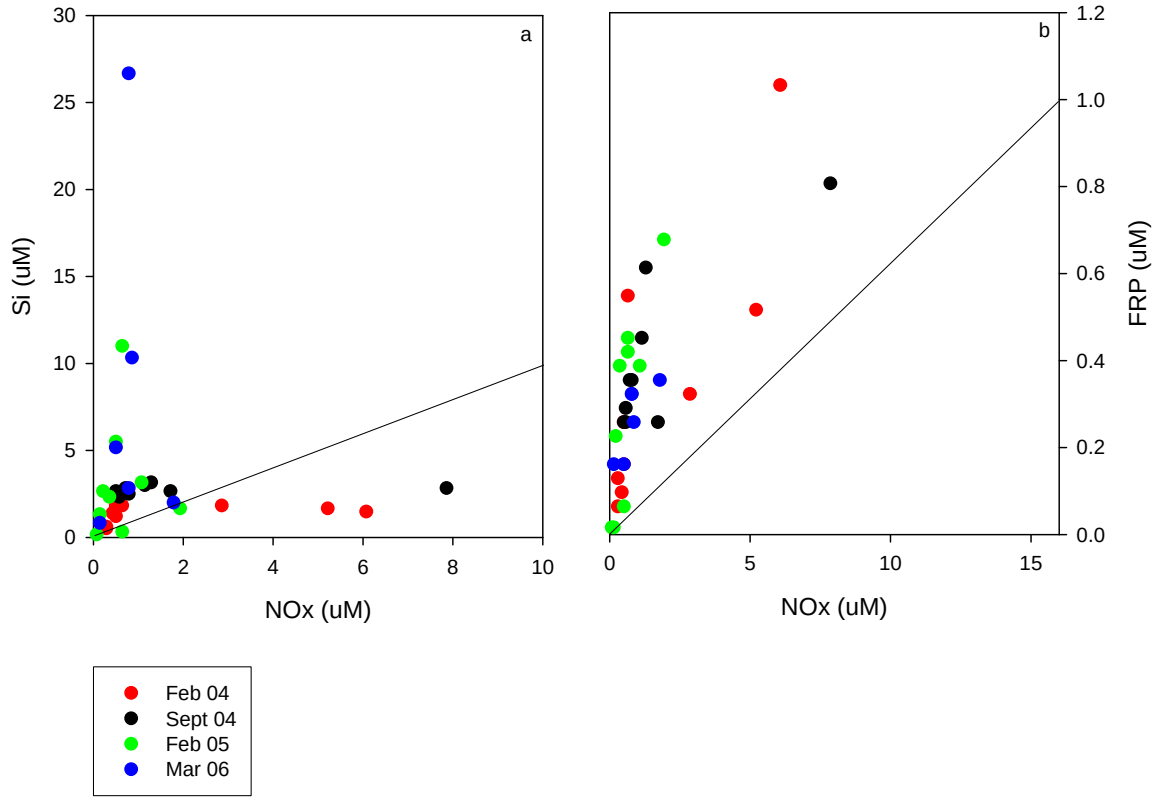

Figure 3.8. Seasonal variation in stoichiometric ratios in waters off south west Eyre Peninsula. Solid black line represents the Redfield ratio for the elemental composition of phytoplankton (1:1 Si:N, 16:1 N:P). Points above the line indicate potential nitrogen limitation. Points below the line indicate potential silica (a) or phosphorus (b) limitation.

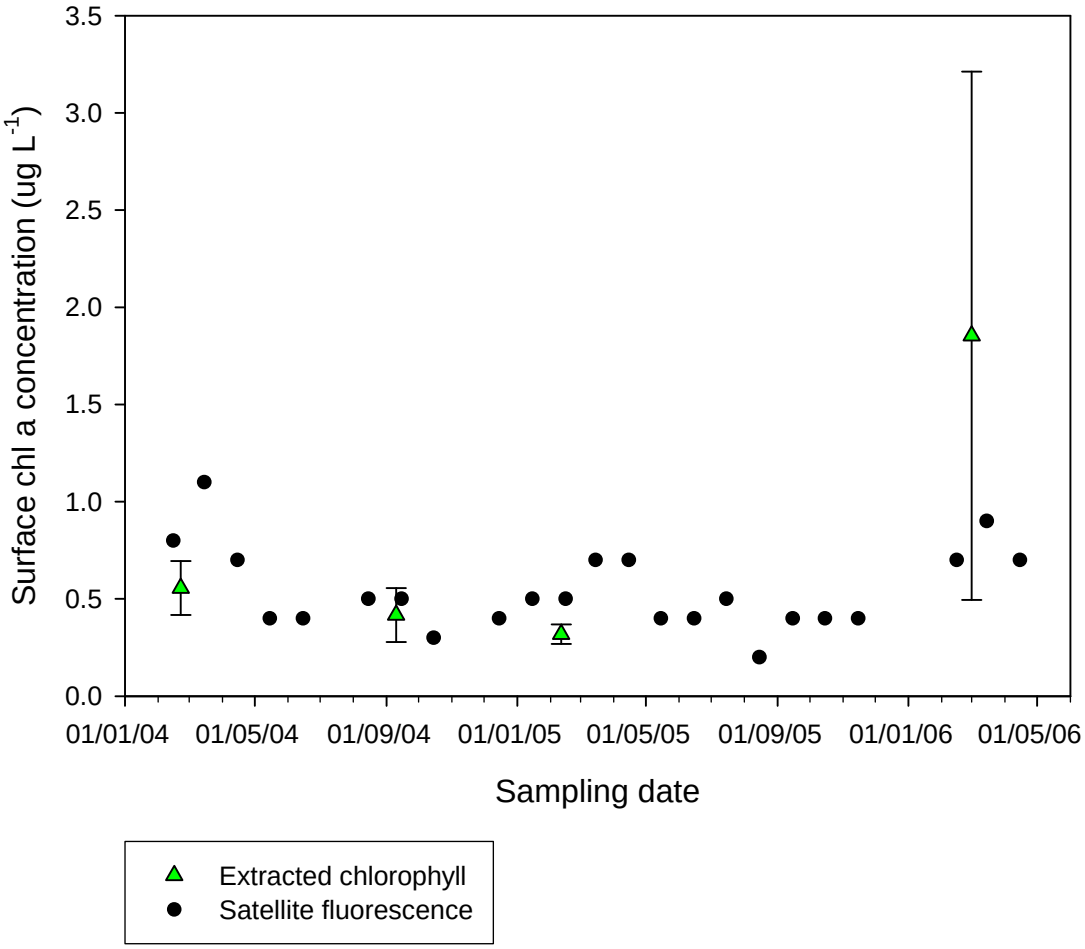

Figure 3.9. Seasonal variation in surface chlorophyll *a* concentrations in waters off south western Eyre Peninsula. Mean calculated using extracted surface chlorophyll *a* concentrations measured at three stations off south western Eyre Peninsula. Black circles represent monthly mean fluorescence taken from the NASA *Giovanni* website (http://reason.gsfc.nasa.gov/OPS/Giovanni/mpcomp.ocean.shtml). Error bars indicate standard deviation.

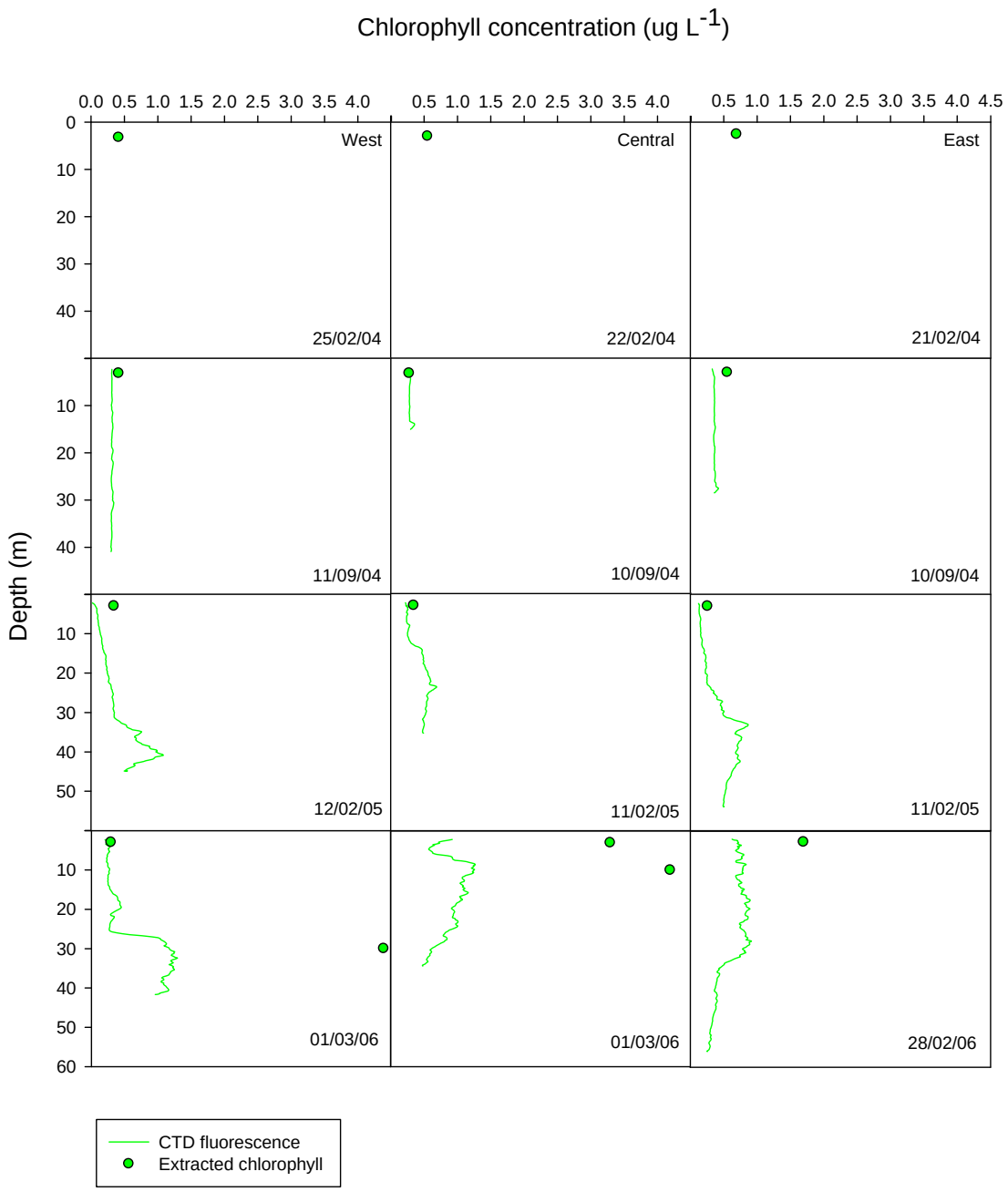

Figure 3.10. Seasonal variation in chlorophyll depth profiles and extracted surface concentrations in waters off south west Eyre Peninsula.

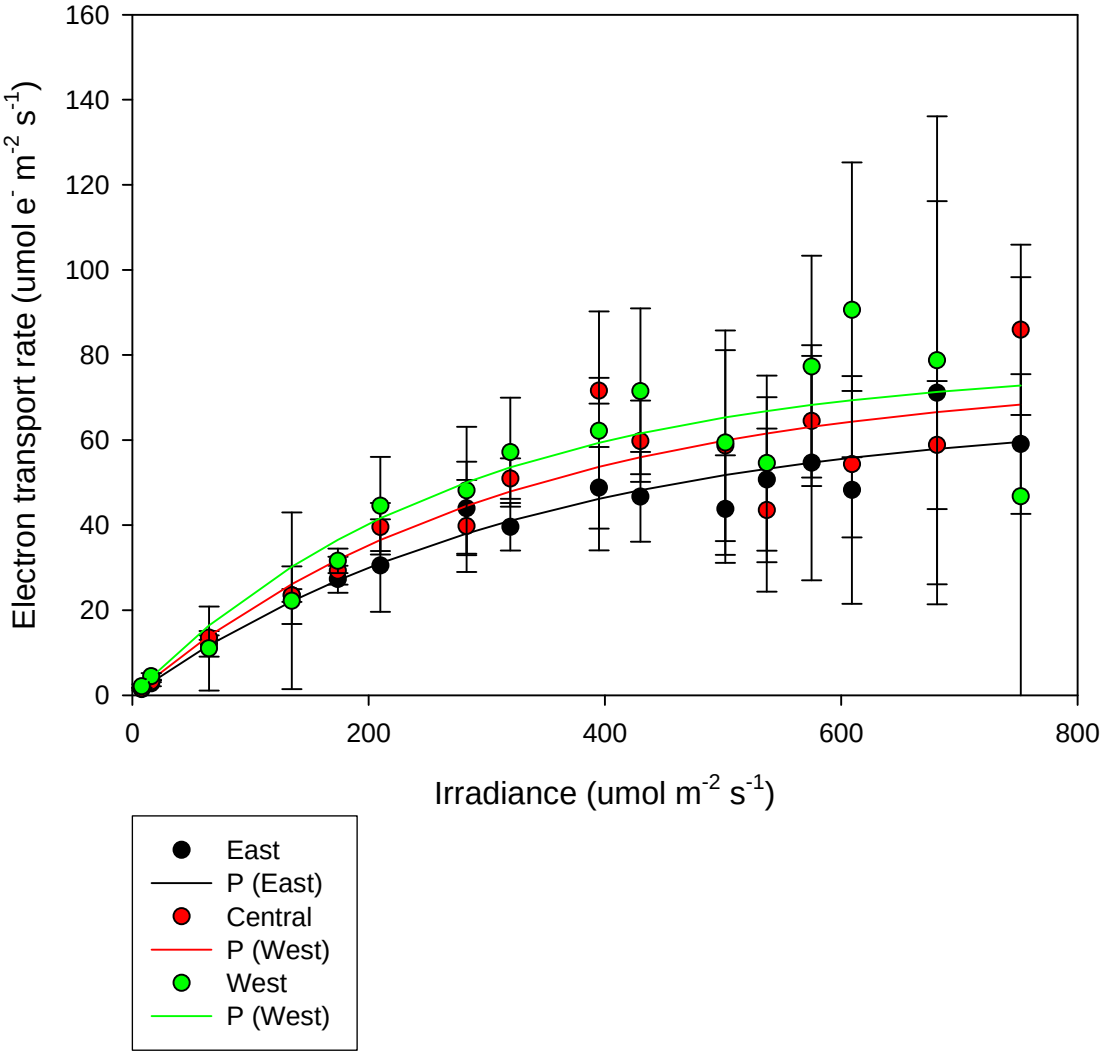

Figure 3.11. Rapid light curves measured with Phyto-PAM in surface waters off south western Eyre Peninsula, February/March 2006. Solid lines represent modelled results using the equation of Ralph and Gademann, (2005). Error bars indicate standard deviation.

4. Spatial and Temporal Variation in Phytoplankton Biodiversity: The Influence of Upwelling and Mixing

4.1. Abstract

Phytoplankton abundance and community composition was examined in the shelf waters of southern Australia, an area with strong seasonal differences in the influence of upwelling and mixing. Phytoplankton abundances were generally higher in near shore waters compared with offshore waters, and during the summer/autumn upwelling season compared with the winter/spring downwelling season. Three distinctly different phytoplankton communities were present in the region during the upwelling and downwelling seasons of 2004, and the upwelling season of 2005, with distinctions manifest in variations in the abundance of dominant types of phytoplankton, and differences in average cell sizes. In summer/autumn, waters influenced by upwelling were characterised by high phytoplankton abundances (particularly diatoms) and larger average cell sizes, while the warmer high-nutrient-low-chlorophyll (HNLC) waters in the region had lower phytoplankton abundances and smaller average cell sizes. The winter/spring community was made up of low abundances of relatively large cells. Diatoms always dominated, but evidence of Si limitation of further diatom growth suggests there may be an upper limit to diatom productivity in the region. The maximum observed diatom concentration of ~164,000 cells L^{-1} occurred in February/March 2004, in an area influenced by the upwelled water mass. Variations in phytoplankton biodiversity in the shelf waters of southern Australia appear to be related to variations in the influence of upwelling in the region.

4.2. Introduction

As micro-organisms in a dynamic environment, phytoplankton are dependent on oceanographic processes like upwelling and vertical mixing to bring nutrients from depths below the euphotic zone to levels where they may be utilized for photosynthesis (Margalef 1978). The dynamic nature of these processes means both nutrients and phytoplankton may be distributed randomly through the water column, and phytoplankton may be exposed to constantly fluctuating nutrient supplies and irradiances. When considering the distribution and dynamics of the phytoplankton community in a given region, it is also necessary to understand the manner in which the physical environment influences individual cells and the community as a whole.

For growth to proceed in lit areas of the water column, nutrients must be available in sufficient levels for phytoplankton use, and must be replenished when levels become too low. Processes like upwelling and turbulent vertical mixing bring nutrient rich water from great depths into the euphotic zone, where they may be utilized for growth via photosynthesis (Margalef 1978). In this way, variations in the physical environment greatly influence the ability of phytoplankton to photosynthesise and grow by effectively determining the availability of nutrients in the euphotic zone.

While extremely effective at redistributing nutrients and other suspended particles on large scales in the euphotic zone, turbulent mixing is only effective across distances of greater than a few millimeters. The distribution of nutrients at scales less than 1 mm relies on molecular diffusion (mixing caused by the random motion of molecules) and is greatly influenced by the boundary layer that forms around individual cells (Mann and Lazier 1996). Turbulence is unable to transport nutrients across the boundary layer to the surface of the cell, and cells must rely on the much

slower process of molecular diffusion. In this situation diffusion limitation may become a problem, as the nutrients used up in the water surrounding the cell are very slowly replenished. The viscous forces of the surrounding water dominate organisms in the 1-10μm size range, and molecular diffusion provides a faster nutrient supply through the boundary layer than water movement (Mann and Lazier 1996). Larger diatoms may overcome diffusion limitation by sinking through the water column during periods of stratification, but only the largest cells (>10 μm) are able to sink fast enough to get any significant increase in nutrient availability. Sinking also has its disadvantages; organisms may sink out of the euphotic zone, thus replacing nutrient limitation with light limitation. Periods of vertical mixing are required to keep cells suspended in the euphotic zone.

The size of phytoplankton that dominates a phytoplankton community depends largely on the nutrient status of the surrounding water. Smaller cells are more effectively able to acquire and use nutrients than larger cells, and thus have an advantage when nutrients are in short supply (Raven 1998). This is due to the combined effect of a thinner boundary layer (and thus reduced impact of diffusion limitation) and a large surface area to volume ratio, which provides a larger area for solute exchange per unit volume (Raven 1998). In upwelling areas with abundant nutrient supplies, larger diatoms tend to dominate. In these regions, the principal form of nitrogen is nitrate (or 'new' nitrogen), which can be stored in the vacuole, giving larger cells an advantage in competing for nitrogen in this situation (Stolte and Riegman 1995). Silica is typically also present in high concentrations in upwelled water (Bidle and Azam 1999; Ragueneau *et al.* 2002), providing diatoms with sufficient levels of the resources required to dominate the community (Brzezinski *et al.* 1990; Sommer 1994). The turbulence present in upwelling areas reduces the

impact of diffusion limitation due to the large boundary layer of large cells, and ensures the large cells remain suspended in the euphotic zone.

The eastern Great Australian Bight (EGAB) in South Australia is characterised by a dynamic, highly variable circulation that drives large between- and within-season differences in water mass characteristics. The prevailing shelf/slope circulation in the EGAB during the upwelling season leads to the formation of a pool of cold, upwelled water in a bottom layer on the shelf south west of Kangaroo Island and south of Eyre Peninsula, the Kangaroo Island pool (McClatchie *et al.* 2006; Middleton and Bye 2007). Coastal upwelling creates an isolated upwelling-influenced hotspot of primary productivity off south west Kangaroo Island (SWKI), with a larger volume of upwelled water brought to the surface off south western Eyre Peninsula (SWEP) influencing nearshore central and western regions of the EGAB (Chapter 2). Offshore waters, especially those of the central and western regions of the EGAB most influenced by the GAB warm pool (McClatchie *et al.* 2006), are less productive (Chapter 2). There are, however, large within-season variations in this characteristic circulation pattern that may significantly affect the overall enrichment and productivity of the upwelling season (Middleton and Bye 2007) (Chapter 3). During the downwelling season, nutrient enrichment via deepwater upwelling is suppressed, and the water column is well mixed. Lower irradiances and shorter daylengths drive lower rates of primary productivity in the EGAB at this time (Chapter 3). These spatial and temporal variations in water mass characteristics and productivity in the EGAB may be driving variations in phytoplankton abundance and community composition.

To date there have been few published studies concerning phytoplankton in the EGAB. The only information for the region consists of estimations of standing stock

via surface chlorophyll *a* measurements (Motoda *et al.* 1978; Kampf *et al.* 2004; McClatchie *et al.* 2006; Ward *et al.* 2006). Little is known about the abundance, composition, and spatial and temporal distribution of the phytoplankton community, although recent studies have been completed in nearby southern Spencer Gulf (van Ruth *et al.* 2008) and Gulf St Vincent (van Ruth 2008). This study represents the first intensive investigation of the phytoplankton community in the EGAB, and was designed to evaluate the hypothesis that spatial and temporal variations in phytoplankton abundance, distribution and community composition in the EGAB are driven by variations in the influence of upwelling on shelf waters in the region. It aims to determine whether the composition of the phytoplankton community can be used to differentiate between the main water masses present in the EGAB, the well mixed winter water mass, the GAB warm pool and the upwelled Kangaroo Island pool.

4.3. Methods

Sampling was conducted during cruises aboard the *RV Ngerin* in February/March and September 2004, and February/March 2005. Eighteen stations were sampled in February/March, with 6 stations sampled in September (Fig. 4.1). Samples were collected at three depths via niskin bottle; 3 m, the deep chlorophyll maximum (DCM) as determined from CTD casts (which generally occurred at or below the thermocline, see chapters 2 and 3), and 10 m below the DCM. One litre samples were fixed with Lugols iodine and returned to the laboratory for identification.

Identification of phytoplankton species to genus level was done via light microscopy using the taxonomic guides of Tomas (1997), Horner (2002), Hallegraef (2002) and Wilkinson (2005). Samples were concentrated 10* prior to counting. A

100 ml subsample from the one litre sample was allowed to settle in a 100 ml measuring cylinder. After 24 hours, the top 90 ml was carefully discarded using a pipette, with the bottom 10 ml retained for analysis. After gentle inversion to re-suspend cells, one ml of this concentrate was pipetted into a Sedgewick-Rafter chamber for counts. Enumeration was continued until 100 specimens of the most dominant species, or contents of the entire one ml subsample, were counted. Phytoplankton biomass was further assessed by converting chlorophyll *a* concentrations reported in chapters 2 and 3 to carbon, using a carbon to chlorophyll *a* ratio of 40:1. Average cell size was calculated by dividing biomass (in mg C m^{-3}) by total number of cells (Irigoien *et al.* 2004).

Regression analyses were performed on abundance values to examine differences in phytoplankton densities between years, seasons, regions and water depths in the EGAB. Annual and seasonal variations in phytoplankton biomass, average cell size and species diversity indices were examined via paired Student's t-tests (Sokal and Rohlf 1995). Annual comparisons were made using data collected from all stations during February/March 2004 and 2005. Seasonal comparisons between February/March 2004, September 2004 and February/March 2005 used only data collected at the six red stations in Figure 4.1. Assumptions of normality and homoscedasticity were examined prior to these analyses, and ln transformation applied to all data to meet these assumptions. Significant differences were indicated by probability values <0.05.

Spatial correlations between physical parameters, phytoplankton abundances, nutrient concentrations, phytoplankton biomass and species diversity indices were examined via Mantel tests in PC-Ord 5 (McCune and Mefford 1999). Essentially, the tests were looking for associations between the distributions of these parameters

around a set of stations. Data were tested for 19 stations across the EGAB in February/March 2004 and 17 stations in February/March 2005. The five matrices compared in the tests included (1) Physical data (temperature and density, from chapters 2 and 3), (2) Diatom abundance data, (3) Dinoflagellate abundance data, (4) Nutrient data (Si, NO_x, FRP, in µmol L^{-1}, from chapters 2 and 3), and (5) Species diversity indices. The distance measure used was Sorensen (Bray-Curtis). The standardised Mantel statistic (r) was calculated via randomization using the Monte Carlo test. Species diversity indices (Species richness (S), Shannon`s diversity index (H), Evenness (E), Simpsons diversity index for infinite population (D)) were calculated using the row and column summary function in PC-Ord 5 (McCune and Mefford 1999). Significant differences were indicated by p values <0.10.

Variations in phytoplankton community structure were examined via non-metric multidimensional scaling (NMS) ordination in PC-Ord 5. Variations between years and regions were examined using data collected in nearshore and offshore stations in the east, central and western regions during February 2004 and February 2005. Variations between sampling periods were examined using data collected from nearshore central and western regions in February and September 2004, and February 2005 (Fig. 4.1). PerMANOVAs were performed on abundance data using methods outlined in Anderson (2001), to examine potential differences in community structure between years, regions, seasons, and depths using a significance value of 0.05. Further examinations of any significance differences were made via pair-wise comparisons corrected for multiple comparisons via the Bonferroni procedure (α = 0.003 for comparisons between regions; α = 0.017 for comparisons between seasons). Indicator species analyses were run to determine the genera that were contributing significantly to differences in community structure between regions and seasons.

Indicator values were calculated using the method of Dufrene & Legendre (1997). Relative abundances were calculated as the average abundance of a given genus in a given group of samples over the average abundance of that genus in all samples, expressed as a percentage. Relative frequencies indicate the percentage of samples in a given group where a given genus is present. Only genera with relative abundances and relative frequencies >40% were considered to be indicators of differences in community composition between groups.

4.4. Results

4.4.1. Phytoplankton abundance and composition

Phytoplankton abundances were generally higher near shore compared with offshore, and in February/March compared with September (Fig. 4.2). In all seasons, regions and depths the phytoplankton community was dominated by diatoms and dinoflagellates. Flagellates were generally less abundant and numbers fluctuated. For example, in February/March 2005 they were present in all regions but not in February/March and September 2004.

The diatom community was dominated by *Pseudonitzschia* in February/March 2004 (61%) and 2005 (36%), September 2004 (42%). Other dominant diatoms included *Leptocylindrus* (16% - 26%), *Thalassiosira* (13%) and *Chaetoceros* (17%). Dominant dinoflagellates included *Gymnodinium* (30%), *Prorocentrum* (24%) and *Ceratium* (18%) in February/March 2004, *Dinophysis* (71%) in September 2004, and *Prorocentrum* (64%) and *Gymnodinium* (12%) in February 2005.

Highest mean diatom abundance (163,333 ± 58,951 cells L^{-1}) occurred at the DCM at the nearshore central region during Feb/Mar 04 (Fig. 4.2) but dinoflagellate

and flagellate abundances were highest at the DCM in the nearshore west region during Feb/Mar 04 (23,229 ± 1,000 cells L^{-1} and 13,411 ± 577 cells L^{-1} respectively, Fig. 4.2). Diatom abundances varied between season ($p = 0.014$), whereas dinoflagellate and flagellates abundances differed between years ($p = 0.001$).

4.4.2. Species diversity and cell size

Mantel tests on February/March 2004 data indicated that there were significant associations between diatom and dinoflagellate abundances and species diversity indices ($p = 0.001$, $r = 0.332$; $p = 0.018$, $r = 0.195$). In September 2004, there was an association between nutrient concentrations and diatom abundances ($p = 0.025$, $r = -0.644$), between physical parameters and species diversity ($p = 0.005$, $r = 0.835$), nutrient concentrations and species diversity ($p = 0.029$, $r = -0.313$), and dinoflagellate abundances and species diversity ($p = 0.044$, $r = 0.542$). Tests on February/March 2005 data indicate significant associations between physical parameters and the diatom community ($p = 0.055$, $r = 0.192$), and between dinoflagellate abundances and species diversity ($r = 0.300$, $p = 0.022$).

Average cell sizes were significantly larger in February/March 2004 than in February/March 2005 ($T = 2.62$, $P = 0.02$, Fig. 4.3), with significantly higher diversity in February/March 2004 ($T = 5.11$, $P = 0.0001$, Fig. 4.3). Average cell sizes were significantly larger in September 2004 compared to the two upwelling seasons ($T < -9.00$, $P < 0.001$, Fig. 4.4), but there were no significant seasonal differences in diversity ($T < 1.95$, $P > 0.1$, Fig. 4.4).

4.4.3. Spatial and temporal variation

NMS ordination indicates similarity in the EGAB phytoplankton communities of February/March 2004 and February/March 2005, although there were outliers in the 2004 data (Fig. 4.5). Further examination suggests that these outliers are driven by variations in community structure in the eastern region. There is a clear similarity in the communities of the nearshore east and offshore east regions (Fig. 4.5). The nearshore central and nearshore west stations also group together, as do stations in the offshore central and offshore west regions (Fig. 4.6). These patterns were confirmed in PerMANOVA results from February/March 2004 and February/March 2005 data, where there were differences in community structure between years and regions, with a significant interaction confirming the difference in community structure in the eastern region identified by the outliers in Figure 4.5 (Table 4.1). Corrected pair-wise comparisons indicated that the community in the nearshore eastern region was different from all other regions ($p < 0.001$) except the nearshore western region ($p = 0.02$). The community in the nearshore central region was not different from the nearshore western region ($p = 0.193$), but was different from communities in the offshore central and western regions ($p < 0.001$). The community in the offshore eastern region was not different from the offshore central region ($p = 0.014$) but was different from all other regions ($p < 0.001$). There was no difference between the communities of the offshore central and offshore western regions ($p = 0.253$). The phytoplankton communities of February/March 2004 and February/March 2005 were homogenous throughout the water column, with no differences in community structure between depths ($p > 0.1$).

Indicator genera for the nearshore eastern region in February/March 2004 and 2005 included *Cylindrotheca*, and *Ceratium* (Table 4.2). Nearshore central indicators

included such potentially toxic/problematic genera as *Gymnodinium*, *Dinophysis*, and *Chaetoceros* (Table 4.2). *Pseudonitzschia* was found in all February samples from the nearshore west region, with the highest mean abundance observed for any genus. 80% of all *Asterionellopsis* occurrences in February were in the nearshore west region, where the genus was present in relatively high abundances but few samples during February/March 2004 and 2005 (Table 4.2).

NMS ordination of seasonal data from the nearshore central and western regions reveals a clear separation between the February/March and September data, and some suggestion of a difference in community structure between February/March 2004 and February/March 2005 samples (Fig. 4.7). PerMANOVA results indicate a significant difference in community structure between sampling periods as suggested by Figure 4.5, with no difference between regions, but a significant interaction between sampling period and region (Table 4.3). Corrected pair-wise comparisons confirm the pattern outlined in Figure 4.7, with the communities in February/March 2004 and 2005 differing significantly from the community in September 2004 ($p < 0.001$). The community in February/March 2004 was also different from the community in February/March 2005 ($p < 0.001$), as indicated in Figure 4.7.

Indicator genera in February/March 2004 include the diatoms *Pseudonitzschia* and *Leptocylindrus* which were present in all samples collected at high mean abundances. 76% of all occurrences of the potentially toxic dinoflagellate *Dinophysis* in the EGAB were during February/March 2004, but the genus was present in low mean abundances during these months (Table 4.4). The vast majority of occurrences of the diatoms *Rhizosolenia*, *Asterionellopsis*, *Guinardia*, and *Cerataulina* were in February/March 2005. A high proportion of occurrences of the potentially toxic

dinoflagellate *Prorocentrum* were also found in February/March 2005, with the genus present in all samples during these months (Table 4.4).

4.5. Discussion

Diatoms dominated the phytoplankton community in the EGAB, but evidence of Si limitation of further diatom growth suggests there may be an upper limit to diatom productivity in the region, which may restrict overall water column primary productivity. The maximum observed diatom concentration was ~164,000 cells L^{-1}. Using a mean average cell size of 3,792 pg C $cell^{-1}$ (from Fig. 4.3), and a Si:C conversion factor of 0.2 g Si g C^{-1} (Paasche and Ostergren 1980), the estimated mean diatom cell would contain ~758 pg Si. A doubling of the population from 82,000 cells L^{-1} to 164,000 cells L^{-1} would require 82,000 * 758 pg Si L^{-1} (62 µg Si L^{-1}). Si concentrations in the nearshore central region in February/March 2004, the time of the maximum diatom concentration, were <56 µg L^{-1} (chapter 3). This suggests that there is very little surplus silica in the system, and implies Si limitation of further diatom growth in the region.

There were significant spatial and temporal variations in EGAB phytoplankton biomass and diversity, but results were in agreement with global phytoplankton biodiversity patterns outlined in Irigoien *et al.* (2004), who observed maximum diversity at mid-level biomass and low diversity during blooms. Variations in phytoplankton biodiversity in the EGAB appear to be driven by between- and within-season variations in circulation that change the influence of upwelling (and thus the supply of Si) in the region.

The EGAB is characterised by significant spatial and temporal variation in meteorology and oceanography which lead to the formation of distinctly different

water masses that may alternate in their influence on overall water column productivity (Chapters 2 and 3). This study indicates that these variations may influence phytoplankton abundance, distribution and community composition. Highest phytoplankton abundances in the EGAB occurred during the summer/autumn upwelling seasons (when rates of primary productivity were an order of magnitude higher than those during periods of downwelling) and were associated with the upwelled water mass (Chapter 3). It appears that there were three distinctly different communities present in the EGAB during the upwelling and downwelling seasons of 2004, and the upwelling season of 2005, with distinctions manifest in variations in the abundance of dominant types of phytoplankton, and differences in average cell sizes. Waters influenced by the Kangaroo Island pool appear to be characterised by high phytoplankton abundances (particularly diatoms) and larger average cell sizes, while the waters of the GAB warm pool have lower phytoplankton abundances and smaller average cell sizes. The winter (downwelling) community was made up of low abundances of relatively large cells. Possible explanations for these characteristic communities are outlined in the following paragraphs.

The upwelling season of 2004 was relatively strong, with extended periods of upwelling and stratification, and sampling in February/March 2004 took place during an upwelling event. This season was characterised by longer periods of upwelling favourable conditions, providing opportunity for larger diatoms to thrive.

The downwelling season of 2004 was stronger than the long term mean, and sampling took place during a strong downwelling event. Waters were well mixed, and biomass was reduced due to lower primary productivity caused by decreased irradiances and shorter daylengths (Chapter 3). Despite this, average cell sizes were still relatively large, with nitrate and silica concentrations at this time adequate

enough to maintain the dominance of diatoms (Chapter 3). There was no association between physical factors and phytoplankton abundances as to be expected in a well mixed water column. However, the strong association between nutrient concentrations and diatoms suggests that diatoms may only be found in areas where nutrient concentrations are high. The lack of association between dinoflagellates and nutrient concentrations suggests the smaller dinoflagellates, which are less susceptible to fluctuating nutrient concentrations, and better able to compete for nutrients at low concentrations, are found throughout the well mixed water column.

The upwelling season of 2005 was weak, with an upwelling index less than the long term-mean (Chapter 3). It was characterised by many downwelling events with few short periods of upwelling favourable winds, and sampling was conducted during a relatively strong downwelling event. As a result, one expects the water column through the 2005 upwelling season to be more mixed than the water column in February/March 2004 (there are signs of recent mixing events in temperature and density depth profiles presented in Chapter 3), having been subject to less upwelling and enrichment in the lead up to sample collection, with a community reflecting this fact. Indeed, the community was made up of smaller cells in February/March 2005, and the high diversity at lower biomass suggests many smaller species in the community. However, there was also a significant association between physical factors and diatoms, reflecting the upwelling signature of a region encompassing clearly defined water masses with distinct physical/biological characteristics, such as might be found during upwelling events, as outlined in Chapter 2. The association between dinoflagellates and species diversity indices suggests that dinoflagellates were driving variations in diversity in 2005. In similar results to February/March

2004, there were no associations between nutrient concentrations and phytoplankton abundances.

Clear spatial and temporal variations in phytoplankton community composition have been identified in this study. Indicator species analyses (Tables 4.3 and 4.4) suggest that spatial and temporal differences are driven by the presence of different genera. However, closer inspection reveals that many of these indicator genera are found in the EGAB in all regions, seasons and years of this study, and their indicator status for a given time or place is due to their presence in significantly higher abundances in that region. Indeed, the diatoms *Chaetoceros*, *Coscinodiscus*, *Guinardia*, *Leptocylindrus*, *Navicula*, *Pseudonitzschia*, *Skeletonema*, *Thalassiosira*, and *Thalassionema*, which showed up as significant indicators of spatial and temporal variations in community composition, are commonly found to dominate coastal phytoplankton communities in Australian waters (Dakin and Colefax 1940; Hallegraeff and Jeffrey 1993; Hanson *et al.* 2007; Thompson *et al.* 2007; van Ruth et al 2008).

Spatial and temporal variations in abundances of common genera in the EGAB may be related to variations in the influence of upwelling in the region. The higher abundances of common genera in the nearshore central and western regions may be driven by exposure of these regions to a larger volume of highly productive upwelled water than the more isolated nearshore eastern region, which may allow high rates of primary productivity to be maintained in these regions for longer periods of time, promoting significant increases in phytoplankton abundance. The absence of indicator genera in September 2004 data suggest that differences between the February/March and September communities are most likely due to significantly lower rates of primary productivity that occur during September 2004, driven by the

absence of upwelling and, low irradiances, and short daylengths (Chapter 3). Variations in the timing and intensity of mixing/stratification events between the upwelling seasons of 2004 and 2005 have been shown to significantly affect rates of primary productivity between years in the upwelling influenced regions of the EGAB (Chapters 2 and 3), and appear to promote variations in phytoplankton abundance and community composition.

Community variations between February 2004 and February 2005 appear to be driven by differences in the nearshore western region in February 2005, which groups closely with the community of September 2004 (Fig. 4.5), and may indicate a transition between the winter and summer phytoplankton communities. The change in seasons in the EGAB is defined by the increased influence of upwelling through summer, with water upwelled from off the shelf south of Kangaroo Island and driven north and then west along constant depth contours (Middleton and Bye 2007). Regions in the west of the EGAB are the last to be influenced by the upwelled water mass and may thus be the last to make the transition from a winter to a summer community. The upwelling season of 2005 was particularly weak (Chapter 3), and the weakened influence of the upwelling in the nearshore western region may be an explanation for the similarities of the February 2005 community with the phytoplankton community of September 2004.

There were no significant differences detected in phytoplankton abundances or community structure with depth, which supports the suggestion in chapter 3 that mixing during downwelling events within the upwelling season allows phytoplankton to entrain from the surface mixed layer into the enriched upwelled water mass, providing the seed for a burst of productivity during the next upwelling event. The reverse may also be true, where phytoplankton from the productive upwelled waters

are mixed into the surface layer following an upwelling event. Both mechanisms promote homogeneity of the phytoplankton community with depth.

4.6. References

Anderson, M. J. (2001). A new method for non-parametric multivariate analysis of variance. *Austral Ecology* **26**(32-46).

Bidle, K. D. and Azam, F. (1999). Accelerated dissolution of diatom silica by marine bacterial assemblages. *Nature* **397**: 508-512.

Brzezinski, M. A., Olson, R. J. and Chisholm, S. W. (1990). Silicon availability and cell cycle progression in marine diatoms. *Marine Ecology Progress Series* **67**: 83-96.

Dakin, W. J. and Colefax, A. N. (1940). The plankton of the Australian coastal waters off New South Wales. Part 1. Sydney, Australian Publishing Company.

Dufrene, M. and Legendre, P. (1997). Species assemblages and indicator species: the need for a flexible asymmetrical approach. *Ecological Monographs* **67**: 345-366.

Hallegraeff, G. M. (2002). Aquaculturalists' Guide to Harmful Australian Microalgae. Hobart, School of Plant Science, University of Tasmania.

Hallegraeff, G. M. and Jeffrey, S. W. (1993). Annually recurrent diatom blooms in spring along the New South Wales coast of Australia. *Marine and Freshwater Research* **44**: 325-334.

Hanson, C. E., Waite, A. M., Thompson, P. A. and Pattiaratchi, C. B. (2007). Phytoplankton community structure and nitrogen nutrition in Leeuwin Current and coastal waters off the Gascoyne region of Western Australia. *Deep Sea Research Part II: Topical Studies in Oceanography* **54**(8-10): 902-924.

Horner, R. A. (2002). A taxonomic guide to some common marine phytoplankton. Bristol, Biopress Ltd.

Irigoien, X., Huisman, J. and Harris, R. P. (2004). Global biodiversity patterns of marine phytoplankton and zooplankton. *Nature* **429**: 863-867.

Kampf, J., Doubel, M., Griffin, D. A., Matthews, R. and Ward, T. M. (2004). Evidence of a large seasonal coastal upwelling system along the southern shelf of Australia. *Geophysical Research Letters* **31**(L09310): doi:10.1029/2003GL019221.

Mann, K. H. and Lazier, J. R. N. (1996). Dynamics of marine ecosystems. London, Blackwell Science.

Margalef, R. (1978). Life forms of phytoplankton as survival alternatives in an unstable environment. *Oceanologica Acta* **1**: 493-509.

McClatchie, S., Middleton, J. F. and Ward, T. M. (2006). Water mass analysis and alongshore variation in upwelling intensity in the eastern Great Australian Bight. *Journal of Geophysical Research* **111**(C08007): doi:10.1029/2004JC002699.

McCune, B. and Mefford, M. J. (1999). PC-ORD. Multivariate Analysis of Ecological Data, Version 5., MjM Software Design, Gleneden Beach, Oregon, USA.

Middleton, J. F. and Bye, J. A. T. (2007). A review of the shelf slope circulation along Australia's southern shelves: Cape Leeuwin to Portland. *Progress in Oceanography* **75**: 1-41.

Motoda, S., Kawamura, T. and Taniguchi, A. (1978). Differences in productivities between the Great Australian Bight and the Gulf of Carpentaria, Australia, in Summer. *Marine Biology* **46**: 93-99.

Paasche, E. and Ostergren, I. (1980). The annual cycle of plankton diatom growth and silica production in the inner Oslofjord. *Limnology and Oceanography* **25**(3): 481-494.

Ragueneau, O., Chauvaud, L., Leynaert, A., Thouzeau, G., Paulet, Y. M., Bonnet, S., Lorrain, A., Grall, J., Corvaisier, R., Le Hir, M., Jean, F. and Clavier, J. (2002). Direct evidence of a biologically active coastal silicon pump: Ecological implications. *Limnology and Oceanography* **47**: 1849-1854.

Raven, J. A. (1998). The twelfth Tansley Lecture. Small is beautiful: the picophytoplankton. *Functional Ecology* **12**: 503-513.

Sokal, R. R. and Rohlf, F. J. (1995). Biometry. United States of America, W.H. Freeman.

Sommer, U. (1994). Are marine diatoms favoured by high Si:N ratios? *Marine Ecology Progress Series* **115**: 309-315.

Stolte, W. and Riegman, R. (1995). Effect of phytoplankton cell size on transient state nitrate and ammonium uptake kinetics. *Microbiology* **141**: 1221-1229.

Thompson, P. A., Pesant, S. and Waite, A. M. (2007). Contrasting the vertical differences in the phytoplankton biology of a dipole pair of eddies in the south-eastern Indian Ocean. *Deep Sea Research Part II: Topical Studies in Oceanography* **54**(8-10): 1003-1028.

Tomas, C. R., Ed. (1997). Identifying marine phytoplankton. San Diego, Academic Press.

van Ruth, P., Thompson, P., Blackburn, S., and Bonham, P. (2008) Temporal and spatial variability in phytoplankton abundance and community composition, and pelagic biogeochemistry in the tuna farming zone *in* Tanner, J.E. and J. Volkman (Eds.) 2008. Aquafin CRC - Southern Bluefin Tuna Aquaculture

Subprogram: Risk and Response – Understanding the Tuna Farming Environment. Technical report, Aquafin CRC Project 4.6, FRDC Project 2005/059. Aquafin CRC, Fisheries Research & Development Corporation and South Australian Research & Development Institute (Aquatic Sciences), Adelaide. SARDI Publication No F2008/000646-1, SARDI Research Report Series No 344, 287 pp.

van Ruth, P.D. (2008) Plankton in Gulf St Vincent and Investigator Strait. *In* Natural History of Gulf St Vincent. Shepherd, S.A., Bryars, S., Kirkegaard, I., Harbison, P., and Jennings, J.T. (eds.) Royal Society of South Australia inc. pp 317-323.

Ward, T. M., McLeay, L. J., Dimmlich, W. F., Rogers, P. J., McClatchie, S., Matthews, R., Kampf, J. and van Ruth, P. D. (2006). Pelagic ecology of a northern boundary current system: effects of upwelling on the production and distribution of sardine (*Sardinops sagax*), anchovy (*Engraulis australis*) and southern bluefin tuna (*Thunnus maccoyii*) in the Great Australian Bight. *Fisheries Oceanography* **15**(3): 191-207.

Wilkinson, C. (2005) Common Microalgae of South Australia. South Australian Shellfish Quality Assurance Program.

4.7. Tables

Table 4.1. Results of PerMANOVA based upon the abundances of phytoplankton in the EGAB during February/March 2004 and February/March 2005.

Source	d.f.	SS	MS	F	p
Year	1	1.91	1.91	9.55	0.0002
Region	5	7.78	1.56	7.77	0.0002
Interaction (Year by Region)	5	4.29	0.86	4.29	0.0002
Residual	96	19.22	0.20		
Total	107	33.21			

Table 4.2. Results of indicator species analysis based upon the abundances of phytoplankton in different regions of the EGAB during February/March 2004 and February/March 2005. Region 1 = nearshore east, region 3 = nearshore central, region 5 = nearshore west. Mean abundances are ± standard error.

Genus	Region	Observed Indicator Value (IV)	IV from randomised groups Mean	IV from randomised groups S.Dev	p *	Mean abundance (cells L^{-1})	Relative abundance (%)	Relative frequency (%)
Cylindrotheca	1	21.8	8.6	3.70	0.0088	764 (±354)	56	39
Ceratium	1	24.7	11	4.42	0.0136	267 (±122)	44	56
Guinardia	3	30.1	7.8	3.79	0.0006	1,031 (±501)	77	39
Thalassiosira	3	43	18.2	5.01	0.0006	8,911 (±5,344)	61	78
Cerataulina	3	33.1	14.6	4.67	0.0036	8,711 (±3,227)	50	67
Coscinodiscus	3	24.4	8.3	3.48	0.004	178 (±67)	63	39
Gymnodinium	3	29	13.7	4.09	0.004	611 (±235)	47	61
Skeletonema	3	24.9	8.8	3.94	0.0044	2,067 (±1,037)	64	39
Thalassionema	3	37.4	19.3	6.21	0.0088	2,011 (±593)	55	61
Proboscia	3	26.8	15	3.78	0.01	997 (±298)	40	67
Chaetoceros	3	23.5	10.3	4.26	0.0124	1,056 (±557)	60	39
Dinophysis	3	21	10.4	3.89	0.0188	208 (±98)	54	39
Pseudonitzschia	5	38.6	25	3.85	0.0038	36,950 (±9,368)	39	100
Asterionellopsis	5	22.2	10.4	5.02	0.0292	3,311 (±2,511)	80	28

Table 4.3. Results of PerMANOVA based upon the abundances of phytoplankton in nearshore central and western regions of the EGAB during February/March 2004, September 2004 and February/March 2005.

Source	d.f.	SS	MS	F	p
Sampling period	2	6.95	3.48	20.06	0.0002
Region	1	0.25	0.25	1.47	0.17
Interaction (Sampling period by Region)	2	0.81	0.41	2.35	0.02
Residual	48	8.32	0.17		
Total	53	16.34			

Table 4.4. Results of indicator species analysis based upon the abundances of phytoplankton in nearshore central and western regions of the EGAB during February/March 2004, September 2004 and February/March 2005. Mean abundances are ± standard error.

Genus	Sampling period	Observed Indicator Value (IV)	IV from randomised groups Mean	IV from randomised groups S.Dev	p *	Mean abundance (cells L^{-1})	Relative abundance (%)	Relative frequency (%)
Eucampia	Feb-04	43.2	14.5	5.75	0.0002	591 (±260)	97	44
Thalassiosira	Feb-04	91.7	29.0	7.95	0.0002	12,589 (±5,259)	97	72
Pseudonitzschia	Feb-04	75.2	42.0	5.28	0.0002	54,722 (±8,935)	75	100
Skeletonema	Feb-04	36.4	14.8	6.02	0.003	2,067 (±1,037)	94	39
Dinophysis	Feb-04	42.0	19.5	6.05	0.005	258 (±97)	76	56
Proboscia	Feb-04	43.2	23.2	5.76	0.006	977 (±255)	55	78
Leptocylindrus	Feb-04	51.5	39.5	6.17	0.045	15,267 (±4,303)	51	100
Cerataulina	Feb-05	68.2	23.0	6.76	0.0002	13,550 (±4,161)	94	72
Rhizosolenia	Feb-05	55.6	14.2	5.79	0.0002	2,100 (±868)	100	56
Asterionellopsis	Feb-05	55.3	17.7	6.75	0.0002	4,094 (±2,475)	99	56
Prorocentrum	Feb-05	85.6	24.2	5.61	0.0002	1,911 (±313)	86	100
Guinardia	Feb-05	43.2	14.9	5.72	0.001	1,294 (±503)	97	44
Cylindrotheca	Feb-05	33.3	10.7	4.79	0.002	567 (±288)	100	33
Flagellate	Feb-05	48.6	29.4	5.63	0.006	1,239 (±310)	58	83
Navicula	Feb-05	40.6	20.1	5.96	0.008	406 (±131)	81	50
Thalassionema	Feb-05	47.8	32.2	6.96	0.030	2,489 (±805)	72	67

4.8. Figures

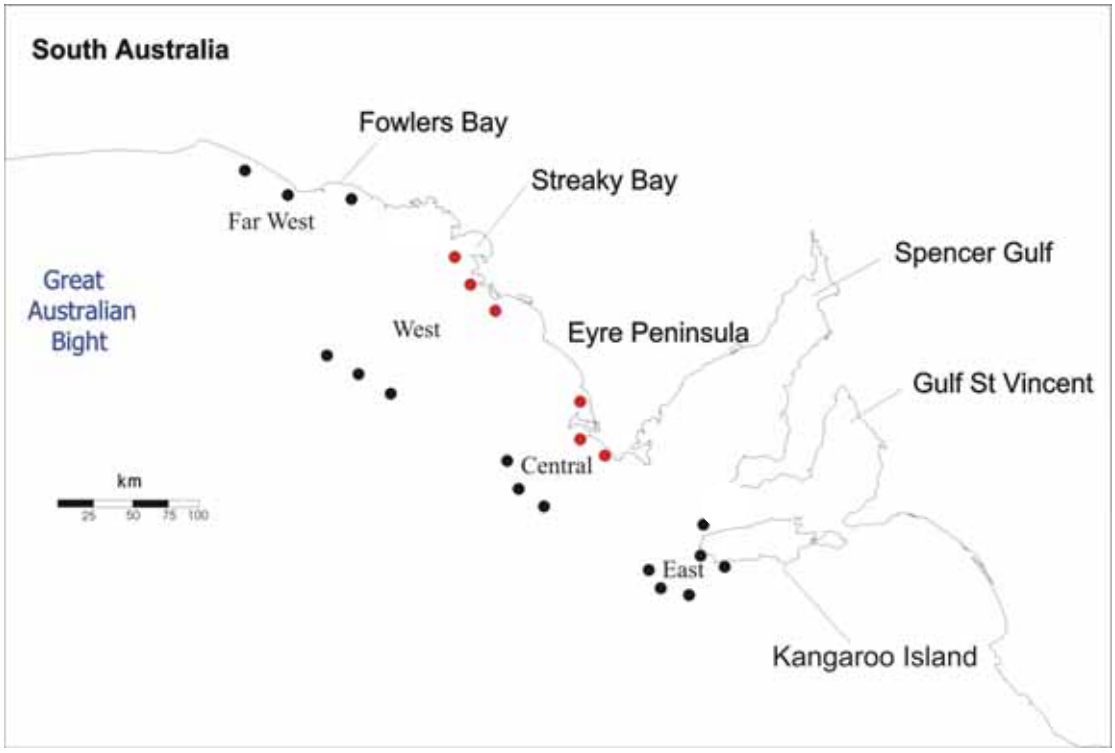

Figure 4.1. Phytoplankton sampling stations. Only red stations were sampled during September 2004. Far west stations were only sampled during February 2005.

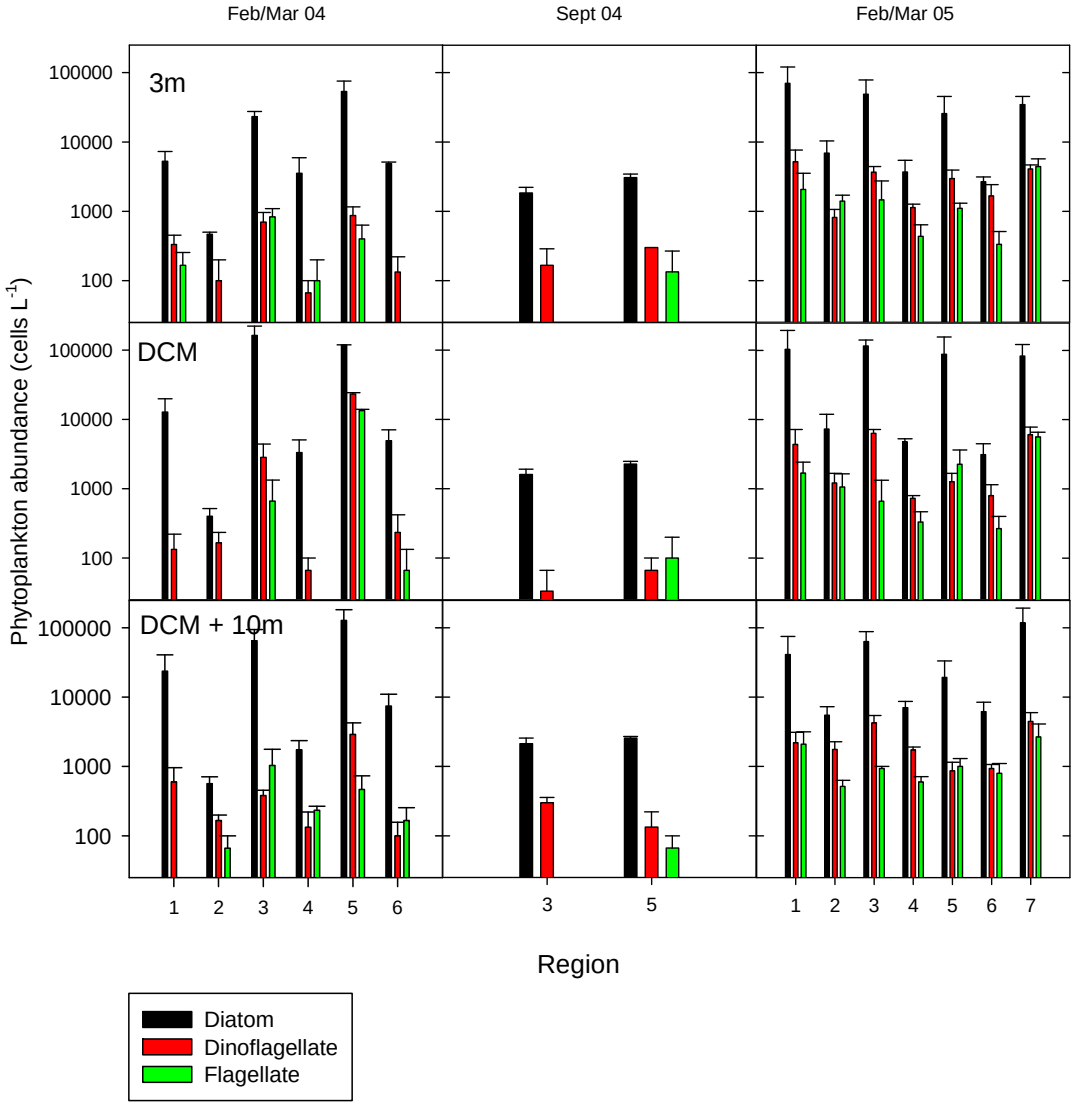

Figure 4.2. Temporal variation in phytoplankton abundance in the EGAB from samples collected at three depths (mean ± standard error, n = 3). Region 1 = nearshore east, region 2 = offshore east, region 3 = nearshore central, region 4 = offshore central, region 5 = nearshore west, region 6 = offshore west, region 7 = nearshore far west (see Fig. 4.1 for regions). Note the log scale on the y axis.

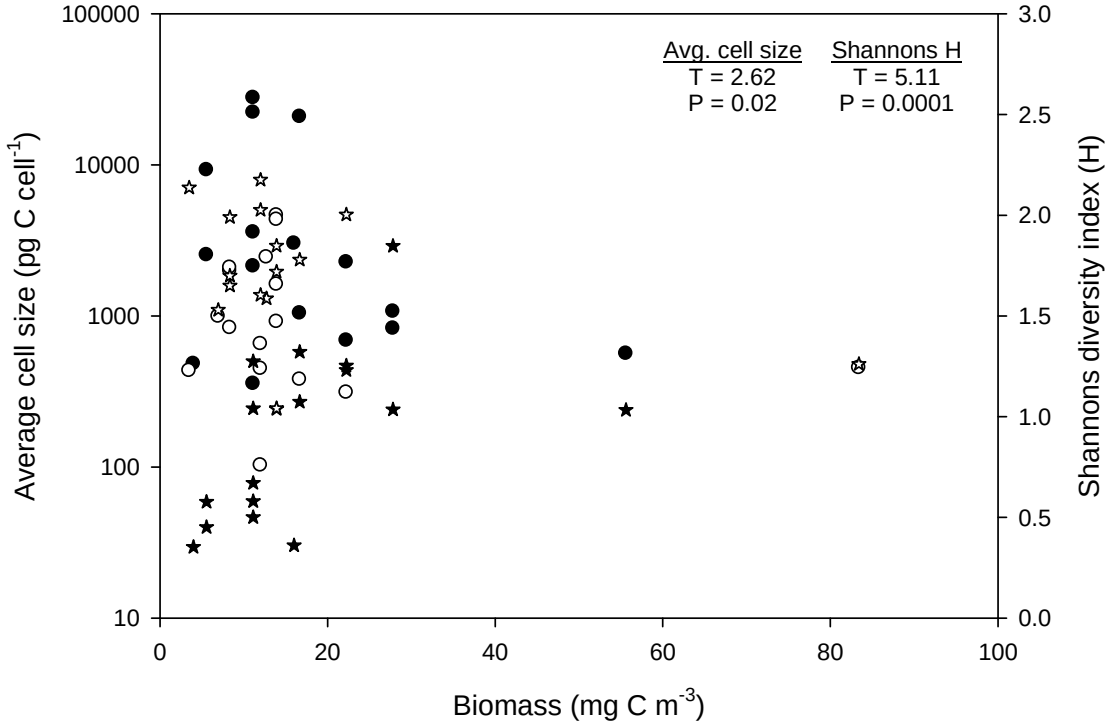

Figure 4.3. Annual variation in phytoplankton biomass, average cell size and diversity in the EGAB. Black symbols represent February/March 2004 data, white symbols represent February/March 2005 data. Circles represent average cell sizes, stars represent Shannon's diversity index. Note the log scale used for average cell size. Text indicates results from t-tests.

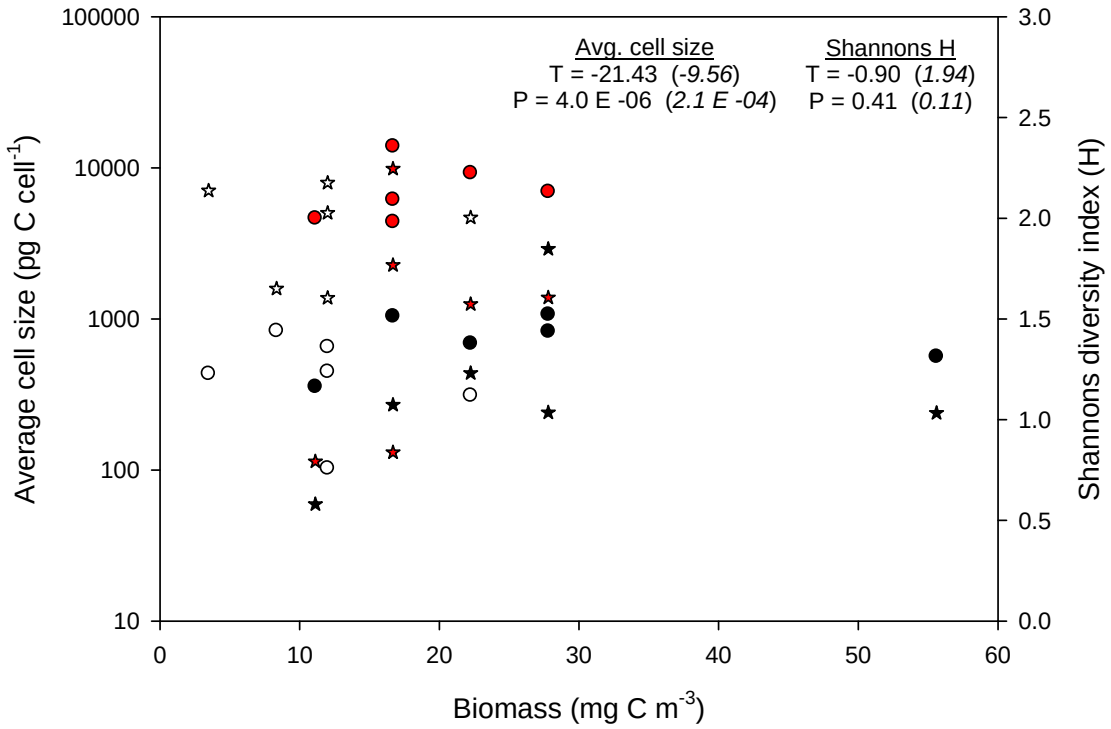

Figure 4.4. Seasonal variation in phytoplankton biomass, average cell size and diversity in the EGAB. Black symbols represent February/March 2004 data, red symbols represent September 2004 data, white symbols represent February/March 2005 data. Circles represent average cell sizes, stars represent Shannon's diversity index. Note the log scale used for average cell size. Text indicates results from t-tests comparing February/March 2004 and September 2004 data. Italicised values in parentheses are from comparisons of September 2004 and February/March 2005 data.

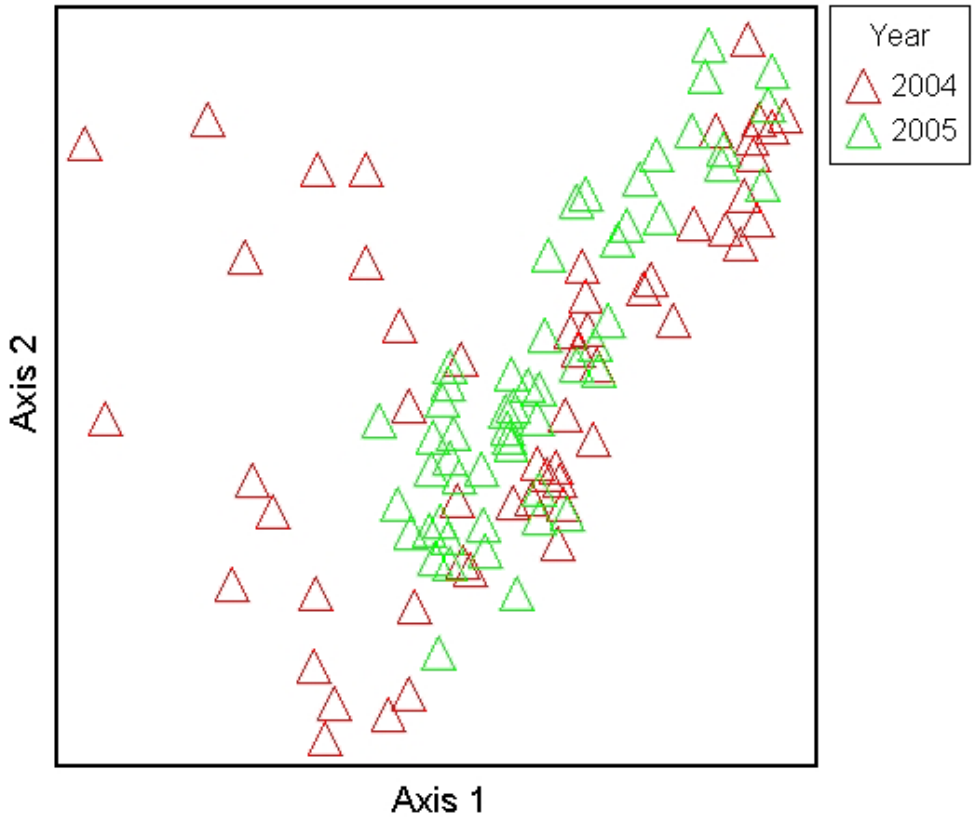

Figure 4.5. NMS ordination of variation in phytoplankton community composition in the EGAB during Feb/Mar 2004 and Feb/Mar 2005. Stress = 15.1 %.

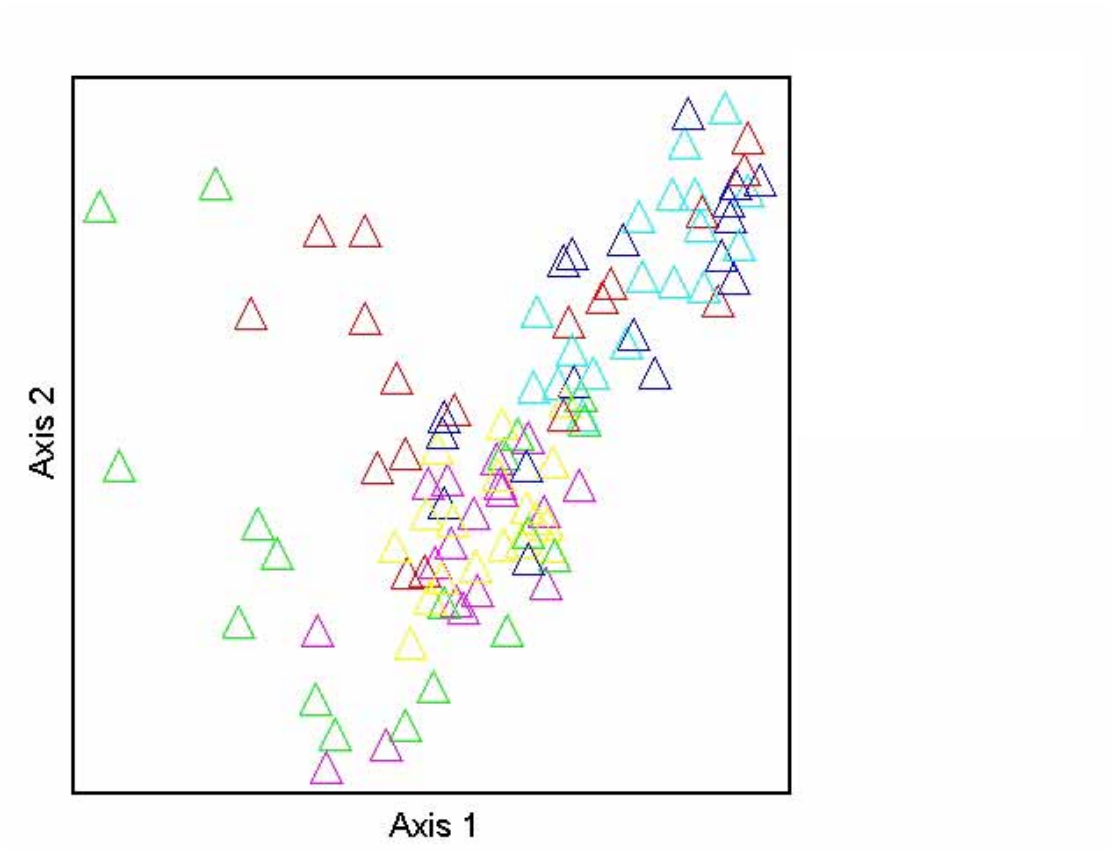

Figure 4.6. NMS ordination of spatial variation in phytoplankton community composition in the EGAB during Feb/Mar 2004 and Feb/Mar 2005. Regions as follows: red = nearshore east, green = offshore east, Light blue = nearshore central, pink = offshore central, dark blue = nearshore west, yellow = offshore west. Stress = 15.1 %.

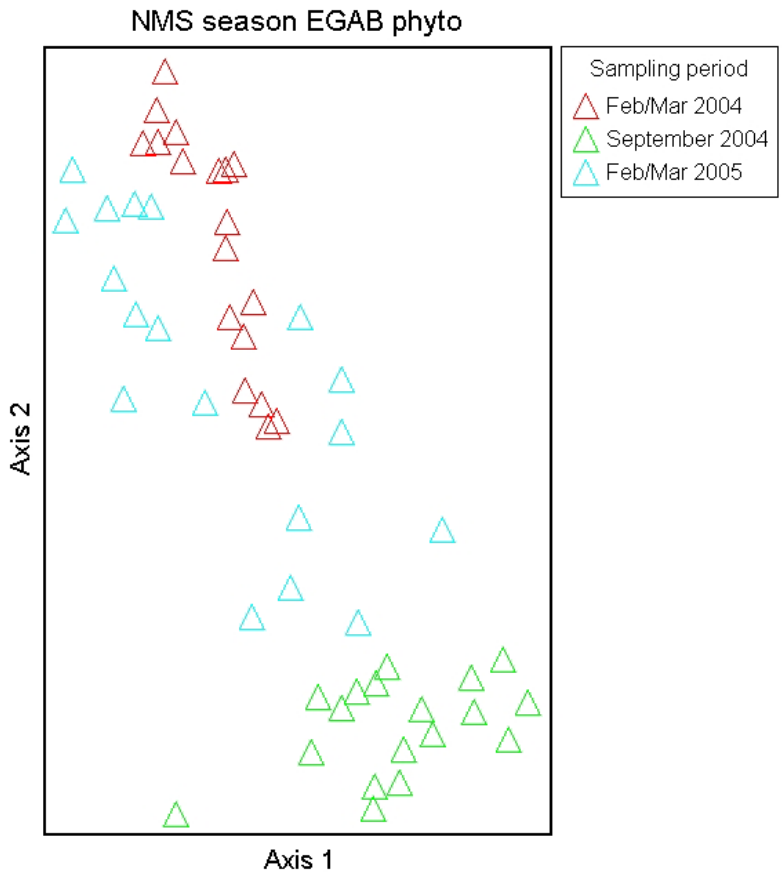

Figure 4.7. NMS ordination of seasonal variation in phytoplankton community composition in the EGAB. Stress = 8.5 %.

5. Can Meso-Zooplankton Community Composition be used to Distinguish between Water Masses in a Coastal Upwelling System?

5.1. Abstract

Meso-zooplankton abundance and community composition was examined in the coastal upwelling system of the eastern Great Australian Bight (EGAB). Spatial and temporal variations were influenced by variations in primary productivity and phytoplankton abundance and community composition, which were driven by variations in the influence of upwelling in the region. Peak meso-zooplankton abundances and biomass occurred in the highly productive upwelling influenced nearshore waters of the EGAB. However, abundances were highly variable between regions and years, reflecting the high spatial and temporal variations in primary productivity and phytoplankton abundance that characterise the shelf waters of the region. Spatial and temporal variations in community composition were driven by changes in the abundance of classes of meso-zooplankton common to all regions in both years of this study. Meroplanktonic larvae and opportunistic colonizers dominated the community through the upwelling season, in response to increased primary productivity and phytoplankton blooms. Differences in community composition between upwelling influenced waters and the more HNLC regions appear to be reflected in the relative abundances of cladocera and appendicularia, with cladocera more abundant in more productive upwelling influenced areas, and appendicularia thriving in the more HNLC regions of the EGAB.

5.2. Introduction

The eastern Great Australian Bight (EGAB) is part of one of the longest stretches of southern facing coastline in the world. As such, the region is dominated by an unusual set of meteorological and oceanographic conditions that together form a coastal upwelling system in summer/autumn (February/March/April) (Middleton and Cirano 2002; Middleton and Platov 2003; Kampf *et al.* 2004; Ward *et al.* 2006). The area supports a rich pelagic ecosystem, with populations of economically and ecologically important predatory species such as southern blue-fin tuna (*Thunnus maccoyii*), New Zealand fur seals (*Arctocephalus forsteri*), and Australian sea lions (*Neophoca cinerea*) (Page *et al.* 2006; Ward *et al.* 2006; Fowler *et al.* 2007; Goldsworthy and Page 2007). These predators feed on small pelagic fish, such as sardine (*Sardinops sagax*), which are highly abundant in shelf waters of the EGAB (Ward *et al.* 2006; Ward *et al.* 2008).

The sardine fishery in South Australia is Australia's largest marine scale-fish fishery by weight (25,000 tonnes in 2006), and is of high economic importance. To adequately manage this fishery, it is necessary to understand the factors that affect the distribution and abundance of the target species. Zooplankton are an important food source for sardine, and an understanding of the distribution and community dynamics of the zooplankton is vital when considering the factors that influence the sardine population of the EGAB.

When examining the distribution and dynamics of zooplankton communities, it is necessary to understand the manner in which the physical environment influences individual organisms and the community as a whole. Biological processes in the EGAB are influenced by seasonally variable meteorological and oceanographic conditions. Upwelling-favourable south-easterly winds and an anticyclonic

circulation dominate the area through summer/autumn (Herzfeld and Tomczak 1997; 1999; Middleton and Cirano 2002; Middleton and Platov 2003), while downwelling-favourable westerly winds and a continuous eastward flow are present through winter/spring (Bye 1983; Godfrey *et al.* 1986; Cirano and Middleton 2004). In an area as large as the EGAB, these seasonal variations in meteorological and oceanographic conditions are likely to result in changes in biological conditions, such as the distribution and abundance of phytoplankton and zooplankton communities, and the pelagic fish that depend on these organisms for food.

Despite the ecological and economical importance of understanding zooplankton dynamics in the EGAB pelagic ecosystem, few studies have examined zooplankton abundance, distribution and composition in this region. Sardine spawning biomass surveys conducted annually from 1995 by researchers from the Aquatic Sciences division of the South Australian Research and Development Institute (SARDI Aquatic Sciences) have provided some information regarding the abundance of the meso-zooplankton community >300 μm in size (Ward *et al.* 2001; Ward *et al.* 2002; Ward *et al.* 2004). However, significant components of the meso-zooplankton may be <300 μm in size, and would therefore not have been collected and reported in these studies. Thus, the importance of meso-zooplankton in the trophic dynamics of the region may have been underestimated. To date there has been no detailed examination of the abundance, distribution and composition of the meso-zooplankton community in the EGAB. This study represents the first step toward bridging this knowledge gap. It was designed to examine the hypothesis that spatial and temporal variations in meso-zooplankton abundance and community composition are driven by variations in phytoplankton abundance and community composition, which are influenced by changes in the timing and intensity of upwelling in the region.

5.3. Methods

Sampling was conducted during cruises aboard the *RV Ngerin* in February/March 2004, and February/March 2005. Eighteen stations were sampled in February/March 2004, twenty one in February/March 2005, with extra samples collected in the far west (Fig. 5.1). A conical zooplankton net with 150 μm mesh size and mouth of 30 cm diameter was lowered to within 10 m of the bottom, or to 70 m at stations greater than 80 m deep. The net was retrieved vertically at approximately 1 m s^{-1}. The entire contents of the net was washed into a 1 L sample jar and fixed with formalin (5% final volume). A General Oceanics flow meter was used to calculate the distance travelled by the net, which was then used to calculate the volume of water swept by multiplying distance travelled by the area of the mouth of the net.

Samples were gently rinsed with running water on a 150 μm mesh sieve to remove all traces of formalin, and the contents of the sieve was rinsed into 100 ml measuring cylinders and allowed to settle for 24 hours. Settling volumes were determined using 100 ml measuring cylinders and a settling time of 24 hours. Samples were then resuspended in 100 ml of water (i.e. concentrated 10x). Identification and enumeration was done via light microscopy. After gently resuspending the sample, a 1ml aliquot was taken for counting using a Sedgewick-Rafter chamber. Counts were continued until 100 specimens of the dominant group were counted, or until three aliquots had been used. Organism numbers were recorded as individuals m^{-3} in the water column using the volume swept, calculated as the depth of the tow multiplied by the area of the net mouth (diameter 30 cm). Organisms were identified using the taxonomic guides of Ritz *et al.* (2003) and Swadling *et al.* (2008).

Spatial correlations between physical parameters, zooplankton abundances and biomass, phytoplankton abundances and biomass and species diversity indices were examined via Mantel tests in PC-Ord 5 (McCune and Mefford 1999), using phytoplankton data reported in chapter 4. Essentially, the tests were looking for associations between the distributions of these parameters around a set of stations. Data were tested for 19 stations across the EGAB in February/March 2004 and 17 stations in February/March 2005. The distance measure used was Sorensen (Bray-Curtis). The standardised Mantel statistic (r) was calculated via randomization using the Monte Carlo test. Significant differences were indicated by p values <0.10. Species diversity indices (Species richness (S), Shannon`s diversity index (H), Evenness (E), Simpsons diversity index for infinite population (D)) were calculated using the row and column summary function in PC-Ord 5 (McCune and Mefford 1999).

Meso-zooplankton grazing pressure was estimated from zooplankton settling volumes, which were converted into biomass (mg C). Settling volumes were first converted into displacement volumes using a factor for samples without gelatinous zooplankton (0.35, (Wiebe *et al.* 1975; Wiebe 1988)). Displacement volumes were converted to biomass (mg C) using a factor of 21 for samples with displacement volumes <1cm^3, and a factor of 41 for samples with displacement volumes 1-10cm^3 (Bode *et al.* 1998). Potential growth of the meso-zooplankton was estimated via the empirical relationship of Huntley and Boyd (1984) (equation 1):

$$G'_{\max} = 0.0542e^{(0.110T)} \qquad (1)$$

where *T* is temperature (in this case, daily mean *SST* from *MODIS Aqua* was accessed via the NASA *Poet* website (http://poet.jpl.nasa.gov/)) and G'_{max} is the maximum mass-specific food-saturated growth rate, which can be used to estimate the assimilative capacity (*AC*) of the meso-zooplankton community via equation 2:

$$AC = 0.7G'_{\max} \qquad (2)$$

Where 0.7 is the estimate of 70% assimilative efficiency proposed by Conover (1978). The assimilative capacity was multiplied by biomass to give an estimate of the potential grazing rate of the meso-zooplankton community.

Variations in zooplankton community structure were examined via non-metric multidimensional scaling (NMS) in PC-Ord 5 (McCune and Mefford 1999). Data were ln(x+1) transformed prior to NMS analysis. PerMANOVAs were performed on transformed data using methods outlined in Anderson (2001), to examine potential differences in community structure between years and regions using a significance value of 0.05. Further examinations of any significance differences were made via pair-wise comparisons corrected for multiple comparisons via the Bonferroni procedure ($\alpha = 0.003$ for comparisons between regions). Indicator analyses were run to determine the classes of meso-zooplankton that were contributing significantly to differences in community composition between regions and years. Indicator values were calculated using the method of Dufrene & Legendre (1997). Relative abundances were calculated as the average abundance of a given species in a given group of samples over the average abundance of that species in all samples, expressed as a percentage. Relative frequencies indicate the percentage of samples in a given group where a given species is present.

5.4. Results

5.4.1. Meso-zooplankton abundance, composition and species diversity

Meso-zooplankton abundance in the summer/autumn upwelling season varied between years (Fig. 5.2). Visual examination of Figure 5.2 suggests the relative abundances by regions were:

2004 Nearshore central > Nearshore east > Nearshore west > Offshore west > Offshore east > Offshore central

2005 Nearshore far west > Nearshore west > Nearshore central > Nearshore east > Offshore east > Offshore central > Offshore west

Despite this visual ranking, neither Spearman's nor Kendall's coefficient of rank correlation (Sokal and Rohlf 1995), confirmed a significant difference. When the 2004 and 2005 data are ranked separately the eastern inshore site has the lowest abundance in 2005 but the second highest abundance in 2004. An explanation is that this site is influenced by the upwelling associated with Kangaroo Island that differed between 2004 and 2005. If this site is considered as an outlier the differences between years is significant with the majority of inshore sites ranked above the off shore sites (Kendall's Tau = 0.46 p = 0.01; Spearman's Rho = 0.64, p = 0.005).

Mantel tests indicated positive associations in 2004 between meso-zooplankton biomass and phytoplankton biomass ($p = 0.022$, $r = 0.285$), and between meso-zooplankton and diatom abundances ($p = 0.013$, $r = 0.273$). There was a weak, negative association between meso-zooplankton and phytoplankton species diversity ($p = 0.065$, $r = -0.111$).

There was a significant positive association between physical parameters and meso-zooplankton abundances in 2005 ($p = 0.084$, $r = 0.131$), with significant positive associations between meso-zooplankton and diatom abundances ($p = 0.013$, $r = 0.277$), and meso-zooplankton and dinoflagellate abundances ($p = 0.069$, $r = 0.142$).

The meso-zooplankton community in the EGAB was dominated by Copepods, which made up 63% of the community in February/March 2004, and 66% of the community in February/March 2005. Other significant contributors to the meso-zooplankton community included Cladocera and Appendicularia, which respectively made up 12% and 10% of the community in 2004, and 16% and 6% of the community in 2005. In 2004, Cladocera were found in higher abundances than Appendicularia in upwelling influenced waters of the nearshore eastern and central regions, while Appendicularia were more abundant than Cladocera in offshore eastern and central regions, and in the west (Fig 5.3). This pattern was not as pronounced in 2005, although Cladocera were clearly present in higher numbers than Appendicularia in the nearshore far western region.

Also identified in the 2004 EGAB meso-zooplankton community, in relatively low proportions, were Bivalvia, Chaetognatha, Copepod nauplii, Gastropoda, Ophiuroidea, Pteropoda and Thaliacea (Fig. 5.4). Meso-zooplankton that contributed <1% to the 2004 community were grouped together as ‘other’, and included Barnacle nauplii, Bryozoa, Decapoda, Euphasiacea, Hydrozoa, Mysidacea, and Siphonophora. In 2005, Bivalvia, Copepod nauplii, Ophiuroidea, and Pteropoda were identified in relatively low proportions in EGAB meso-zooplankton samples (Fig. 5.4), while ‘other’ meso-zooplankton included Barnacle nauplii, Bryozoa, Chaetognatha, Ctenophora, Decapoda, Euphasiacea, Gastropoda, Hydrozoa, Isopoda, Mysidacea, Scyphozoa and Thaliacea.

5.4.2. Biomass and grazing

Highest phytoplankton biomass was associated with low meso-zooplankton biomass, with high meso-zooplankton biomass associated with low-mid level phytoplankton biomass (Fig. 5.5). Meso-zooplankton diversity was generally higher in 2004, and phytoplankton diversity was generally higher in 2005 (Fig. 5.6).

Potential grazing rates varied considerably between years, but were typically highest at nearshore stations. The exception occurred in the western region where grazing rates were higher offshore than nearshore (Fig. 5.7). Greatest mean biomass and mean potential grazing rates occurred in the nearshore eastern region in February/March 2004 and the nearshore far western region in February/March 2005 (Table 5.1). Greatest mean potential growth rates occurred in the offshore western region in both years of this study (Table 5.1).

5.4.3. Spatial and temporal variation

NMS ordination indicates that the EGAB meso-zooplakton communities of February/March 2004 and February/March 2005 had similar compositions, although distinct outliers in each year's data suggest that there are some annual differences (Fig. 5.8). Further examination indicates a clear grouping based on the distance of the sample site from shore (Fig. 5.9). These patterns are confirmed in PerMANOVA analysis, with significant differences in community composition identified between years ($p = 0.012$) and regions ($p = 0.0002$), and a significant year by region interaction ($p = 0.018$, Table 5.2). Corrected pairwise comparisons indicate that the community in the nearshore eastern region was not significantly different to the

communities in any of the other EGAB study regions ($p > 0.03$). The community in the offshore eastern region was significantly different to the nearshore central and western regions and the offshore western region ($p = 0.0002$), but not the offshore central region ($p > 0.1$). The communities in the nearshore central and western regions were significantly different to the communities in the offshore central and western regions ($p = 0.0002$). The nearshore central and western regions did not differ significantly in community composition ($p > 0.4$).

Indicator analyses suggest that variations in the presence/abundance of Gastropods and Siphonophores contributed significantly to the uniqueness of the February/March 2004 community (Table 5.3). Both classes were present in higher mean abundances in February/March 2004 (Gastropod 42.8 ± 9.3 individuals m^{-3} in 2004, 17.0 ± 5.9 individuals m^{-3} in 2005; Siphonophore 7.4 ± 2.6 individuals m^{-3} in 2004, 0.3 ± 0.3 individuals m^{-3} in 2005), and both were present in more samples in February/March 2004 (Gastropod in 83% of samples in 2004, 50% of samples in 2005; Siphonophore in 44% of samples in 2004, in only one sample in 2005). Several classes of zooplankton were indicators of significant variation in community composition between regions in the EGAB (Table 5.4). Decapods were present in the nearshore eastern region in abundances more than double those found in other nearshore regions, and an order of magnitude greater than abundances in offshore regions. Cladocera, Copepods and Pteropods were found in all samples in all regions, but highest abundances of these classes occurred in the nearshore central region. Bivalves were most abundant in the nearshore western region where they were present in numbers two to four times greater than other nearshore regions, and an order of magnitude greater than offshore regions.

5.5. Discussion

Spatial and temporal variations in meso-zooplankton abundance and community composition in the EGAB appear to be influenced by variations in primary productivity and phytoplankton abundance and community composition, which are driven by variations in the influence of upwelling in the region (Chapters 2, 3, 4). Peak meso-zooplankton abundances and biomass occurred in the highly productive upwelling influenced nearshore waters of the EGAB, in areas with greatest phytoplankton abundances (Chapter 4). However, abundances were highly variable between regions and between years, most likely reflecting the high spatial and temporal variations in primary productivity and phytoplankton abundance that characterise the shelf waters of the EGAB (Chapters 2, 3, 4). Abundances and biomass in the EGAB in February/March 2004 and 2005 were ~4-5 times less than those measured in southwestern Spencer Gulf in March 2007, except in the nearshore far western region in February/March 2005, when abundances were about half those measured in southwestern Spencer Gulf in March 2007 (van Ruth *et al.* 2008). Peak abundances measured in the EGAB in February/March 2004 were similar to abundances measured in the Huon Estuary in February 2005 (6,800 individuals m^{-3}, Thompson *et al*. 2008). However, abundances in the nearshore far western region in February/March 2005 were ~3 times greater than abundances measured in the Huon Estuary in February 2005 (Thompson *et al.* 2008).

Spatial and temporal variations in meso-zooplankton community composition were driven by changes in the abundance of classes of zooplankton common to all regions in both years of this study. Spatial variations in community composition identified in the PerMANOVA analysis revealed similar regional community groupings to those identified in the EGAB phytoplankton community (Chapter 4),

suggesting that variations in phytoplankton abundances resulting from changes in the influence of upwelling in different regions of the EGAB are driving variations in meso-zooplankton abundances. Indeed, some zooplankton are known to time their spawning to take advantage of phytoplankton blooms (such as those that may occur during the EGAB upwelling season) which provide an abundant food supply for emerging larvae. An increase in larval zooplankton numbers usually occurs in spring/summer, with meroplanktonic larvae particularly abundant in shallow coastal waters (Ritz *et al.* 2003). An upwelling driven phytoplankton bloom may also facilitate the dominance of certain species in the zooplankton community with reproductive strategies that allow the rapid colonization of areas with an abundant supply of food. For example, cladoceran populations can quickly increase in size in response to phytoplankton blooms via parthenogenesis (Kim *et al.* 1989; Larsson 1997; Ritz *et al.* 2003), which may explain their position as one of the major components of the EGAB meso-zooplankton community, especially in the upwelling influenced nearshore areas with higher primary productivity.

Cladocera were important components of the meso-zooplankton, but copepods clearly dominated the community in the EGAB during February/March 2004 and 2005, in agreement with studies in other coastal regions of Australia including southwestern Spencer Gulf, South Australia (van Ruth *et al.* 2008), and the Huon estuary in southeastern Tasmania (Thompson *et al.* 2008). Copepods generally dominate marine meso-zooplankton communities (Parsons and Takahashi 1973; Omori and Ikeda 1984), and have been reported to constitute >70% of the zooplankton community observed in studies of the equatorial Pacific (Roman *et al.* 1995), the northeast Atlantic (Clark *et al.* 2001), and the waters off central Chile (Grunewald *et al.* 2002). Copepods have also been reported to dominate zooplankton

communities in the Arabian sea (Roman *et al.* 2000), and off southwestern Africa (Verheye *et al.* 1992). Appendicularia were also important components of the meso-zooplankton. However, these organisms were only found in abundances greater than cladocera in offshore and western areas influenced by the GAB warm pool (Chapter 2). This result may be explained by the fact that appendicularia are targeting a different food source to copepods and cladocerans. Appendicularians are well adapted for living in oligotrophic or HNLC waters, with feeding mechanisms that efficiently concentrate and filter the smaller pico and nano-plankton that generally dominate these waters (Davoll and Silver 1986; Bedo *et al.* 1993; Ritz *et al.* 2003). By consuming the smaller pico and nanoplankton, appendicularia make available to higher trophic levels areas of primary productivity that would be otherwise unavailable. These smaller phytoplankton may be present in higher numbers in areas of the EGAB not influenced by upwelling (i.e. offshore and western regions with lower phytoplankton abundances), and may not have shown up in the phytoplankton results presented in chapter 4 since they are too small to be identified with a light microscope. Pico-plankton may also be present in high numbers during periods of relaxation between upwelling events, possibly explaining the abundance of appendicularia during the weak upwelling season of 2005.

Highest potential grazing rates in the EGAB occurred in nearshore regions with highest meso-zooplankton biomass, most likely in response to the high phytoplankton biomass that occurs in the same regions. However, highest grazing rates were not associated with highest mass specific food saturated growth rates (G'_{max}). Estimates of G'_{max} varied with SST (as implicitly required in it's calculation via equation 1), suggesting that the significant impact of SST on zooplankton abundances identified in the regression analysis in this study reflects the influence of SST on potential

zooplankton growth rates. Peak meso-zooplankton growth rates in the EGAB were ~26% less than peak meso-zooplankton growth rates reported for southwestern Spencer Gulf in March 2007 (van Ruth *et al.* 2008), but were ~47% greater than rates reported for the Huon estuary in February 2005 (Thompson *et al.* 2008). Peak meso-zooplankton grazing rates in the EGAB were ~80% less than those measured in south west Spencer Gulf in March 2007 (van Ruth *et al.* 2008), and ~35% greater than grazing rates in the Huon Estuary in February 2005 (Thompson *et al.* 2008).

The seasonal differences in zooplankton community composition observed during this study appear to be associated with differences in primary productivity, with the dominance of meroplanktonic larvae and opportunistic colonizers in the EGAB through the upwelling season driven by increased primary productivity and phytoplankton blooms. Differences in community composition between the upwelling influenced waters of the nearshore eastern and central regions, and the more HNLC offshore and western regions appear to be reflected in the relative abundances of cladocera and appendicularia, with cladocera more abundant in more productive upwelling influenced areas, and appendicularia thriving in the more HNLC regions of the EGAB.

5.6. References

Anderson, M. J. (2001). A new method for non-parametric multivariate analysis of variance. *Austral Ecology* **26**(32-46).

Bedo, A. W., Acuna, J. L., Robins, D. and Harris, R. P. (1993). Grazing in the micronic and submicronic particle size range: the case of *Oikopleura dioica* (Appendicularia). *Bulletin of Marine Science* **53**: 2-14.

Bode, A., Alvarez-Ossorio, M. T. and Gonzalez, N. (1998). Estimations of meso-zooplankton biomass in a coastal upwelling area off NW Spain. *Journal of Plankton Research* **20**(5): 1005-1014.

Bye, J. A. T. (1983). The general circulation in a dissipative ocean basin with longshore wind stresses. *Journal of Physical Oceanography* **13**: 1553-1563.

Cirano, M. and Middleton, J. F. (2004). The mean wintertime circulation along Australias southern shelves: a numerical study. *Journal of Physical Oceanography* **34**(3): 668-684.

Clark, D. R., Aazem, K. V. and Hays, G. C. (2001). Zooplankton abundance and community structure over a 4000 km transect in the north-east Atlantic. *Journal of Plankton Research* **23**(4): 365- 372.

Conover, R. J. (1978). Transformations of organic matter. Marine Ecology V. 4. Dynamics. O. Kinne. Chichester, John Wiley**:** 221-456.

Davoll, P. J. and Silver, M. W. (1986). Marine snow aggregates: Life history sequence and microbial community of abandoned larvacean houses from Montery Bay, California. *Marine Ecology Progress Series* **33**: 111-120.

Dufrene, M. and Legendre, P. (1997). Species assemblages and indicator species: the need for a flexible asymmetrical approach. *Ecological Monographs* **67**: 345-366.

Fowler, S. L., Costa, D. P. and Gales, N. (2007). Ontogeny of movements and foraging ranges in the Australian sea lion. *Marine Mammal Science* **23**: 598-614.

Godfrey, J. S., Vaudrey, D. J. and Hahn, S. D. (1986). Observations of the shelf-edge current south of Australia, winter 1982. *Journal of Physical Oceanography* **16**: 668-679.

Goldsworthy, S. D. and Page, B. C. (2007). A risk assessment approach to evaluating the significance of seal bycatch in two Australian fisheries. *Biological Conservation* **139**: 269-285.

Grunewald, A. C., Morales, C. E., Gonzalez, H. E., Sylvester, C. and Castro, L. R. (2002). Grazing impact of copepod assemblages and gravitational flux in

coastal and oceanic waters off central Chile during two contrasting seasons. Journal *of Plankton Research* **24**(1): 55-67.

Herzfeld, M. and Tomczak, M. (1997). Numerical modelling of sea surface temperature and circulation in the Great Australian Bight. *Progress in Oceanography* **39**: 29-78.

Herzfeld, M. and Tomczak, M. (1999). Bottom-driven upwelling generated by eastern intensification in closed and semi-closed basins with a sloping bottom. *Marine and Freshwater Research* **50**: 613-627.

Huntley, M. and Boyd, C. M. (1984). Food-limited growth of marine zooplankton. *The American Naturalist* **124**: 455-478.

Kampf, J., Doubel, M., Griffin, D. A., Matthews, R. and Ward, T. M. (2004). Evidence of a large seasonal coastal upwelling system along the southern shelf of Australia. *Geophysical Research Letters* **31**(L09310): doi:10.1029/2003GL019221.

Kim, S. W., Onbe, T. and Yoon, Y. H. (1989). Feeding habits of marine cladocerans in the inland sea of Japan. *Marine Biology* **100**: 313-318.

Larsson, P. (1997). Ideal free distribution in Daphnia? Are daphnids able to consider both the food patch quality and the position of competitors? *Hydrobiologia* **360**: 143-152.

McCune, B. and Mefford, M. J. (1999). PC-ORD. Multivariate Analysis of Ecological Data, Version 5., MjM Software Design, Gleneden Beach, Oregon, USA.

Middleton, J. F. and Cirano, M. (2002). A northern boundary current along Australia's southern shelves: the Flinders current. *Journal of Geophysical Research-Oceans* **107**(C9): 3129-3143.

Middleton, J. F. and Platov, G. (2003). The mean summertime circulation along Australia's southern shelves: a numerical study. *Journal of Physical Oceanography* **33**(11): 2270-2287.

Omori, M. and Ikeda, T. (1984). Methods in marine zooplankton ecology. New York, Wiley-Interscience.

Page, B. C., McKenzie, J., Sumner, M. D., Coyne, M. and Goldsworthy, S. D. (2006). Spatial separation of foraging habits among New Zealand fur seals. *Marine Ecology Progress Series* **323**: 263-279.

Parsons, T. R. and Takahashi, M. (1973). Biological oceanographic processes. New York, Pergamon Press.

Ritz, D. A., Swadling, K. M., Hosie, G. and Cazassus, F. (2003). Guide to the zooplankton of south eastern Australia, Fauna of Tasmania Committee, University of Tasmania.

Roman, M., Smith, S., Wishner, K., Zhang, X. and Gowing, M. (2000). Mesozooplankton production and grazing in the Arabian sea. *Deep Sea Research 2* **47**: 1423-1450.

Roman, M. R., Dam, H. G., Gauzens, A. L., Urban-Rich, J., Foley, D. G. and Dickey, T. D. (1995). Zooplankton variability on the equator at 140 deg W during the JGOFS EqPac study. *Deep Sea Research 2* **42**(2-3): 673-693.

Sokal, R. R. and Rohlf, F. J. (1995). Biometry. United States of America, W.H. Freeman.

Swadling, K. M., Slotwinski, A. S., Ritz, D. A., Gibson, J. A. E. and Hosie, G. W. (2008). Guide to the marine zooplankton of south eastern Australia. Version 1.0 June 2008 www.tafi.org.au/zooplankton.

Thompson, P. A., Bonham, P. I. and Swadling, K. M. (2008). Phytoplankton blooms in the Huon Estuary, Tasmania: top down or bottom up control? *Journal of Plankton Research* **30**: 735-753.

van Ruth, P., Thompson, P., Bonham, P., and Jones, E. (2008) Primary productivity and zooplankton ecology in the Lincoln Offshore Subtidal Aquaculture Zone. Technical report, Aquafin CRC Project 4.6, FRDC Project 2005/059. Aquafin CRC, Fisheries Research & Development Corporation and South Australian Research & Development Institute (Aquatic Sciences), Adelaide. SARDI Publication No F2008/000789-1, SARDI Research Report Series No 343, 58 pp.

Verheye, H. M., Hutchings, L., Huggett, J. A. and Painting, S. J. (1992). Mesozooplanktonm dynamics in the Benguela ecosystem, with emphasis on the herbivorous copepods. *South African Journal of Marine Science* **12**: 561-584.

Ward, T. M., McLeay, L. J., Dimmlich, W. F., Rogers, P. J., McClatchie, S., Matthews, R., Kampf, J. and van Ruth, P. D. (2006). Pelagic ecology of a northern boundary current system: effects of upwelling on the production and distribution of sardine (*Sardinops sagax*), anchovy (*Engraulis australis*) and southern bluefin tuna (*Thunnus maccoyii*) in the Great Australian Bight. *Fisheries Oceanography* **15**(3): 191-207.

Ward, T. M., McLeay, L. J. and McClatchie, S. (2004). Spawning biomass of Sardine (*Sardinops sagax*) in South Australia in 2004, SARDI Aquatic Sciences**:** 38p.

Ward, T. M., McLeay, L. J., Rogers, P. J. and Dimmlich, W. F. (2001). Spawning biomass of Pilchard (*Sardinops sagax*) in South Australia in 2001, SARDI Aquatic Sciences**:** 31.

Ward, T. M., McLeay, L. J., Rogers, P. J., Dimmlich, W. F., Schmarr, D. and Deakin, S. (2002). Spawning biomass of Pilchard (*Sardinops sagax*) in South Australia in 2002, SARDI Aquatic Sciences**:** 33.

Ward, T. M., Rogers, P. J., Keane, J. P., Lowry, M., McLeay, L. J., Neira, F. J., Ovenden, J. R., Saunders, R. S., Schmarr, D., Whittington, I. D. and Williams, D. (2008). Development and evaluation of egg-based stock assessments for blue mackerel *Scomber australasicus* in southern Australia. Final report to Fisheries Research and Development Council, SARDI Aquatic Sciences.

Wiebe, P. H. (1988). Functional regression equations for zooplankton displacement volume, wet weight, dry weight, and carbon. A correction. *Fisheries Bulletin* **86**: 833-835.

Wiebe, P. H., Boyd, S. and Cox, J. L. (1975). Relationship between zooplankton displacement volume, wet weight, dry weight and carbon. *Fisheries Bulletin* **73**: 777-786.

5.7. Tables

Table 5.1. Temporal variation in settling volume (ml m^{-3}) meso-zooplankton biomass (mg C m^{-3}) and grazing rate (mg C m^{-3} d^{-1}). SST = CTD measured sea surface temperature (°C), G'_{max} = potential growth rate (d^{-1}). Means are ± standard error.

Year	Region	Settling vol.	Mean biomass	SST	G'_{max}	Mean grazing rate
2004	Nearshore east	5.1 (±1.5)	37.2 (±11.0)	18.7 (±0.4)	0.42 (±0.02)	22.7 (±6.9)
	Offshore east	1.2 (±0.2)	8.9 (±1.5)	18.8 (±0.1)	0.43 (±0.01)	5.4 (±0.9)
	Nearshore central	2.7 (±0.4)	19.9 (±3.0)	16.5 (±0.3)	0.33 (±0.01)	9.6 (±1.7)
	Offshore central	0.8 (±0.3)	5.9 (±2.3)	19.0 (±0.1)	0.44 (±0.01)	3.7 (±1.4)
	Nearshore west	2.4 (±1.1)	17.7 (±8.0)	16.7 (±0.4)	0.34 (±0.02)	8.5 (±3.9)
	Offshore west	2.2 (±0.5)	16.3 (±3.9)	19.3 (±0.1)	0.45 (±0.01)	10.5 (±2.6)
2005	Nearshore east	4.1 (±2.7)	30.3 (±19.6)	18.9 (±0.3)	0.43 (±0.01)	18.9 (±12.3)
	Offshore east	3.2 (±0.5)	23.3 (±3.5)	18.2 (±0.1)	0.40 (±0.01)	13.3 (±2.0)
	Nearshore central	3.1 (±0.7)	23.0 (±5.4)	17.8 (±0.3)	0.38 (±0.01)	12.7 (±3.0)
	Offshore central	1.0 (±0.6)	7.0 (±4.1)	19.3 (±0.1)	0.45 (±0.01)	4.5 (±2.7)
	Nearshore west	2.6 (±0.4)	19.0 (±2.9)	18.4 (±0.4)	0.41 (±0.02)	11.0 (±1.2)
	Offshore west	2.5 (±0.8)	18.3 (±5.8)	19.7 (±0.2)	0.47 (±0.01)	12.5 (±4.2)
	Nearshore far west	4.2 (±1.5)	31.1 (±11.2)	18.9 (±0.1)	0.44 (±0.01)	19.4 (±7.3)

Table 5.2. Results of PerMANOVA based upon the abundances of meso-zooplankton in the EGAB during February/March 2004 and February/March 2005.

Source	d.f.	SS	MS	F	p
Year	1	0.14	0.14	2.63	0.01
Region	5	0.84	0.16	3.08	0.0002
Interaction (year by region)	5	0.44	0.09	1.63	0.02
Residual	24	1.30	0.05		
Total	35	2.72			

Table 5.3. Results of indicator species analysis based upon the abundances of meso-zooplankton in the EGAB during February/March 2004. Mean abundances are ± standard error.

Class	Year	Observed Indicator Value (IV)	IV from randomised groups Mean	S.Dev	p *	Mean abundance (individuals m^{-3})	Relative abundance (%)	Relative frequency (%)
Siphonophora	2004	40.8	19.5	5.75	0.0046	7.4 (±2.6)	92	44
Gastropoda	2004	54.5	40.2	5.49	0.0134	42.8 (±9.3)	65	83

Table 5.4. Results of indicator species analysis based upon the abundances of meso-zooplankton in different regions of the EGAB during February/March 2004 and February/March 2005. Region 1 = nearshore east, region 3 = nearshore central, region 5 = nearshore west. Mean abundances are ± standard error.

Class	Region	Observed Indicator Value (IV)	IV from randomised groups Mean	S.Dev	p *	Mean abundance (individuals m^{-3})	Relative abundance (%)	Relative frequency (%)
Decapoda	1	38.8	15.9	7.6	0.0204	25.3 (±10.7)	58	67
Cladocera	3	25.9	21.2	2.12	0.0114	684.3 (±188.7)	26	100
Copepoda	3	23.9	20.3	1.34	0.0048	4,596.3 (±1,014.8)	18	100
Pteropoda	3	25.4	20.7	1.62	0.0002	388.2 (±90.3)	25	100
Bivalvia	5	28.9	21.1	3.17	0.0026	287.8 (±120.3)	29	100

5.8. Figures

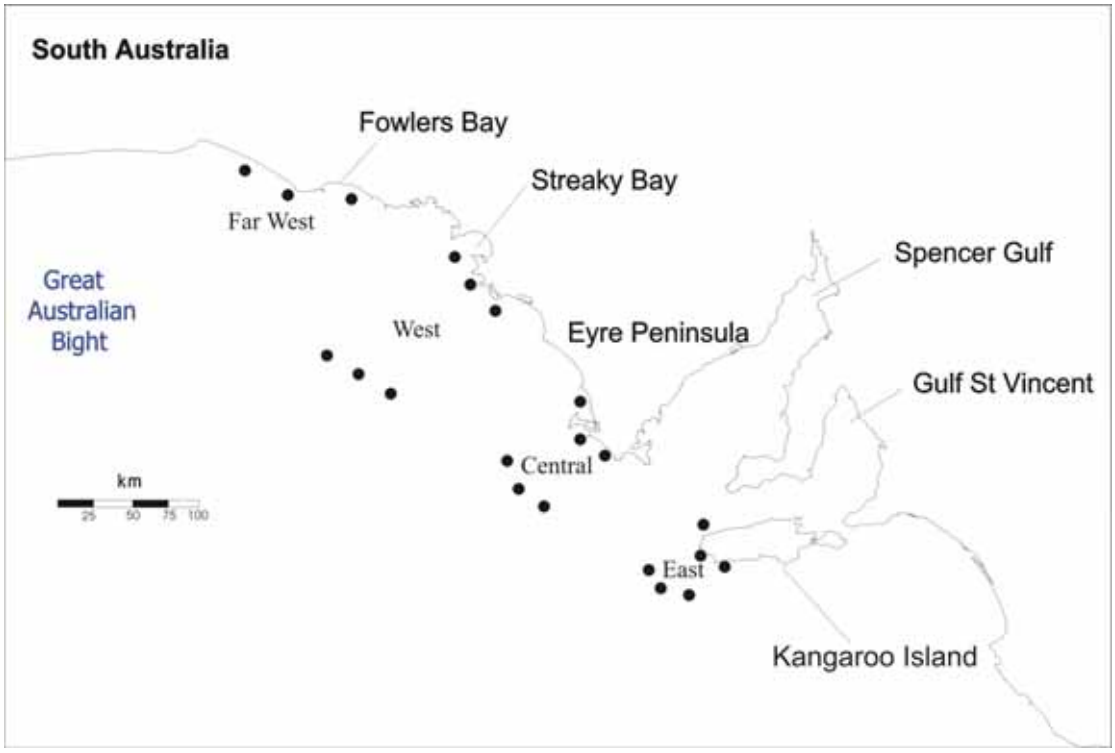

Figure 5.1. Zooplankton sampling stations. Far west stations were only sampled during February/March 2005.

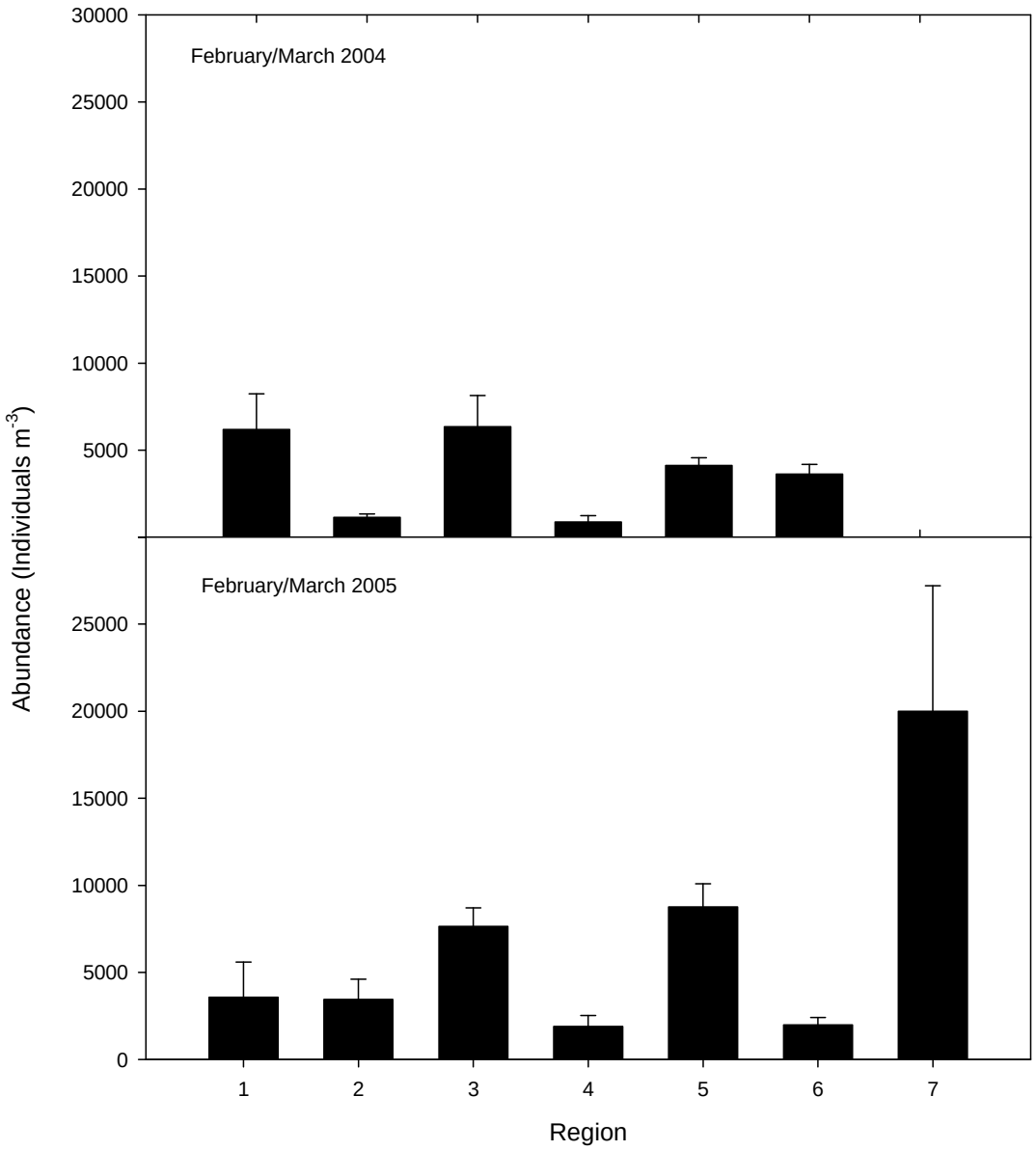

Figure 5.2. Spatial variations in meso-zooplankton abundance between years (mean ± standard error, n = 3). Region 1 = nearshore east, region 2 = offshore east, region 3 = nearshore central, region 4 = offshore central, region 5 = nearshore west, region 6 = offshore west, region 7 = nearshore far west (see Fig. 5.1).

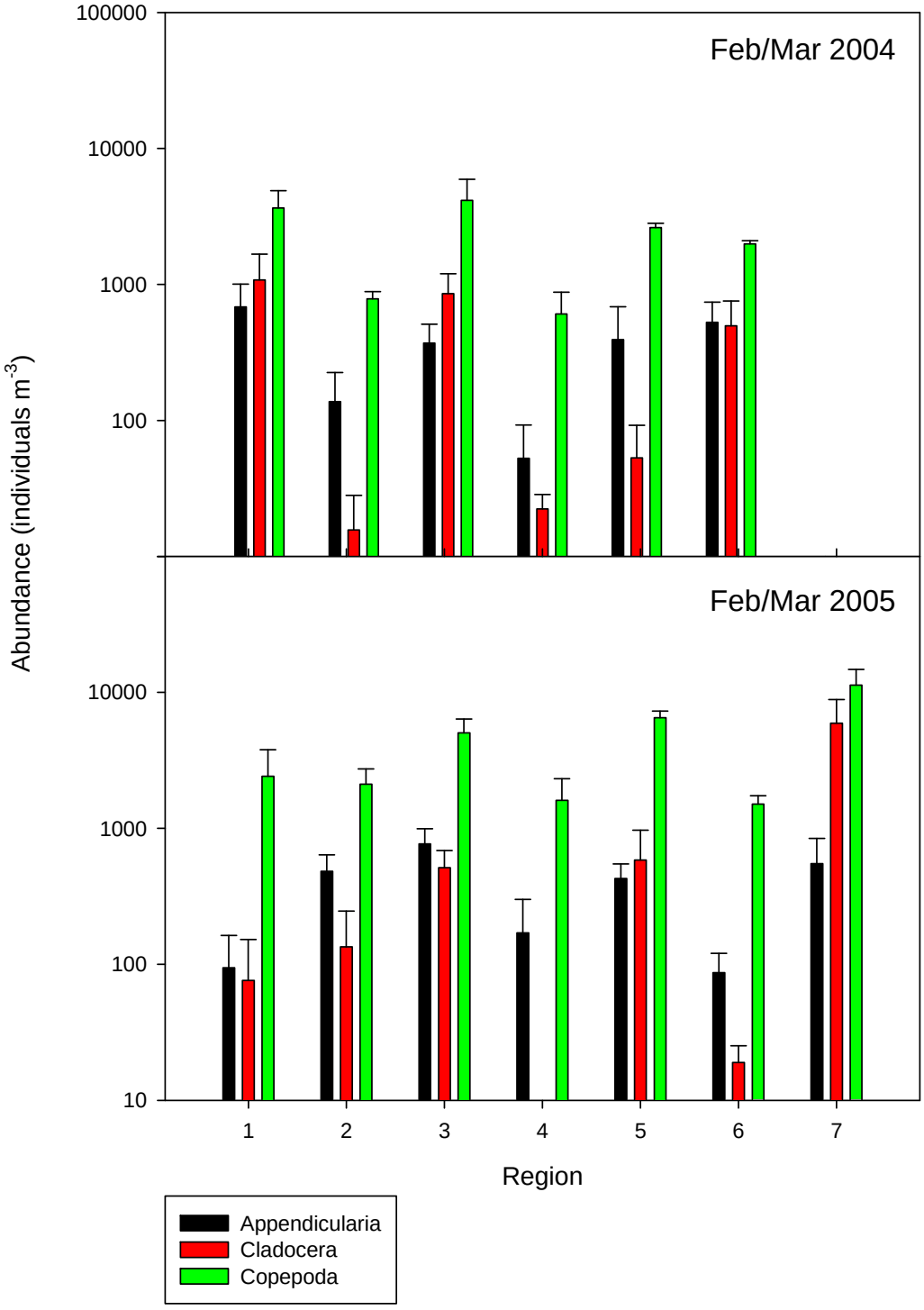

Figure 5.3. Spatial and temporal variation in abundances of dominant meso-zooplankton in the EGAB (mean ± standard error, n = 3). Region 1 = nearshore east, region 2 = offshore east, region 3 = nearshore central, region 4 = offshore central, region 5 = nearshore west, region 6 = offshore west, region 7 = nearshore far west (see Fig. 5.1 for regions). Note the log scale on the y axis.

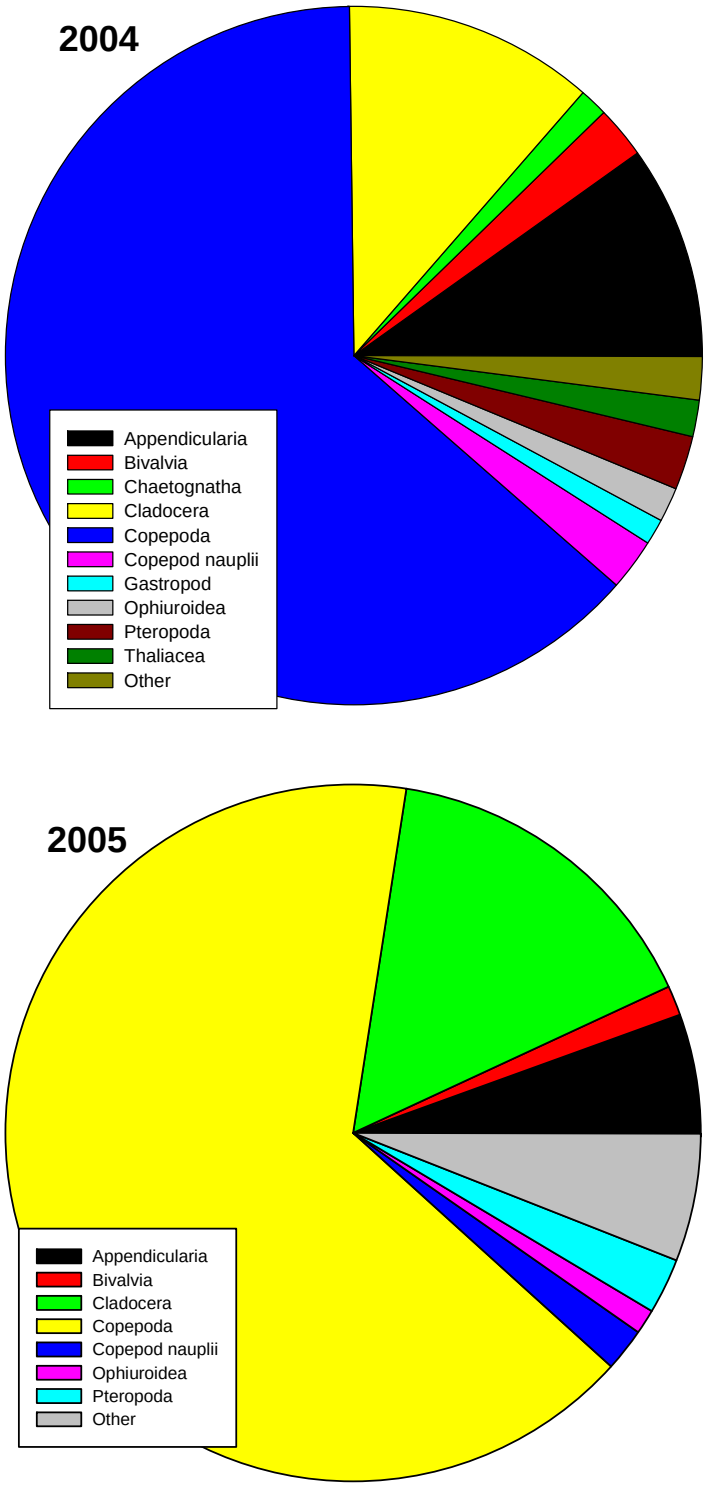

Figure 5.4. Meso-zooplankton community composition (proportions of total community) in the EGAB, February/March 2004 and 2005.

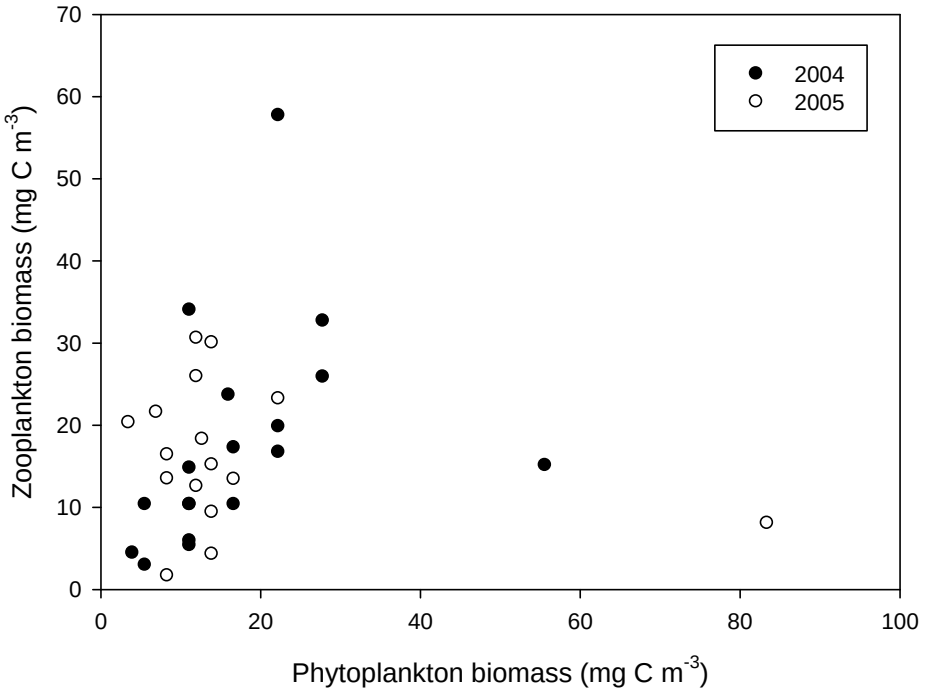

Figure 5.5. Variation in phytoplankton and meso-zooplankton biomass in the EGAB.

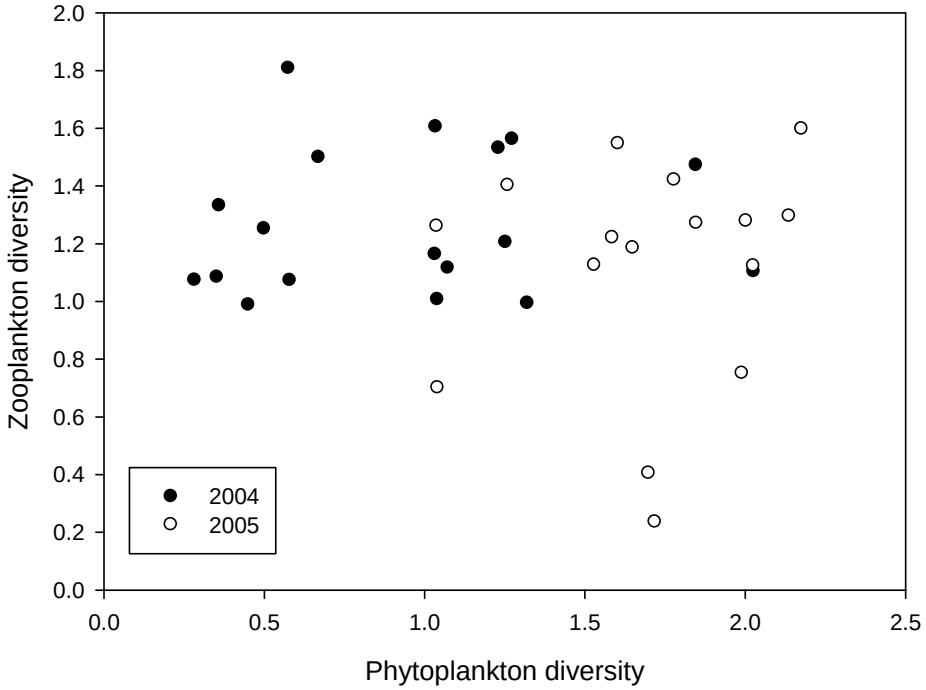

Figure 5.6. Variation in phytoplankton and meso-zooplankton diversity in the EGAB.

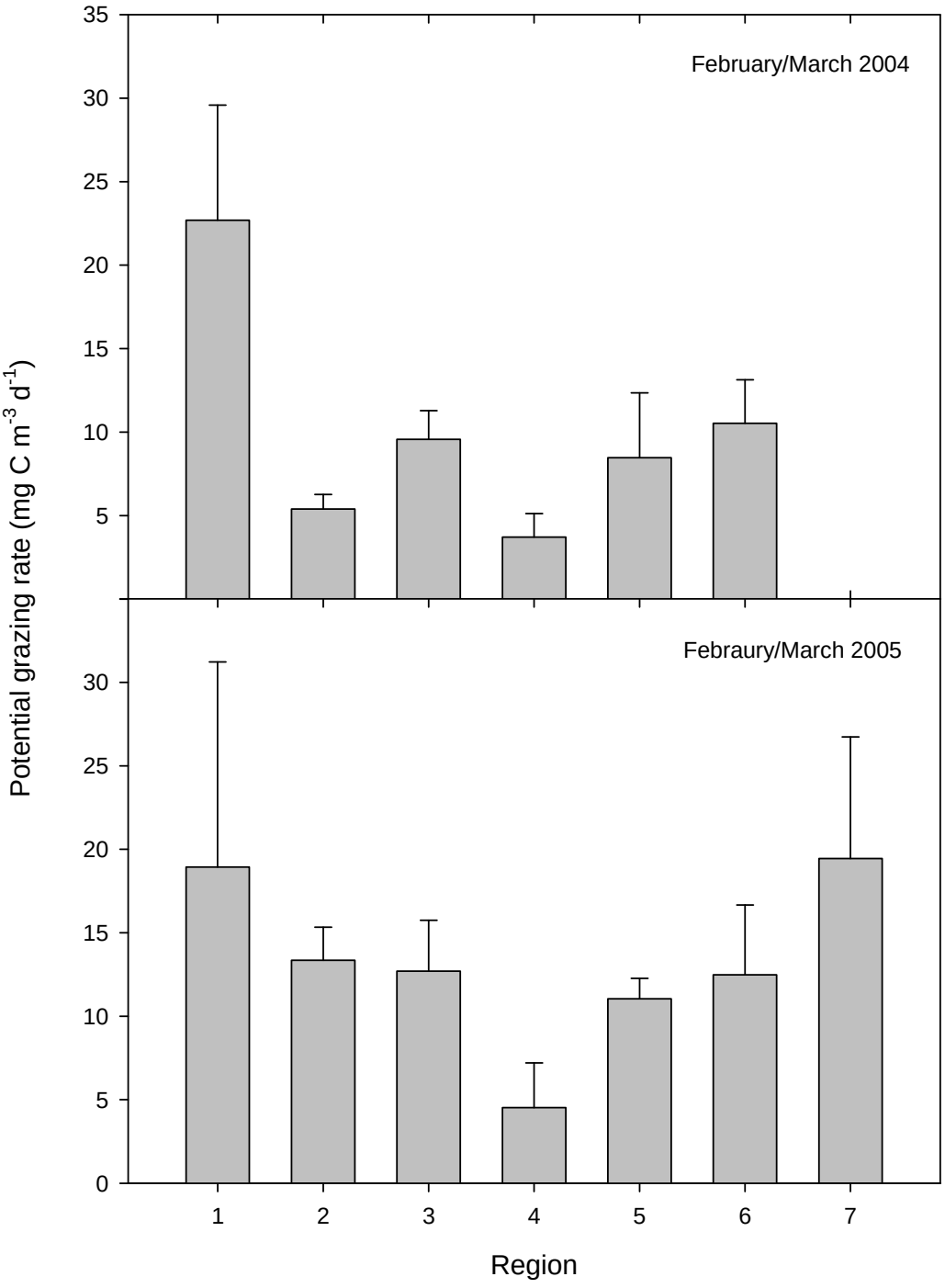

Figure 5.7. Spatial variations in meso-zooplankton potential grazing rate between years (mean ± standard error n = 3). Region 1 = nearshore east, region 2 = offshore east, region 3 = nearshore central, region 4 = offshore central, region 5 = nearshore west, region 6 = offshore west, region 7 = nearshore far west (see Fig. 5.1).

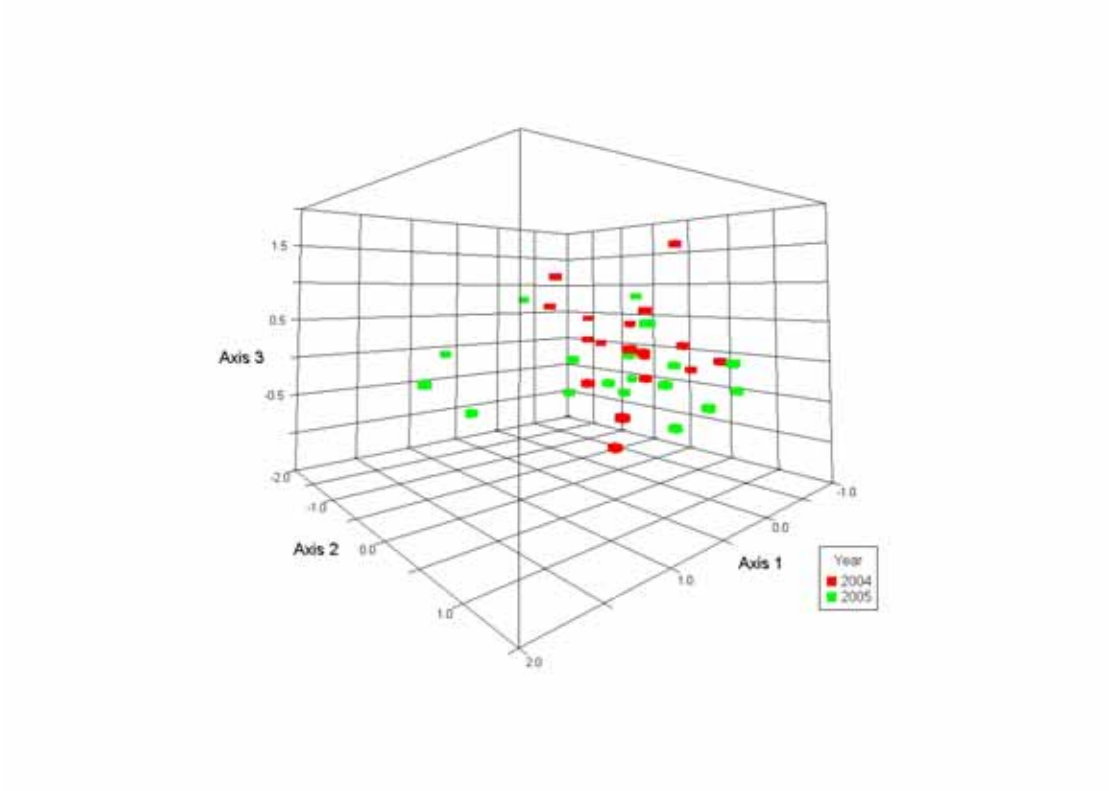

Figure 5.8. NMS ordination of temporal variation in meso-zooplankton community composition in the EGAB during February/March 2004 and February/March 2005. Stress = 13.8 %.

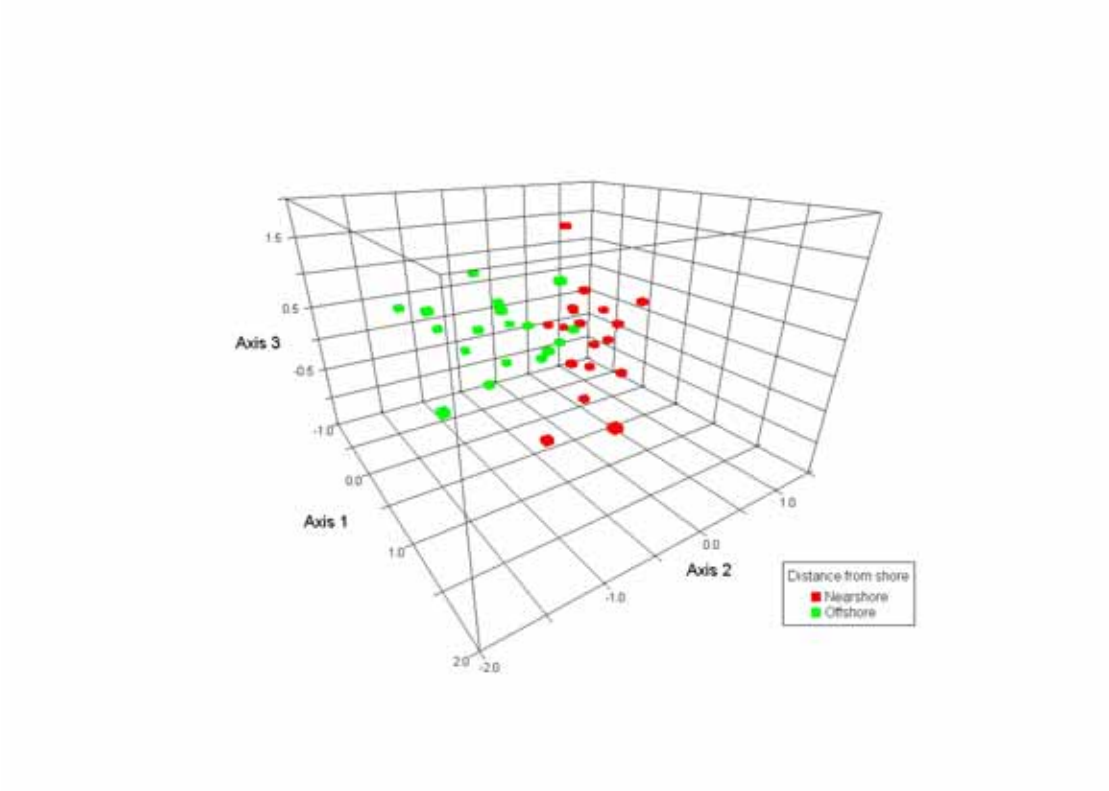

Figure 5.9. NMS ordination of spatial variation in meso-zooplankton community composition in the EGAB during February/March 2004 and February/March 2005. Stress = 13.8 %.

6. General discussion

Productivity in the EGAB shows significant spatial and temporal variation, with changes reflecting regional and seasonal variation in meteorology and oceanography, and the water masses present in the region. During the winter downwelling season, shelf waters were characterised by a well mixed water mass, and productivity throughout the EGAB was low due to deep mixing arising after long periods of downwelling favourable winds, and the absence of micro-nutrient enrichment via suppression of the upwelling associated with the Flinders current (Middleton and Cirano 2002; Middleton and Bye 2007). Primary productivity was also inhibited by lower irradiances and shorter daylengths which are characteristic of winter and early spring in the region. Daily integral productivities for winter fell towards the higher end of the range reported for the oligotrophic waters of the Leeuwin current (110-530 mg C m^{-2} d^{-1}, Hanson *et al.* 2005). Chlorophyll concentrations measured during September 2004 were relatively low by global standards, and were comparable to those measured throughout the year in the oligotrophic waters off western and south eastern Australia (Gibbs *et al.* 1986; Hallegraeff and Jeffrey 1993; Hanson *et al.* 2005).

Primary productivity was higher during the summer/autumn upwelling season, although there was considerable spatial variation. Offshore areas of the eastern, central and western waters had low daily integral productivities (<800 mg C m^{-2} d^{-1}), comparable to values reported for the oligotrophic waters of the Leeuwin current off south west Western Australia (110-530 mg C m^{-2} d^{-1}, Hanson *et al.* 2005), the AuSW and SSTC provinces of Longhurst *et al.* (1995) and the north and south Atlantic sub-tropical gyres (18-362 mg C m^{-2} d^{-1}, Maranon *et al.* 2003). They were significantly

higher than the average values reported by Ryther (1969) and those of Motoda *et al.* (1978). Mid-shelf and coastal waters had intermediate productivities (800-1600 mg C m^{-2} d^{-1}) that were similar to those reported for localised upwellings off south west Western Australia (840-1310 mg C m^{-2} d^{-1}, Hanson *et al.* 2005), and for the waters of Bass Strait and the east coast of Tasmania (336-2880 mg C m^{-2} d^{-1}, highest rates associated with the spring bloom: Harris *et al.* 1987). Higher productivities were measured, but were restricted to distinct hotspots off SWEP, SWKI, and Cape Adieu (1600-3900 mg C m^{-2} d^{-1}). In these regions, productivities were within ranges measured in the highly productive upwelling systems of the Benguela current off southern Africa (1000-3500 mg C m^{-2} d^{-1}, Brown *et al.* 1991), and the Humboldt current off the coast of Chilè (800-5100 mg C m^{-2} day^{-1}, Daneri *et al.* 2000).

High rates of primary productivity in the EGAB were not restricted to surface waters. The deeper region of the euphotic zone at times encompassed a significant portion of the upwelled water mass, with highest chlorophyll fluorescences measured in this water below the surface mixed layer. This study has shown that the contribution of the surface mixed and bottom layers of the euphotic zone to total primary productivity in the EGAB can vary considerably between years. At times, the surface mixed layer accounted for <40% of total productivity despite the fact that it made up >50% of the euphotic zone. Therefore, it is highly likely that daily integral productivity levels in some areas of the EGAB, most likely in the mid shelf waters of the eastern and central regions that include the upwelled Kangaroo Island pool, are higher than indicated by modelled results which use surface measured values in calculations. Overall primary productivity in the EGAB was heavily influenced by the presence of the upwelled water mass, but did not require that water mass to reach the surface. High productivity levels appear to be achievable after the first upwelling

event which drives the formation of the Kangaroo Island Pool. These results have implications for previous conclusions about productivity in the region based on satellite derived data, and emphasise the importance of ground-truthing satellite and modelled data.

The overall productivity of a summer/autumn upwelling season was highly dependent on within-season variations in wind strength and direction, which dictate the number, intensity, and duration of upwelling events. Rates of primary productivity in the EGAB at a given time depended on the meteorological and oceanographic conditions in the region in the lead up to, and during, the sampling event. In February 2004, sampling took place during an upwelling event, signified by a peak in three day averaged wind stress that occurred within a relatively strong upwelling season. High productivity was driven by stratification and the intrusion of upwelled waters above Z_{cr}. Low productivity in September 2004 was due to high mixing rates arising after long periods of downwelling favourable winds and the absence of micro-nutrient enrichment via upwelling. Primary productivity in September 2004 also appears to have been inhibited by lower irradiances and shorter daylengths which are characteristic of winter and early spring in the region. In February 2005 sampling occurred during a downwelling event at the end of a short peak in upwelling favourable winds, but within a season of weak mean upwelling favourable wind stress. During this time, increased mixing from downwelling favourable winds was suppressing wind driven upwelling, but gradually enriching surface waters of the SWEP via entrainment of upwelled water into the surface mixed layer. These periods of mixing may also provide the seed for a burst of primary productivity during the next upwelling/stratification event, by allowing phytoplankton from the surface mixed layer to entrain into areas of the water column influenced by

the upwelled water mass. Productivity levels were highest in February/March 2006, after a sustained period of upwelling favourable winds. Sampling occurred during a strong upwelling event, in a season of greater than average upwelling favourable wind stress. During this time, high daily integral productivity was driven by shallow MLD's which allowed the entrainment of upwelled waters to areas above Z_{cr}, and gradual overall enrichment of shelf waters during a two month period of strong upwelling events that occurred in the lead up to the sampling period. Thus, variations in productivity in the EGAB are not dictated by variations in mixing in the classical sense. The waters off SWEP in the EGAB appear to represent a unique situation that doesn't always comply with conventional theory regarding mixing and productivity, which is generally used to explain the phytoplankton spring bloom. Results from February 2005 seem to resemble the conventional model. MLD were ~7 m deeper than the critical depth and productivity was low. This was the weakest upwelling season of the study, and sampling occurred during a period of downwelling and mixing. In the waters off SWEP in February/March 2006, however, MLD were shallow at the western and eastern stations. At the western station, MLD was 1.7 m above Z_{cr}. Despite this result, integrated losses were greater than integrated production, due to a high grazing impact. At the eastern station, MLD was 13.5 m above Z_{cr}, and productivity was high. Primary productivity in the surface mixed layer in February/March 2006 was accounting for <40% of primary productivity in the euphotic zone. It follows that >60% of primary productivity was occurring in the waters below the surface mixed layer but above Z_{cr}. Higher productivity during 2006, the strongest upwelling season, was due to the entrainment of a larger volume of upwelled water from the bottom layer on the shelf southeast of Eyre Peninsula (the Kangaroo Island pool) into nearshore areas of the water column above Z_{cr}. The high

rates of primary productivity, medium biomass and low grazing impact observed at the eastern station may indicate the onset of a phytoplankton bloom driven by access to large volumes of upwelled water. In contrast, at the central station off SWEP in 06, no credible Z_{cr} could be calculated since losses were always > productivity. Indeed, integrated losses were ~650% of primary productivity, due to high grazing impact. Despite this fact, biomass was largest at the central station in February/March 2006. The presence of such a large biomass, despite relatively low rates of primary productivity, and such high grazing losses may signal the peak/decline of a phytoplankton bloom.

There were three distinct water masses identified in the EGAB during this study, the winter well-mixed water mass, the upwelled Kangaroo Island pool, and the GAB warm pool. Our results indicate that despite large contrasts in productivity between the GAB warm pool and the upwelled water mass, there were no patterns in nutrient concentrations that could be used to differentiate between them. Macro-nutrient concentrations in this study were highly variable with no clear pattern between periods of upwelling/downwelling, and there was no evidence of macro-nutrient limitation in waters off SWEP at any time during this study. Despite this, productivity levels in the GAB warm pool can be up to an order of magnitude lower than productivities in areas influenced by the upwelled water mass. Iron has been shown to limit growth in large parts of the ocean particularly high nutrient low chlorophyll (HNLC) regions such as the sub-arctic and equatorial Pacific, and the southern ocean around Antarctica (Martin and Fitzwater 1988; Martin *et al.* 1989; Martin 1990). Iron deficiency may explain the low levels of primary productivity associated with the HNLC waters of the GAB warm pool. The absence of direct

measurements of dissolved iron concentrations in the different water masses, however, makes it impossible to confidently draw conclusions.

As mentioned above, the blooming of phytoplankton in the waters off SWEP appears to be regulated by changes in MLD, but not because it leads to an increase in surface layer primary productivity. Variations in MLD drive phytoplankton blooms by dictating the volume of upwelled water that can entrain from the bottom layer into nearshore areas of the water column above Z_{cr}. These results suggest that there is some component of the upwelled water mass that is not present in the overlying surface water that promotes primary productivity. In the absence of any evidence of macro-nutrient limitation, differences in micro-nutrient concentrations between the upwelled water mass and the overlying surface water of the GAB warm pool may be responsible for variations in primary productivity between the two water masses. Higher productivity during the upwelling season may be driven by enrichment of shelf waters with micro-nutrients, which is absent during winter/spring due to the suppression of upwelling by the coastal current, and the dominant downwelling favourable winds. Temporal variations in mixing scenarios between and within seasons may affect primary productivity in the EGAB by changing the influence of the upwelled water mass on waters in the region.

Although the three water masses in the EGAB could not be differentiated by variations in nutrient concentrations, they could be identified by variations in the phytoplankton and meso-zooplankton communities. In the case of phytoplankton, distinctions between water masses were manifest in variations in the abundance of dominant types of phytoplankton, and differences in average cell sizes. The phytoplankton community in the well-mixed winter water mass was made up of low abundances of relatively large cells. Waters were well mixed, and biomass was

reduced due to lower primary productivity caused by decreased irradiances and shorter daylengths. Despite this, average cell sizes were still relatively large, with nitrate and silica concentrations at this time adequate enough to maintain the dominance of diatoms. During the summer/autumn upwelling season, waters influenced by the Kangaroo Island pool were characterised by high phytoplankton abundances (particularly diatoms) and larger average cell sizes, as might be expected to be found in productive upwelling regions, while the waters of the GAB warm pool had lower phytoplankton abundances and smaller average cell sizes, as might be expected to be found in more oligotrophic, or HNLC waters (Ryther 1969; Mann and Lazier 2006). Differences in meso-zooplankton community composition between the upwelling influenced waters of the nearshore eastern and central regions, and the more oligotrophic offshore and western regions appear to be reflected in the relative abundances of cladocera and appendicularia, with cladocera, as opportunistic colonisers, able to quickly multiply in more productive areas influenced by the Kangaroo Island pool, and appendicularia, with specialised feeding mechanisms for consuming smaller plankton, thriving in the HNLC waters of the GAB warm pool.

The shelf waters of the EGAB have a potential productivity that could rival even the most productive areas of the ocean. However, more accurate indications of primary and secondary productivity in these economically and ecologically important waters will require finer scale (monthly/weekly) direct measurements of primary productivity (via ^{14}C or equivalent technique) and community respiration, and direct measurements of secondary productivity and grazing rates. ^{14}C productivity experiments and grazing experiments using the dilution method of Landry and Hasset (1982) were attempted in this study, but difficulties associated with inadequate laboratory facilities onboard the primary research vessel (*RV Ngerin*) made the results

difficult to interpret. Consideration in future studies should also be given to the components of the microbial food web, which may be playing an important part in the productivity of the region, particularly in the less productive offshore waters in the central and western EGAB. These studies will require dedicated cruises, with the provision of suitable onboard laboratory facilities. Finer scale studies of spatial variations in macro and micro nutrient cycling in the water masses of the EGAB will provide a better understanding of the factors that promote high productivity in the upwelled water. Future studies should include analysis of iron concentrations/deposition rates, sedimentation rates, the influence of benthic-pelagic and ocean-atmospheric coupling on nutrient cycling, and potential nutrient limitation in phytoplankton.

6.1. References

Brown, P. C., Painting, S. J. and Cochraine, K. L. (1991). Estimates of phytoplankton and bacterial biomass and production in the northern and southern Benguela ecosystems. *South African Journal of Marine Science* **11**: 537-564.

Daneri, G., Dellarossa, V., Quinones, R., Jacob, B., Montero, P. and Ulloa, O. (2000). Primary production and community respiration in the Humboldt Current System off Chile and associated oceanic areas. *Marine Ecology Progress Series* **197**: 41-49.

Gibbs, C. F., Tomczak, M. and Longmore, A. R. (1986). The nutrient regime of Bass Strait. *Marine and Freshwater Research* **37**: 451-466.

Hallegraeff, G. M. and Jeffrey, S. W. (1993). Annually recurrent diatom blooms in spring along the New South Wales coast of Australia. *Marine and Freshwater Research* **44**: 325-334.

Hanson, C. E., Pattiaratchi, C. B. and Waite, A. M. (2005). Seasonal production regimes off south-western Australia: influence of the Capes and Leeuwin Currents on phytoplankton dynamics. *Marine and Freshwater Research* **56**: 1011-1026.

Harris, G., Nilsson, C., Clementson, L. and Thomas, D. (1987). The water masses of the east coast of Tasmania: seasonal and interannual variability and the influence on phytoplankton biomass and productivity. *Australian Journal of Marine and Freshwater Research* **38**: 569-590.

Landry, M. R. and Hasset, R. P. (1982). Estimating the grazing impact of marine microzooplankton. *Marine Biology* **67**: 283-288.

Longhurst, A., Sathyendranath, S., Platt, T. and Caverhill, C. (1995). An estimate of global primary production in the ocean from satellite radiometer data. *Journal of Plankton Research* **17**(6): 1245-1271.

Mann, K. H. and Lazier, J. R. N. (2006). Dynamics of marine ecosystems: biological - physical interactions in the oceans. London, Blackwell Science.

Maranon, E., Behrenfeld, M. J., Gonzalez, N., Mourino, B. and Zubkov, M. V. (2003). High variability of primary production in oligotrophic waters of the Atlantic ocean: uncoupling from phytoplankton biomass and size structure. *Marine Ecology Progress Series* **257**: 1-11.

Martin, J. H. (1990). Glacial-interglacial carbon dioxide change: The iron hypothesis. *Paleoceanography* **5**: 1-13.

Martin, J. H. and Fitzwater, S. E. (1988). Iron deficiency limits phytoplankton growthin the north-east Pacific subarctic. *Nature* **331**: 341-343.

Martin, J. H., Gordon, R. M., Fitzwater, S. and Broenkow, W. W. (1989). VERTEX: phytoplankton/iron studies in the Gulf of Alaska. *Deep Sea Research* **36**: 649-680.

Middleton, J. F. and Bye, J. A. T. (2007). A review of the shelf slope circulation along Australia's southern shelves: Cape Leeuwin to Portland. *Progress in Oceanography* **75**: 1-41.

Middleton, J. F. and Cirano, M. (2002). A northern boundary current along Australia's southern shelves: the Flinders current. *Journal of Geophysical Research-Oceans* **107**(C9): 3129-3143.

Motoda, S., Kawamura, T. and Taniguchi, A. (1978). Differences in productivities between the Great Australian Bight and the Gulf of Carpentaria, Australia, in Summer. *Marine Biology* **46**: 93-99.

Ryther, J. H. (1969). Photosynthesis and Fish Production in the Sea. *Science* **166**: 72-76.